PolyPublie
Polytechnique Montréal

POLYTECHNIQUE MONTRÉAL
UNIVERSITÉ D'INGÉNIERIE

| | |
|---|---|
| **Titre:** Title: | Olivine-based castables for copper industry |
| **Auteur:** Author: | Eugen Kosc |
| **Date:** | 2003 |
| **Type:** | Mémoire ou thèse / Dissertation or Thesis |
| **Référence:** Citation: | Kosc, E. (2003). Olivine-based castables for copper industry [Master's thesis, École Polytechnique de Montréal]. PolyPublie. https://publications.polymtl.ca/7129/ |

**Document en libre accès dans PolyPublie**
Open Access document in PolyPublie

| | |
|---|---|
| **URL de PolyPublie:** PolyPublie URL: | https://publications.polymtl.ca/7129/ |
| **Directeurs de recherche:** Advisors: | Michel Rigaud, & Stefan Palco |
| **Programme:** Program: | Unspecified |

**Ce fichier a été téléchargé à partir de PolyPublie, le dépôt institutionnel de Polytechnique Montréal**
This file has been downloaded from PolyPublie, the institutional repository of Polytechnique Montréal

https://publications.polymtl.ca

In compliance with the
Canadian Privacy Legislation
some supporting forms
may have been removed from
this dissertation.

While these forms may be included
in the document page count,
their removal does not represent
any loss of content from the dissertation.

UNIVERSITÉ DE MONTRÉAL

# OLIVINE – BASED CASTABLES FOR COPPER INDUSTRY

EUGEN KOSC
DÉPARTEMENT DE MATHÉMATIQUES ET DE GÉNIE INDUSTRIEL
ÉCOLE POLYTECHNIQUE DE MONTRÉAL

MÉMOIRE PRÉSENTÉ EN VUE DE L'OBTENTION
DU DIPLÔME DE MAÎTRISE ÈS SCIENCES APPLIQUÉES
(GÉNIE MÉTALLURGIQUE)
MAI 2003

© Eugen Kosc, 2003.

National Library
of Canada

Acquisitions and
Bibliographic Services

395 Wellington Street
Ottawa ON K1A 0N4
Canada

Bibliothèque nationale
du Canada

Acquisisitons et
services bibliographiques

395, rue Wellington
Ottawa ON K1A 0N4
Canada

*Your file Votre référence*
*ISBN: 0-612-86406-5*
*Our file Notre référence*
*ISBN: 0-612-86406-5*

The author has granted a non-exclusive licence allowing the National Library of Canada to reproduce, loan, distribute or sell copies of this thesis in microform, paper or electronic formats.

The author retains ownership of the copyright in this thesis. Neither the thesis nor substantial extracts from it may be printed or otherwise reproduced without the author's permission.

L'auteur a accordé une licence non exclusive permettant à la Bibliothèque nationale du Canada de reproduire, prêter, distribuer ou vendre des copies de cette thèse sous la forme de microfiche/film, de reproduction sur papier ou sur format électronique.

L'auteur conserve la propriété du droit d'auteur qui protège cette thèse. Ni la thèse ni des extraits substantiels de celle-ci ne doivent être imprimés ou aturement reproduits sans son autorisation.

Canada

UNIVERSITÉ DE MONTRÉAL

ÉCOLE POLYTECHNIQUE DE MONTRÉAL

Ce mémoire intitulé:

**OLIVINE – BASED CASTABLES FOR COPPER INDUSTRY**

présenté par : KOSC Eugen

en vue de l'obtention du diplôme de: Maîtrise ès sciences appliquées

a été dûment accepté par le jury d'examen constitué de:

M. ALLAIRE Claude, Ph.D., président

M. BENHOOD Nosrad, Ph.D., membre externe

M. RIGAUD Michel, D.Sc.A., membre et directeur de recherche

M. PALCO Stefan, Ph.D., membre et codirecteur de recherche

# ***ACKNOWLEDGEMENTS***

I would like to express my sincere gratitude to my supervisor, Professor Michel Rigaud, for his expert guidance, valuable advice and constructive criticism throughout this work. I do appreciate his constant support and encouragement during my M.Sc.A program at École Polytechnique de Montréal.

Special thanks go to Dr. Štefan Palčo, for his valuable help during all my study in everything I needed. Stefan's technical advises and discussions helped me significantly to write this thesis.

Special thanks go to Mr. Vladimír Kováč, for his kindly support and help on experimental work.

Grateful thanks also go to my colleagues at CIREP, Professor C. Allaire, Dr. R. Pelletier, Dr. H. He, E. Divry, Ch. Gaubert, Dr. N. Ntakaburimvo for their friendship, helpful discussion and valuable assistance. My particular thanks are due to J.P.Bouchard and H.Rioux at CIREP for their technical and administrative help.

Finally, I would like to express my deepest appreciation to my wife Katka for her love, sacrifice, encouragement and constant support.

# ABSTRACT

Magnesia - chrome bricks have been widely used in copper industry for more than 50 years. Their very good performances against copper making slags mainly fayalite slag explain this situation. The growing concern comes from an environmental issue. The formation of a $Cr^{6+}$, and its carcinogenic consequences, are well known. The $Cr^{6+}$ presented in used chrome containing refractory is easy dissolved in water and is then considered as a contaminant.

In steel and cement industries the process of replacement of that potential risk has already begun and chromium free solution have been successfully installed and proven. An effort to use new refractory with no health hazard in copper industry, as well, is needed, and has already started.

In this work, olivine has been selected as one of the possible new alternatives. Chemical compatibility of olivine with fayalite slag, as well as its very attractive price were the main factors considered in selection. Olivine as a solid solution of forsterite and fayalite should offer, a priori, good resistance to fayalite slag. Calcium ferrite slags, which are also in use in copper industry, will also be tested.

Current tendency in refractory applications is to use castables over bricks. Advantages like fast installation and possibility of local repairing lead to significant money saving. Castables unlike the bricks have no joins – the easiest path for possible penetration causing significant damage of refractory lining. Therefore part of this work is focusing upon castables, their design and characterization.

The essential part of this work has been to study the olivine-MgO refractory, their interaction with fayalite and calcium ferrite slags and to determine their corrosion resistance against those slags.

Four olivine-MgO castables (C-2, 3, 4 and 5) with graded olivine/MgO mutual proportion have been prepared and undergone corrosion testing at 1400°C for 8 hours. A

magnesia-chrome brick (REF) as a reference and a commercial olivine-based castable (C-1) as an additional reference were involved in the corrosion testing. Rotary slag test was chosen to evaluate those five castable and magnesia-chrome brick in order to determine their corrosion wear in fayalite and calcium ferrite slags. Then rates of dissolution-erosion as well as maximum penetration depth were measured and used to evaluate the corrosion resistance in the slags.

With each slag, a test with the same configuration of specimens was repeated three times. Comparing the results obtained from those tests has shown that reproducibility of the corrosion test was satisfactory.

As for dissolution-erosion is concerned, the magnesia-chrome brick (REF), as expected, has shown the best performance in both slags. A tendency in decreasing the dissolution-erosion rate with increasing of amount of MgO in castable was observed in all 3 tests in fayalite and 3 tests in calcium ferrite slags. Castable C-5 containing of 60% of MgO has got close to reference magnesia-chrome brick. Possible improvement on C-5 is foreseeable in a very near future. In all six cases, the same ranking REF > C-5 > C-4 > C-3 > C-1 >C-2 has been observed.

As far as penetration is concerned, the tested olivine-MgO castables (C-2, 3, 4 and 5) have been penetrated only up to 1 mm in both slags. A self-protecting mechanism as a result of the castable-slags interactions keeps the penetration at a very low level.

As a whole this work has revealed that olivine based castables enriched with magnesia, do offer a valuable potential, worthwhile to explore further.

# ***RÉSUMÉ***

Les réfractaires de magnésie-chrome sont très couramment utilisés dans l'industrie du cuivre, et ce depuis plus de 50 ans. Leurs excellentes performances vis à vis des scories, principalement les scories fayalitiques expliquent à elles seule cette situation. La menace grandissante contre ce quasi monopole vient de considération environnementaliste. La formation d'ion $Cr^{+6}$, avec ses conséquences cancérigènes, sont bien connues. Les ions $Cr^{+6}$ présents dans les briques de magnésie-chrome usagées se dissolvent facilement dans l'eau et ceux-ci sont considérés comme des contaminants majeurs.

Dans l'industrie des aciers et des ciments le processus de remplacement des « magnésie-chrome » pour pallier à ce risque est en bonne partie complet; les solutions « sans-chrome » sont en place. Des efforts pour utiliser de nouveaux réfractaires, sans risque au point de vue de la santé publique, sont entamés dans l'industrie du cuivre, mais les taux de substitution sont encore faibles.

Dans ce travail, des matériaux à base d'olivine ont été évalués. La compatibilité chimique de l'olivine avec les scories fayalitiques, de même que le coût raisonnable de ce minéral, ont été les principaux facteurs pris en compte, dans ce choix. L'olivine, une solution solide de forsterite et de fayalite devrait avoir, a priori, une bonne résistance à l'attaque des scories fayalitiques. Comme les scories à base de ferrite de calcium deviennent de plus en plus utilisées, elles seront aussi utilisées dans ce projet.

Une autre tendance lourde c'est l'utilisation de plus en plus fréquente des réfractaires non-façonnés, qui remplacent les réfractaires façonnés, c'est-à-dire les briques. Les avantages des non-façonnés sur les façonnés se situent au niveau de l'installation et des possibilités de réparation, deux facteurs économiques importants. Les non-façonnés sont dits monolithiques, c'est-à-dire sans joints (entre les briques) qui sont des inconvénients vis à vis de la pénétration des métaux dans les parois. Dès lors, le

choix dans cette thèse, de se centrer sur la mise au point et la caractérisation de bétons réfractaires à base d'olivine apparaît tout à fait justifié.

La partie essentielle de ce travail a donc été d'étudier le comportement de réfractaires à base d'olivine et de magnésie, de préciser les interactions de ces deux minéraux avec des scories de fayalite et de ferrite de calcium et de mesurer la résistance de tels bétons réfractaires à la dégradation dans de telle scories.

Quatre bétons d'olivine-magnésie (C-2, 3, 4 et 5) avec des proportions graduelles d'olivine-magnésie ont été préparés et soumis à l'action des scories, à 1400°C pendant 8 heures. Une brique de magnésie-chrome et un béton commercial d'olivine ont été choisis comme matériau de comparaison. Les essais de corrosion ont été effectués dans un four rotatif. Des mesures de taux de dissolution-érosion et de pénétration ont été effectuées pour évaluer la résistance à la corrosion de ces produits vis à vis des scories.

Les essais de corrosion, avec chaque scorie, ont été répétés trois fois, dans les mêmes conditions expérimentales. Les résultats obtenus ont démontré que ces résultats sont reproductibles.

Pour la dissolution, la brique de référence des magnésie-chrome est demeurée supérieure aux bétons d'olivine-magnésie. Pour les bétons, une quantité croissante de magnésie est bénéfique, et ce pour les deux scories traitées. C'est donc le béton contenant le plus de magnésie 60% (37% d'olivine) qui dans les 4 bétons testés est le plus performant. Des améliorations à ce béton sont encore possible.

Pour la pénétration, tous les bétons à base d'olivine et de magnésie offrent un net avantage sur la brique de magnésie-chrome. Un mécanisme d'auto-protection, résultant des interactions béton-scorie, permet d'obtenir des taux de pénétration à un niveau très faible.

Dans l'ensemble, il a pu être établi, sur une base expérimentale, que les bétons à base d'olivine enrichis de magnésie, offrent un bon potentiel, qui mérite d'être exploré davantage.

# *TABLE OF CONTENT*

**ACKNOWLEDGEMENTS**.....iv

**ABSTRACT**.....v

**RÉSUMÉ**.....vii

**TABLE OF CONTENT**.....ix

**LIST OF TABLES**.....xi

**LIST OF FIGURES**.....xiii

**LIST OF APPENDIXES**.....xv

**INTRODUCTION**.....1

**CHAPTER I - ON THE DESIGN OF THE REFRACTORY CASTABLES**.....7

1. PARTICLE PACKING.....7
2. FACTORS INFLUENCING PROPERTIES OF CASTABLES.....10
3. TECHNIQUES TO MEASURE PROPERTIES OF CASTABLES.....12

**CHAPTER II - ON MAKING THE OLIVINE CASTABLES – PRELIMINARY WORK**.....17

1. DESCRIPTION OF RAW MATERIALS USED.....17
2. DISPERSANTS TESTING.....21
3. MgO - ADDITION TO THE CASTABLE.....23
4. CHARACTERIZATION OF THE TESTED CASTABLE AND REFERENCE BRICK.....27

**CHAPTER III - ON CORROSION TESTING**.....29

1. EXPERIMENTAL SETUP.....30
   1.1. EQUIPMENT.....30
   1.2. SPECIMEN PREPARATION.....31
   1.3. CONFIGURATION OF THE TESTED SPECIMENS.....32
   1.4. SLAGS.....33
2. PROCEDURE.....33
3. DETERMINATION OF DISSOLUTION – EROSION AND PENETRATION RATES.....35

**CHAPTER IV - EXPERIMENTAL RESULTS**.....37

1. DISSOLUTION – EROSION.....37
2. PENETRATION.....44
   2.1. VISUAL OBSERVATION.....44
   2.2. OPTICAL MICROSCOPY.....46

**CHAPTER V - INTERPRETATION AND DISCUSSION**.....52

1. OLIVINE CASTABLE IN FAYALITE AND CALCIUM FERRITE SLAG.....52
   1.1. MgO - FAYALITE SLAG.....54
   1.2. FORSTERITE - FAYALITE SLAG.....56
   1.3. MgO - CALCIUM FERRITE SLAG.....58
   1.4. FORSTERITE - CALCIUM FERRITE SLAG.....59
2. GENERAL DISCUSSION.....62

CHAPTER VI - CONCLUSIONS AND RECOMMENDATIONS.....66

REFERENCES.....70
APPENDIX I.....73
APPENDIX II.....85
APPENDIX III.....87
REFERENCES FOR APPENDIX.....90

# LIST OF TABLES

***Table 1:*** Chemical composition of olivine used.....16

***Table 2***: *Sieve analyses of received olivine fractions 1-5mm, 0.5-2mm, AFS 50 and AFS 120*.....19

***Table 3:*** Chemical composition of used MgO as aggregate and MgO for matrix.....19

***Table 4:*** Chemical analyses of the Elkem Microsilica grade 971.....20

***Table 5***: Composition of the castable used to select the dispersant.....22

***Table 6:*** Flowability of the castable tested with 5 different dispersants after 30 seconds of vibration with amplitude of 0.4mm.....23

***Table 7***: Composition of the castables with comparative Olivine/MgO ratio.....25

***Table 8***: Rheological, physical and mechanical properties of the castables with comparative olivine/MgO ratio dried and fired at 1450°C/6hrs .....26

***Table 9***: Flowability of the commercial castables depending on water addition.....27

***Table 10:*** Chemical composition of testing castables.....27

***Table 11:*** Characteristics of the castables selected for rotary slag corrosion test in fayalite and calcium ferrite slags .....28

***Table 12:*** Chemical composition and relevant physical and mechanical properties of the magnesia-chrome brick – REXAL 60DB .....28

***Table 13:*** Chemical composition of the testing fayalite and calcium ferrite slags .....33

***Table 14*** Values of dissolution-erosion as measured and calculated, averages and standard deviations for fayalite slag .....43

***Table 15***: Values of dissolution-erosion as measured and calculated, averages and standard deviations for calcium ferrite slag .....43

# LIST OF TABLES IN APPENDIX I

***Table 16:*** Chemical analyses of some commercial olivine (%).....**74**

***Table 17:*** Physical properties of olivine.....**76**

# LIST OF TABLES IN APPENDIX III

***Table 18***: Calculation Packing Density using Andreasen Formula for coefficient n=0.26, 0.27 and 0.28.....**87**

***Table 19:*** Depth of dissolution-erosion mass of REXAL 60 DB in 9 tests in Fayalite slag/1400°C/8hrs.....**88**

***Table 20:*** Depth of dissolution-erosion mass of REXAL 60 DB in 9 tests in Calcium Ferrite slag/1400°C/8hrs.....**89**

# LIST OF FIGURES

**Figure 1:** Grain size distribution curves for the three equations with different coefficient "n".....9

**Figure 2:** A flow measurement as described in ASTM C1445 has been accomplished by using the flow cone on vibration table.....14

**Figure 3:** Determination of cold modulus of rapture.....15

**Figure 4**: Sieve analyses of received olivine fractions 1-5mm, 0.5-2mm, AFS 50 and AFS 120.....18

**Figure 5:** The rotary slag testing equipment – a general view .....28

**Figure 6:** Heating program for the castable specimens prior to rotary slag test, and determination of physical properties .....31

**Figure 7**: Shape and dimensions of a test specimen for rotary slag test .....32

**Figure 8:** Configuration of 6 test samples .....32

**Figure 9:** The rotary slag testing furnace – a longitudinal section view .....31

**Figure 10**: Rotary slag test – time/temperature evolution .....35

**Figure 11:** Way to determine of corrosion resistance of samples (penetration and dissolution-erosion).....36

**Figure 12**: Averages of dissolution – erosion rates of samples tested at 1400 °C for 8 hours in fayalite slag over three tests .....38

**Figure 13**: Averages of dissolution – erosion rates of samples tested at 1400 °C for 8 hours in calcium ferrite slag over three tests .....38

**Figure 14**: Contribution of MgO additions to the total dissolution-erosion rate in fayalite *slag* .....39

**Figure 15**: Contribution of MgO addition to total dissolution-erosion rate in calcium ferrite slag .....40

**Figure 16**: Apparent porosity of the castables after firing at 1450°C/8 hrs .....41

**Figure 17**: Dissolution-erosion rates of three tests in fayalite slag .....42

**Figure 18**: Dissolution-erosion rates of three tests in calcium ferrite slag .....42

**Figure 19:** Depth of penetration as determined macroscopically for samples tested in fayalite slag at 1400°C for 8 hours .....45

**Figure 20**: Depth of penetration as determined macroscopically for samples tested in calcium ferrite slag at 1400°C for 8 hours .....45

**Figure 21:** Apparent (macroscopically) versus microscopically determined penetration in fayalite slag, at 1400°C for 8 hours .....46

**Figure 22**: Apparent (macroscopically) versus microscopically determined penetration in calcium ferrite slag, at 1400°C for 8 hours .....47

**Figure 23**: Olivine grain in contact with fayalite slag .....47

**Figure 24**: Samples after 8 hrs in fayalite slag at 1400°C.....49

**Figure 25**: Samples after 8 hrs in calcium ferrite slag at 1400°C.....50

**Figure 26:** Olivine-MgO-$SiO_2$ proportion of the commercial (C-1) and CIREP's castable (C-2 and C-3).....51

**Figure 27:** The FeO-MgO phase diagram.....54

**Figure 28**: MgO - fayalite slag interface after rotary slag test at 1400°C/8hrs, 20x.....55

**Figure 29**: The FeO-$SiO_2$-MgO system.....56

**Figure 30:** Forsterite-Fayalite phase diagram.....57

**Figure 31:** Olivine – fayalite slag interaction after rotary slag test at 1400°C/8hrs, 20x.....57

**Figure 32**: The CaO – MgO - $Fe_2O_3$ phase diagram.....58

**Figure 33:** The $SiO_2$ – CaO – MgO – $Fe_2O_3$ system.....58

**Figure 34:** MgO – calcium ferrite slag interaction after 1400°C/8hrs, 20x.....59

**Figure 35:** Olivine in contact with calcium ferrite slag, 20x.....60

**Figure 36**: Reaction layer between olivine grain and calcium ferrite slag, 100x.....**61**
**Figure 37**: MgO and olivine grains in contact with fayalite slag, 20x.....**63**
**Figure 38**: MgO and olivine in contacts with Fayalite slag, 5x .....**64**
**Figure 39**: Features of olivine – MgO – fayalite slag interactions .....**65**
**Figure 40**: Features of olivine – MgO – calcium ferrite slag interactions.....**65**

## *LIST OF FIGURES IN APPENDIX I*

***Figure 41:*** Binary system forsterite ($Mg_2SiO_4$) – fayalite ($Fe_2SiO_4$) as a solid solution with unlimited mutual solubility.....**73**
***Figure 42***: The Binary system MgO – $SiO_2$ after Bowen and Anderson [35].....**78**

# ***LIST OF APPENDIXES***

APPENDIX I.....**73**
APPENDIX II.....**85**
APPENDIX III.....**87**

# ***INTRODUCTION***

In this introduction the main words in the title will be explained; then the goal and objectives as well as the scope of the experimental work are being presented.

This thesis is about olivine. ***Olivine*** is greenish magnesium silicate mineral more precisely solid solution of forsterite and fayalite with a very high melting point, heaving high magnesia content, excellent heat-storage properties due to its relatively high density. Olivine is chemically stable and olivine products can be handled without any health' hazard. Forsterite is represented by its formula $Mg_2SiO_4$, corresponding to 57,3 % magnesia (MgO) and 42.7 % silica ($SiO_2$). Fayalite, $Fe_2SiO_4$, contains only 29.49 % silica ($SiO_2$).

This thesis is about olivine castables. ***Castables*** are hydraulically bonded monolithics or unshaped refractories; others unshaped refractory materials are ramming mixes, plastics, mortars, gunning mixes. Castables are fabricated and supplied usually as mixes ready for the application; only a specific amount of water has to be added to the dry mixture, and after mixing, the castable can be installed. Simple casting technique can be used for the installation of conventional castables, together with some vibration technique (of the mold or in the mold).

The evaluation of the olivine castables, which have been elaborated, is mainly based upon ***corrosion testing***. Numerous methods have been tried and some reasonable correlations have been obtained for very specific conditions, but very few methods have reached the status of standard operating practices and non have yet been accepted for universal use.

The main reason is that corrosion resistance rate obtained in a laboratory environment very rarely simulate the conditions that prevail in service: sample size and geometry, state of stresses in the lining, thermal gradient and thermal cycling, as well as time, which are very difficult to be scaled down to fit with acceptable laboratory test conditions. It must always be remembered that accelerated tests, especially those done using very severe conditions, can lead to erroneous predictions.

Compared with laboratory testing, field trial testing is, of course, much more costly, and, in some instances, unsafe. It may then be worthwhile to test small panels rather than to carry out full size testing; the larger the installation the more confidence one will have in the selection of the proper material to use.

The primary goal of this work is to induce the development of new refractory materials tailored-made to meet the needs of the copper producers in order:

i. To bring savings on refractory materials
ii. To adjust to the requirements imposed by new metallurgical process (changes in slag composition)
iii. To be able to offer more environmentally friendly solution, compared to magnesia-chrome bricks, where their disposal, as waste solid may become a very serious issue.

The objectives of this thesis are:

i. To initiate the development of monolithic refractories taking into consideration new systems: magnesia - forsterite, magnesia - spinel, magnesia - hercynite instead of magnesia – chrome
ii. To select the most proper testing method for that refractory and verify reproducibility of the results
iii. To test and evaluate those unshaped refractory materials in comparison with magnesia-chrome brick presently the most used refractory in copper industry
iv. To evaluate and compare the performances of refractory materials against fayalite and calcium ferrite slags

The general context, under in which this work has been done, is as follows. The specific consumptions of refractory materials in the steel, the cement, the glass industry have decreased respectively from 20kg/ton to 10kg/ton, 2kg/ton to 1kg/ton, 8kg/ton to 4kg/ton during the last 20 years [1] through a series of improvements in the material (new bricks, new monolithic) in the installation method (self-flow then shotcreted castables) and in the process control (standardization of the key input variables). In the copper industry, mag-chrome bricks have been in use for more that 50 years. It is true to say that an impressive evaluation in mag-chrome bricks have been made during that intervals from silicate bonded or chemically bonded bricks, to the direct – bonded bricks, using co-clinkers and fused-grains [2-6], but the specific consumption in kg of refractories per ton of copper, has not decreased as significantly as in other industries. Mag-chrome bricks in the steel industry have been displaced by more performing products in most

units. Mag-chrome bricks in the cement industry have been displaced by doloma and magnesia-spinel for both improved performances and environmental concerns.

In copper industry, some magnesia-spinel bricks are used but adjustments to use the appropriate spinel grains (magnesia-rich) or other new spinel (hercynite) are slow to come about. Several corrosion test results on magnesia-spinel bricks in contact with fayalite slag have been reported [7-11], and comparison with mag-chrome bricks are well documented; many papers [12-17] have pointed out, that apart from the erosion by fayalite slag, the role of the penetration of metallic copper and copper compounds (oxide, sulfide) into the bricks are dominant factors to account for the wear and degradation of refractories. This has been documented in several post-mortem analyses [18].

The inherent penetration, which occurs, causes spalling and slabbing. It has to be remembered that one of the easiest and fastest paths for deep penetration in the refractory lining are the joints between bricks, and the second important paths are the cracks generated by thermal and thermo-mechanical stresses. Adjustment of the permeability of the bricks, of the micro-texture and of the composition of the matrix materials (the bonding phases and the additives to act as getter) are key issues to design new refractories suited for the copper industry. In this thesis two different themes are developed.

The first theme is centered on the making of proper castables. It is to be underlined that today, more than 60% of the refractory materials used in steel industry in developed countries are unshaped rather than bricks. The advantages to use castables normally include:

i. Easier and faster installation, mainly now since the shotcreting technique has been well developed, using the industrial experience which already exist in other fields of application (civil construction, tunneling);
ii. Less penetration (less joints in lining, lower permeability in low and no-cement castables as compare to bricks);
iii. Easier repair and veneering, minimizing waste solid disposal;
iv. Easier to manufacture large pre-cast blocks, partially or totally pre-fired,
v. Possibility to use steel-fibers reinforcement to improve the wear-resistance of the refractory materials in zones subjected to intensive thermal and mechanical abuses.

The combined application of bricks with castables is meant to bring cost saving mainly because of the labor-saving and cutting down the time for repairs, reducing the refractory consumption by using veneering technique and making overall the operation smoother without long-time delays for bricks lining.

The second is about the use of calcium ferrite slags rather than fayalite slags. According to A. Yazawa [19] and L. Molnar et al. [20], the main advantages to use such slags should be:

- Better physical properties of the melt.
- Wider concentration field of melting.
- No problems with the formation of magnetite.
- Lower loss of copper in slags.
- Less aggressive slag against basic refractories.

In terms of selection of the most appropriate refractory materials, it is clear that the alumina-based refractories which are not suited for fayalite slags, could be acceptable for calcium ferrite slags

In this thesis, materials to be tested are cement free castables made of olivine and magnesia additions. Two sources of olivine have initially been tested; at the end only one source was considered. Apart from magnesia, initially other additions were considered - hercynite and zircon but at the end only magnesia was considered.

# CHAPTER I

## ON THE DESIGN OF THE REFRACTORY CASTABLES

Design of a castable involves steps, which will rule out final properties of the castables. Final characteristics of the castable directly depend mainly on grain size distribution, dispersants and retarders used to make the castable. Water addition is also critical and has to be determined precisely to get a sufficient amount to wet surface of the smallest particles and to react with binder to provide strength at room temperature. The basic principles of design as well as measuring of the main characteristics of castables are described further.

### 1. PARTICLE PACKING

The packing of particles is a subject of both theoretical and practical interest in a vast number of technical disciplines. If powder packing efficiency can be maximized, the apparent volume of the powder compact is minimized and solids loading is maximized.

The high packing density of cast body is achieved by the proper, graded grain sizing of particles (aggregates and matrix) up to the finest particles in the mixture (matrix).

It is known that the maximum solid content of monospheres (spheres of the same size), in a cube, is 74.05%. Using different size of monospheres, it is possible to achieve much higher densities, (by filling the spacing between large particles with smaller particles), and such experiments have been done. Although, these experiments have shown that the packing densities achieved in practice was always lower than the calculated ones.

There are many reasons to explain such results:

- Each particle in a mixture should be in its proper position; the internal friction among the smallest particles prevents them to reach the optimum position
- The shape of real particles in not uniform and spherical
- The number of different fractions, used in practice, is limited
- The smallest particles are always more or less flocculated, and form aggregates

In practice, for the calculation of the optimum packing density of the particular mixture, composed of the definite number of fractions, the following formulas are used:

FURNAS

$$\frac{CPFT}{100} = \frac{r^{\log D} - r^{\log D_S}}{r^{\log D_L} - r^{\log D_S}} \qquad (1)$$

Where: - *CPFT* – is the cumulative percentage of particles finer than....

- $r$ – is the ratio of volume of particles on one sieve to the volume on the next smaller sieve
- D – is the upper limit size of particles of a fraction
- $D_S$ – is the size of the smallest particles in the mixture
- $D_L$ – is the size of the largest particles in the mixture

ANDREASEN

$$\frac{CPFT}{100} = \left(\frac{D}{D_L}\right)^n \qquad (2)$$

MODIFIED ANDREASEN

$$\frac{CPFT}{100} = \frac{D^n - D_S{}^n}{D_L{}^n - D_S{}^n} \qquad (3)$$

Generally, the acceptable range of n values (for both equation) is around $^1/_3$, but in the case of castables values lower than $^1/_3$ are used. ***Figure 1*** shows the calculated grain size distribution curves for the three equations.

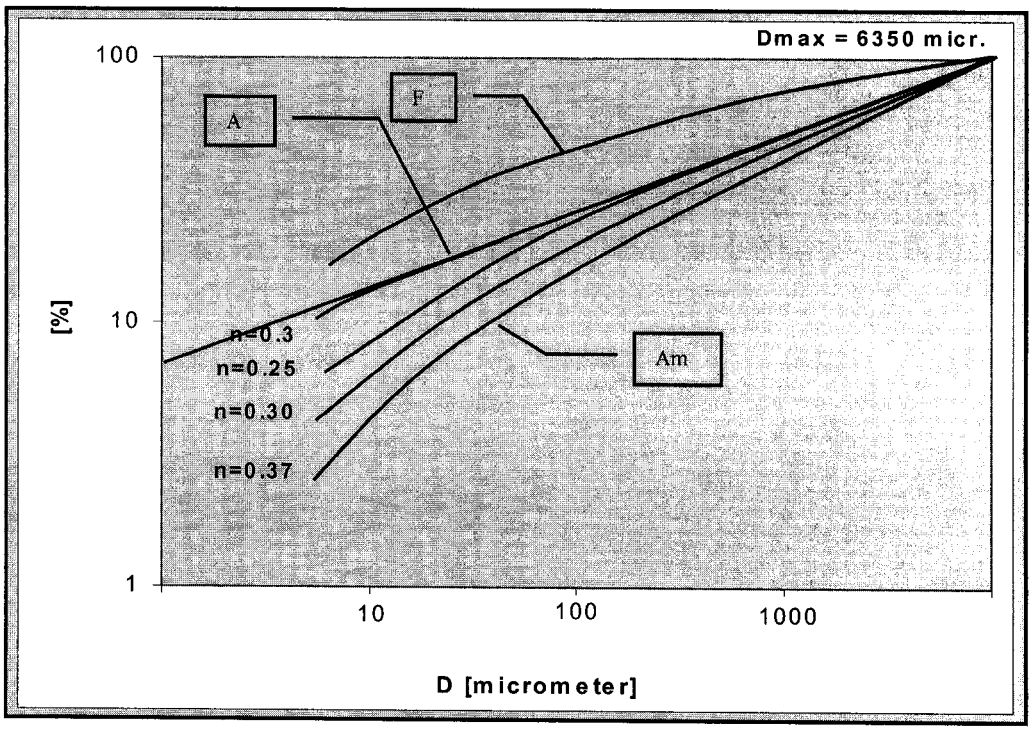


***Figure 1***: *Different grain size distribution curves derived from Furnas or Andreasen equations.*

For castables, mostly continuous sizing is used, to achieved a proper flowability of the mixture, and minimize the segregation.

For instance, the mixture is composed of 4 - 6 particular grain size ranges, with continuous sizing, e.g. 4 - 6mm, 2 – 4mm, 0.5 – 2mm, 0.1 – 0.5mm, 0.04 – 0.1mm, -

0.04mm. Though, quite often, particular fractions overlap each other so after calculation some corrections have to be done.

## 2. ***FACTORS INFLUENCING PROPERTIES OF CASTABLES***

Workability of a castable is affected in a great measure by the gralnulometry of the dry mixture. The proper sizing of aggregates, as well as the finest (matrix) is very important. For the calculation of the grain size distribution, one of the previously described models is used, but the optimum composition has to be always determined experimentally. To prevent the segregation, usually continuous curves are utilized.

Additives - ***dispersants***, which control the deflocculation of the smallest particles, have to be added, because they control the viscosity of the system. The setting of the binder during the mixing is not desirable. It can be controlled by addition of ***retarders.*** The temperature can also play an important role, since at higher temperatures (25 to 35°C) the chemical and physical processes responsible for the setting are accelerated.

There are many factors that can affect the porosity of the castable, and both the manufacturer and the user can influence it. The packing density after casting depends on the granulometry of the mixture, and the processing parameters such as: mixing, water addition, and installation. The proper mixing influences the rheology of the mixture after the water addition. If the time is too short, the homogeneity of the mixture is not appropriate. That is reflected by higher viscosity, while prolonged mixing can cause, when too much energy of mixing is introduced in the system, premature setting, which also leads to the deterioration of the rheological properties and consequently the porosity of the casted body.

The ***water amount*** added to the dry mixture is the most critical. The amount has to be sufficient for the reaction with a binder, and for covering the surface of fine particles, to control the fluidity of the system. Each quantity contributes more or less to the increasing of the porosity (less – the flowability of the mixture is not sufficient for the proper rearrangement of particles and the deaeration of the mixture; more – after drying, when the free water escapes, only pores can remain there).

The mostly used technique for installation of low moisture castable is vibration. The time, frequency and the amplitude of vibration are important. The time has to be sufficient for the rearrangement of particles and for the deaeration of the mixture, but not too long to avoid the segregation. As for the frequency, 50 Hz is recommended and the amplitude can be usually varied in the range of 1 mm up to approximately 3 mm.

It is obvious that the porosity is closely connected with the workability of the mixture, and so parameters, which control the workability, will also influence the porosity. The porosity of aggregates used in mixtures contributes to the total porosity of the castable, and at the same time affects the necessary mixing water demand. The porosity after heat treatment depends on another factors, as the formation of liquid phases, chemical reactions, relative thermal expansion of present phases, sintering of the matrix, and the formation of bonds among aggregates and fine particles of the matrix. The phenomenon is complex and each case is to be treated individually.

## 3. TECHNIQUES TO MEASURE PROPERTIES OF CASTABLES

Rheological, physical and mechanical behaviors are the main characteristics that characterize refractory castables.

*Flowability*, as an indicator of rightness of particle packing density, selection of a proper dispersant and determination of water addition, is an important property of the castables. *Apparent porosity, water absorption, apparent specific gravity, and bulk density* are primary properties of refractories shapes. These properties are widely used in the evaluation and the comparison of product quality and as part of the criteria for selection and use of refractory product in a variety of industrial applications

The *mechanical properties* have to be evaluated separately for room temperature, intermediate temperature (700 – 1200°C), and high temperature, when intensive sintering process occurs.

The strength after drying is determined mainly by the bonding system and the amount of binder, as well as the particle sizing (particle size distribution, max and min size) and consequently the porosity. The strength at room temperature has to be sufficient to allow the casted shape to be demolded. In most cases, it does not have any connection with the strength at intermediate and high temperatures. The strength at intermediate temperature depends mostly on the character of binder, the initial content of the binder and the packing density of the mixture. Generally, the higher initial content of the binder the lower the packing density, the higher drop of the strength at intermediate temperature can be expected. Hydraulic bonds decompose in the interval between 500 and 800°C and the castable in this temperature range will loose its strength. Phosphate bonds, on the other hand, are stable at those temperatures, because the products of the chemical reactions, formed in the setting process, do not decompose.

The strength at high temperatures is given by the ceramic bonding, which is the result of sintering processes. The high-temperature strength is affected mainly by the porosity, which reflects the number of mutual contacts (or bonds) among particles (with lower porosity, higher strength can be expected). The phase composition at high temperature determines the amount of the liquid phase in the system, as well as the quality of phases boundaries. This is the factor that affects the high-temperature strength predominately. It is very important to pay attention, when the composition of the castable has to be designed, to the proper choice of the raw materials and the binder, considering the possible reaction products and eutectics formed at temperatures of service.

Transition from dry castable to fired one brings some dimensional changes that can cause partial or more significant damage of the refractory lining. Dimensional shrinkage or expansion is common in case of unshaped refractories and has to be determined to make the characterization of the castable completed. *Permanent linear change - PLC* is the accepted measure to characterize such a behavior.

- **FLOWABILITY**

Flow measurements are accomplished using a flow cone a described in ASTM Standard C1445. The testing has been performed on a vibration table set at amplitude of 0.4 mm. The cone is filled up with castable, vibration table is activated and than the cone is removed; the castable is subjected to vibration for 30 seconds as defined in ***Figure 2***, diameter - $D_2$ of the "pancake-castable" is measured with a caliper and value of the flowability determined according to following formula **(4):**

$$flowabilit\ y[\%] = \frac{D_2 - D_1}{D_1} \times 100 \qquad (4)$$

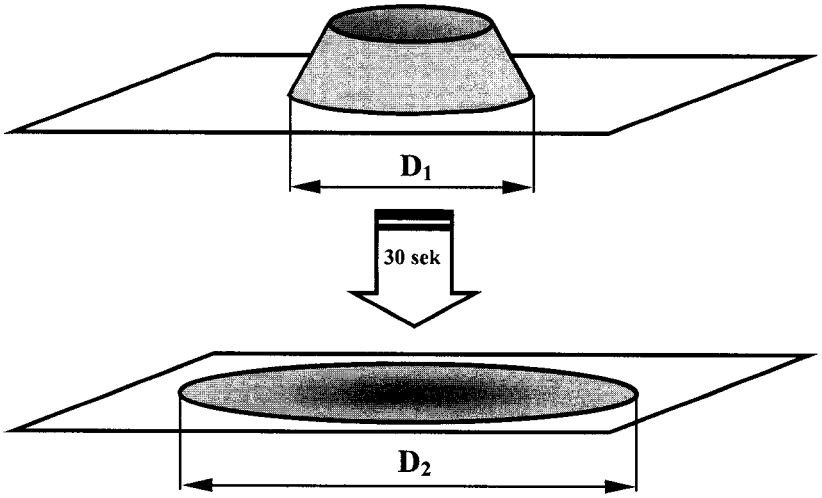


***Figure 2:*** *A flow measurement as described in ASTM C1445 has been accomplished by using the flow cone on vibration table.*

- **APPARENT POROSITY – *A.P.***

The apparent porosity expresses, as a percentage, is calculated as follows:

$$A.P.[\%] = [\frac{W-D}{V}] \times 100 \qquad (5)$$

Where: **D** – dried weight

**V** – exterior volume

**W** – water absorbed weight

- **WATER ABSORPTION – W.A.**

The water absorption expresses, as a percentage, the weight of water absorbed to the weight of the dry test specimen.

$$W.A.[\%] = [\frac{W-D}{D}] \times 100 \qquad (6)$$

- **BULK DENSITY – B.D.**

The bulk density of the test specimen in grams per cubic centimeter is the ratio of its dry weight divided by its exterior volume.

$$B.D.[g/cm^3] = \frac{D}{V} \tag{7}$$

- **COLD MODULUS OF RAPTURE – CMOR**

Determination of CMOR is carried put according to ASTM Standard C133 as shown at ***Figure 3*** than calculated according to formula ***(8)***.

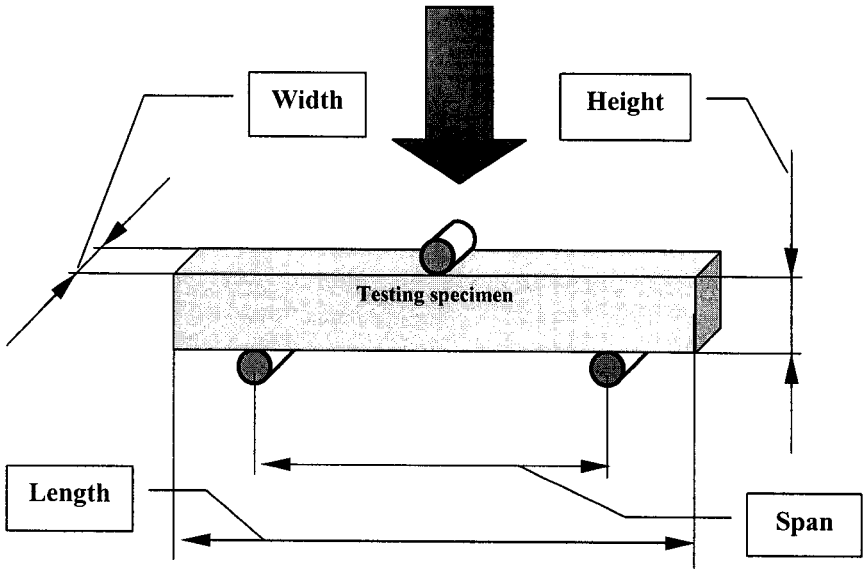


***Figure 3:*** *Determination of cold modulus of rapture*

$$CMOR[MPa] = \frac{3}{2} \times \left( \frac{F * l}{w \times h^2} \right) \tag{8}$$

Where: F - load, l – span, w – width, h – height

- **PERMANENT LINEAR CHANGES**

Permanent linear changes of the castables depicted in % are determined by measurement of samples in dried and in fired conditions and calculated by following formula:

$$PLCH[\%] = \frac{length_{dried} - length_{fired}}{length_{fired}} \times 100 \qquad (9)$$

# CHAPTER II

## ON MAKING THE OLIVINE CASTABLES – PRELIMINARY WORK

As mentioned before, olivine-based refractory were considered as one alternative to at least compete with magnesia-chrome bricks.

Initial idea to test olivine-based castable with copper making slags comes from the fact that fayalite slag is quite often used in copper making units, and olivine, being a solid solution of fayalite and forsterite, should be compatible.

Olivine castables, which have been designed and prepared, were composed of two major constituents: olivine and MgO. The objective of this preliminary work was to develop olivine - MgO castable of acceptable rheological, physical and mechanical properties from the installation point of view and make a selection of some of them to test their corrosion resistance.

### 1. DESCRIPTION OF RAW MATERIALS USED

The castables were basically made of olivine and MgO as major components with addition of 3% of microsilica as the finest fraction. Dispersant, retarder and water have been naturally used as well to develop the castables.

#### OLIVINE

The chemical composition of the olivine is depicted in ***Table 1***. The olivine comes from Norway (the biggest world source), from company Olivine A/S.

***Table 1:*** *Chemical composition of olivine used.*

| $MgO$ | $SiO_2$ | $Fe_2O_3$ | $Cr_2O_3$ | $Al_2O_3$ | $MnO$ | $CaO$ |
|---|---|---|---|---|---|---|
| 49.3 | 42 | 7.32 | 0.32 | 0.35 | 0.1 | 0.07 |

Olivine fractions of 1-5mm, 0.5-2mm, AFS 50 and AFS 120 have been received and by crushing and sieving prepared as needed. Sieve analyses of the 4-olivine fractions are shown in ***Figure 4*** and ***Table 2***.

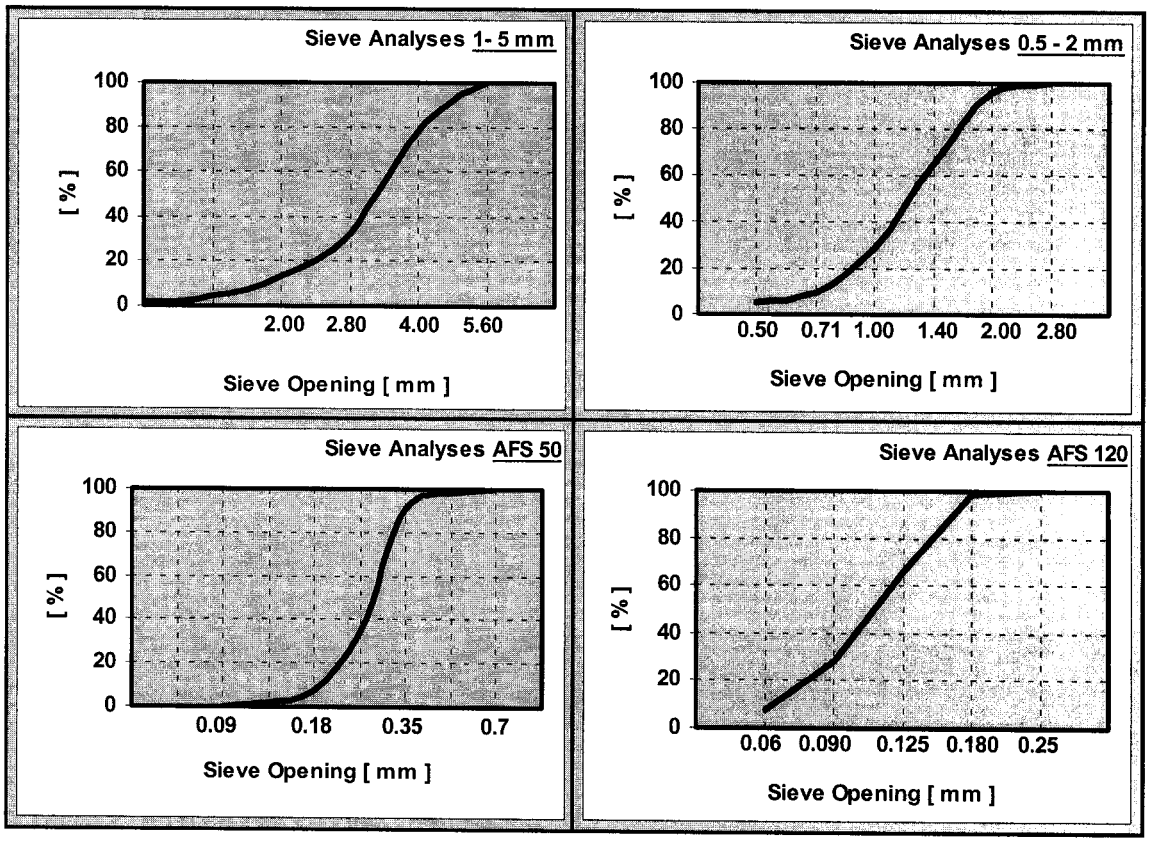


***Figure 4****: Sieve analyses of received olivine fractions 1-5mm, 0.5-2mm, AFS 50 and AFS 120*

***Table 2***: *Sieve analyses of received olivine fractions 1-5mm, 0.5-2mm, AFS 50 and AFS 120*

| 1 - 5 mm | | 0.5 - 2 mm | | AFS - 50 | | AFS - 120 | |
|---|---|---|---|---|---|---|---|
| [mm] | Typical [%] | [mm] | Typical [%] | [mm] | typical [%] | [mm] | Typical [%] |
| 5.6 | 0 | 2.8 | 0 | 1.000 | 0 | 0.250 | 0 |
| 4.0 | 22 | 2.0 | 2 | 0.500 | 0.8 | 0.180 | 0.5 |
| 2.8 | 46 | 1.4 | 28 | 0.355 | 8 | 0.125 | 35 |
| 2.0 | 20 | 1.0 | 40 | 0.250 | 54 | 0.090 | 39 |
| 1.0 | 10 | 0.7 | 20 | 0.180 | 27 | 0.063 | 18 |
| -1.0 | 0 | 0.5 | 5 | 0.125 | 7 | -0.630 | 8 |
| | | -0.5 | 5 | 0.900 | 2 | | |
| | | | | -0.900 | 0.6 | | |

Some of the fractions have been used as received but most of them have been prepared by crushing and sieving form those four. The finest fraction of –0.045 mm was prepared by crushing of higher fraction (AFS 50) in ball mill (attritor) and the granulometry was determined by COULTER LS 200. An amount of 400g of olivine of fraction 0.3mm and 250 ml of water was used for each crushing procedure. After 20 minutes of crushing at 400rpm crushed olivine was removed and dried in a drier at 110°C for 12 hrs. **(MORE ABOUT OLIVINE IN APPENDIX I)**

## MAGNESIA

MgO has been used as either aggregate or fine particles in matrix. As far as corrosion resistance of the castable against slag is concerned matrix plays the key role. Therefore MgO (Ludington 98 – BMF) of higher purity has been preferentially used in matrix and MgO (RY 99AD) of purity 97.6% with slightly higher content of CaO as aggregates in the castables. Chemical analyses of both are shown in ***Table 3.***

***Table 3:*** *Chemical composition of used MgO as aggregate and MgO for matrix.*

| | | | | | | |
|---|---|---|---|---|---|---|
| AGGREGATES (RY 99AD) | 97.6 | 0.15 | 0.17 | 0.13 | 1.05 | 0.18 |
| MATRIX – LUDINGTON 98 - BMF | 98.13 | 0.66 | 0.14 | 0.08 | 0.91 | - |

All fractions (3.35-5mm, 1.7-3.35mm, 0.3-1.18mm, 0.2-0.5mm, 0.06-0.2mm and BMF of 75μm) needed to compose the castable as will be shown further were available and were used as received. **(MORE ABOUT MgO IN APPENDIX I)**

## MICROSILICA

Elkem - microsilica of the chemical composition depicted in ***Table 4*** has been used as the finest particles in the olivine – MgO castable. The average diameter of microsilica is about 0.15 micron. Although some of the silica spheres exist as single entities, most of them are sintered together during production to form primary agglomerates. The sizes of these vary between 0.1 and 1 micron.

***Table 4:*** *Chemical analyses of the Elkem Microsilica grade 971*

| [%] | | | | | | | | | | | |
|---|---|---|---|---|---|---|---|---|---|---|---|
| $SiO_2$ | C | $Fe_2O_3$ | $Al_2O_3$ | CaO | MgO | $K_2O$ | $Na_2O$ | $P_2O_5$ | $SO_3$ | Cl | $H_2O$ |
| 97.5 | 0.5 | 0.1 | 0.4 | 0.2 | 0.1 | 0.3 | 0.1 | 0.1 | 0.1 | 0.1 | 0.4 |

## DISPERSANTS

The following 5 dispersants have been selected and involved in the preliminary study:

- *DARVAN 811D* – 2-Propenoic acid, 2-methyl-, polymer with 2-propenoic acid, sodium salt
- *CASTAMENT FS-10* – dispersant based on polyglykol
- *CASTAMENT FS-20* – polymeric dispersant based on polycarboxylates
- *Calgon* – Sodium hexa-metha-phosphate
- *Galoryl PA 120* – Sodium salt of sulfonic acid polycondensate

**RETARDER**

Sodium dihydrogencitrate 99% was always used in all castables at a level of 0.05% in weight percentage, based upon accumulated experience in CIREP's group.

## 2. *DISPERSANTS TESTING*

In order to make the selection of the proper dispersant for olivine-MgO castables with matrix composed of BMF-MgO, fine olivine and 3% of microsilica 5 dispersants have been tested.

Previous experience had indicated that for particle size distribution calculated using the Andreasen formula, a coefficient "n" between 0.26 – 0.29 gives an optimal packing of the grains and particles. With intended dealing with proportional MgO/olivine ratio (further will be engage with) a base castable composed of 70% of olivine, 28% of MgO and 3% of microsilica was proposed. According to our idea the matrix should contain in addition to microsilica also at least 15% of MgO –BMF (-75μm) and around 10 % of fine olivine. Following the intention in terms of amount of particular constituents composing matrix a castable of composition depicted in ***Table 18*** (***APPENDIX III***) was theoretically calculated. Eventually the final composition, depicted in ***Table 5,*** was adjusted to a theoretical one calculated using the Andreasen formula with coefficient **n = 0.27**.

***Table 5**: Composition of the castable used to select the dispersant.*

| Constituents of the tested castable | [%] |
|---|---|
| Olivine 3.35 - 6.3 mm | 13 |
| Olivine 1.7 - 3.35mm | 14 |
| Olivine 0.6 - 1.7mm | 18 |
| Olivine 0 - 2mm | 15 |
| Olivine – 0.075mm | 10 |
| MgO - 0.6mm | 10 |
| MgO – MBF | 18 |
| $SiO_2$ – microsilica | 3 |
| Tested Dispersant | 0.15 - 0.2 |
| Sodium dihydrogencitrate 99% | 0.05 |
| Water | 6% |

Total 5 dispersants (DARVAN 811D, CASTAMENT FS-10, CASTAMENT FS-20 in 0.15% in weight and Calgon and Galoryl PA 120 in 0.2% in weight in mutual combination) have been tested to determine their suitability for certain system of certain composition of matrix. Dispersants Calgon and Galoryl Pa 120 were used in combination with each other for well-known suitability of the Calgon for microsilica and Galoryl Pa 120 for fine MgO. 6% of water addition has been determined as optimal amount and kept in all four mixtures. The experiment was to find out the best dispersant for olivine-MgO castable or at least eliminate improper ones. Preparation procedures, like mixing time (8 minutes) and speed, adding of water to the dry mixtures, were identical in all cases.

Flowability of the mixtures, as an indicator of suitability of the dispersant for the particular castable, was measured (determined) immediately after mixing by way described earlier and their values depicted in ***Table 6*** are averages of 3 measurements of the same "pancake-castable"

***Table 6:*** *Flowability of the castable tested with 5 different dispersants after 30 seconds of vibration with amplitude of 0.4mm.*

| Dispersants | Flowability [%] |
|---|---|
| DARVAN 811D | 92 |
| CASTAMENT FS-10 | 61 |
| CASTAMENT FS-20 | 88 |
| Calgon + Galoryl | 88 |

As obvious from ***Table 6*** the dispersant DARVAN 811D has shown the best effect on the rheological behavior of the castable. Flowability in this case has reached value of 92%, which is promising for prospective application. **CASTAMENT FS-20** and **Calgon with Galoryl** in mutual combination each other have reached value of 88%, which is quite close to the **DARVAN 811D** and could be considered as **equal**.

## 3. *MgO - ADDITION TO THE CASTABLE*

Magnesia added to olivine (apart from filling need fraction in castables) fulfills following purposes:

- Transformation of the enstatite to forsterite

  $MgSiO_3 + MgO \Rightarrow Mg_2SiO_4$

- Formation of forsterite in-situ by reaction with microsilica in matrix

  $SiO_2 + 2MgO \Rightarrow Mg_2SiO_4$

- Binding of FeO to magnesio-wustitte (solid solution of MgO and FeO) or $Fe_2O_3$ to magnesio-ferrite ($MgFe_2O_4$)

  $FeO + MgO \Rightarrow (Mg, Fe)O$

  $Fe_2O_3 + MgO \Rightarrow MgFe_2O_4$

In addition, previous corrosion testing with samples composed of pure MgO have shown very good performance as for dissolution-erosion in both fayalite and calcium ferrite slag. But how much MgO addition to olivine castable should be and what contribution to corrosion resistance of olivine-MgO system would this bring was unknown matter.

Hence an olivine-MgO castable series with graded MgO/olivine ratio was tested for corrosion. Ratios of 5/92, 15/82, 30/67, 45/52, 60/37, 75/22 were chosen as the olivine/MgO ratio. 3% of $SiO_2$ (microsilica) was added to each mixture.

In total 6 fractions of olivine and 5 fractions of MgO have been tested. Since some of the fractions overlapped each other and that could not be involved into the theoretical calculation, a remedial grain size range (5mm, 2mm, 0.6mm, 0.2mm, 0.075mm) had to be used and then an adjustment to the real compositions was made as shown in ***Table 7***. Initial fraction proportions calculated using Andreasen formula with coefficient **n = 0.27**, are depicted in ***Table 17*** (**APPENDIX III**).

Compositions are expressed in weight percentage. Grain size distribution of the castables should have been calculated in volume percentage of particular fraction. However, specific gravity of the olivine and MgO (3.33 $g/cm^3$ and 3.6 $g/cm^3$ respectively) is close enough to each other, to consider their weight percentage for volume percentage as well.

***Table 7**: Composition of the castables with comparative Olivine/MgO ratio.*

| | | Ratio MgO/olivine | | | | | |
|---|---|---|---|---|---|---|---|
| | Fractions [mm] | 5/92 | 15/82 | 30/67 | 45/52 | 60/37 | 75/22 |
| Olivine | 2.00 - 5.00 | 22 | 22 | 22 | 22 | 7 | ~ |
| MgO | 3.35 - 5.00 | ~ | ~ | ~ | ~ | 7 | 10 |
| MgO | 1.70 - 3.35 | ~ | ~ | ~ | ~ | 8 | 12 |
| Olivine | 0.50 - 2.00 | 25 | 25 | 25 | 10 | 10 | ~ |
| MgO | 0.30 - 1.18 | ~ | ~ | ~ | 15 | 15 | 25 |
| Olivine | 0.20 - 0.50 | 12 | 12 | 7 | 6 | 5 | 4 |
| MgO | -0.3 | ~ | ~ | 15 | 15 | 15 | 15 |
| Olivine | 0.06 - 0.20 | 15 | 12 | 2 | 3 | 4 | 5 |
| MgO-BMF | -0.075 | 5 | 15 | 15 | 15 | 15 | 15 |
| Olivine | -0.02 | 20 | 11 | 11 | 11 | 11 | 11 |
| Castament FS-20 | | 0.15 | 0.15 | 0.15 | 0.15 | 0.15 | 0.15 |
| Citr Na 99% | | 0.05 | 0.05 | 0.05 | 0.05 | 0.05 | 0.05 |
| Water | | 6% | 6% | 6% | 6% | 6% | 6% |
| | Olivine | 92 | 82 | 67 | 52 | 37 | 22 |
| | MgO | 5 | 15 | 30 | 45 | 60 | 75 |
| | $SiO_2$ | 3 | 3 | 3 | 3 | 3 | 3 |

Initially *5/92, 15/82, 30/67, 45/52, 60/37, 75/22* MgO/olivine rations were fixed, and then calculated percentages were filled up with available or pre-prepared fractions to keep the ratios. Keeping the pre-defined amount of water (6%), dispersant (FS-20), retarders (Citr Na 99%), and identical mixing conditions (speed and time), influence of the different composition on the rheological behaviour of the castable as well as their physical properties were determined. Since, olivine and MgO grains have different shapes, changing the olivine/MgO ratio causes some differences in rheology of the mixture and subsequently in physical properties as shown in ***Table 8***.

***Table 8**: Rheological, physical and mechanical properties of the castables with comparative olivine/MgO ratio dried and fired at 1450°C/6hrs.*

| | | DRIED | | | FIRED | | | |
|---|---|---|---|---|---|---|---|---|
| Olivine/MgO | Flowability [%] | B.D. [%] | A.P. [%] | MOR [N/mm²] | P.L.CH [%] | B.D. [%] | A.P. [%] | MOR [N/mm²] |
| 92 / 05 | 70 | 2.774 | 13.57 | 3.9 | -0.160 | 2.750 | 16.50 | 6.5 |
| 82 / 15 | 81 | 2.799 | 12.42 | 7.9 | 0.120 | 2.740 | 16.86 | 6.8 |
| 67 / 30 | 67 | 2.796 | 13.02 | 10.3 | 0.000 | 2.753 | 17.35 | 7.1 |
| 52 / 45 | 68 | 2.795 | 13.88 | 9.2 | -0.050 | 2.774 | 17.52 | 6.1 |
| 37 / 60 | 67 | 2.770 | 15.08 | 9.7 | 0.390 | 2.757 | 18.58 | 5.0 |
| 22 / 75 | 55 | 2.760 | 16.44 | 10.3 | 0.218 | 2.797 | 18.23 | 5.6 |

Flowability of the six castables, with an exception of castable of "22/75" where flowability has reached only 55%, do not differ from each other significantly. Apparent porosity in both unfired and fired conditions increases with increasing of amount of MgO, which is probably caused by the shape of MgO grains, which are sharper then olivine grains and thus making particle packing more difficult.

It appears that the biggest effect on the flowability of the castables is due to the intermediate fraction between 0.06-0.5mm. In case of 15/82 castables, the fraction consisted of two precisely defined fractions 0.06-0.2mm and 0.2-0.5mm. Flowability in this olivine high containing castables has reached value of 81%, which is more that 10% higher in comparison with the others. With increasing of amount of MgO in castables, olivine has been steadily replaced with MgO. Significant part of the intermediate olivine fraction of 0.06-0.5mm has been replaced with MgO -0.3mm (15% by weight), which caused decreasing flowability to 67-68% as shown in ***Table 8***.

For the permanent linear changes, in all 6 cases acceptable values were obtained and no problem should occur if installed and fired. The same conclusion can be stated as for physical and mechanical properties.

However only the following 4 castables (15/82, 30/67, 45/52, 60/37) have been included in the next step of corrosion testing for the reason stated further.

## 4. *CHARACTERIZATION OF THE TESTED CASTABLES AND REFERENCE BRICK*

Six samples can be tested in one rotary slag test. It has been decided to add in each test one magnesia-chrome brick as a reference. A commercial olivine-based castable (also from the same Norway supplier) was made available to us, thus was added to leaving 4 other castables with different "olivine/MgO ratio" to test.

C-1 - the commercial olivine-MgO castable was involved as a secondary material of reference. Producer has recommended amount of water between 5 – 7%. In order to prepare a castable with similar properties to CIREP'S ones, 7 mixes with different amount of water have been prepared to obtain flowability of comparable values to castables C-2 – C-5 (70-80%). Water addition and flowability of those 7 mixes are depicted in ***Table 9.*** An addition of 4.75% of water was thus selected.

***Table 9****: Flowability of the commercial castables depending on water addition*

| Water Addition | [Weight %] | 4.00 | 4.25 | 4.50 | 4.75 | 5.00 | 6.00 | 7.00 |
|---|---|---|---|---|---|---|---|---|
| Flowability | [%] | **0** | **53** | **63** | **82** | **95** | **123** | **138** |

Chemical compositions of the 5 castables to be used in the rotary slag test are shown in ***Table 10*** where Olivine, MgO and microsilica as major constituents are in weight percentage.

***Table 10:*** *Chemical composition of tested castables, C-1 being a commercial one.*

| | C – 1 | C - 2 | C - 3 | C - 4 | C - 5 |
|---|---|---|---|---|---|
| Constituents | [%] | | | | |
| Olivine | 76 | 82 | 67 | 52 | 37 |
| MgO | 20 | 15 | 30 | 45 | 60 |
| $SiO_2$ | 4 | 3 | 3 | 3 | 3 |

All castables were prepared in the same way keeping uniform conditions of mixing and casting, 6% of water addition has been made to castables C-2 to C-5 and 4.75% to the castable C-1. Characterization of the castables included values of flowability, physical properties in dried as well fired conditions has been made and the results are shown in ***Table 11.***

***Table 11:*** *Characteristics of the castables selected for rotary slag corrosion test in fayalite and calcium ferrite slags.*

| | Rheological Properties | Physical Properties | | | | | |
|---|---|---|---|---|---|---|---|
| | | DRIED | | | | | |
| | Flowability [%] | A.P. [%] | B.D. [g/cm$^3$] | CMOR [MPa] | | | |
| C – 1 | 85 | NA | NA | NA | | | |
| C – 2 | 81 | 12.5 | 2.802 | 8.2 | | | |
| C – 3 | 67 | 12.9 | 2.807 | 9.3 | | | |
| C – 4 | 68 | 13.9 | 2.805 | 9.7 | | | |
| C – 5 | 67 | 14.8 | 2.792 | 9.2 | | | |

***REXAL 60 DB – magnesia - chrome brick***, commonly used in copper metallurgy has been chosen as a reference. Chemical composition and relevant physical properties of the brick are collected in ***Table 12***.

***Table 12:*** *Chemical composition and relevant physical and mechanical properties of the magnesia-chrome brick – REXAL 60DB*

| CHEMICAL ANALYSIS | | PHYSICAL PROPERTIES | | |
|---|---|---|---|---|
| MgO | 67.0 % | Bulk density | [g/cm$^3$] | 3.02 |
| $Cr_2O_3$ | 12.7 % | Apparent porosity | [%] | 18.5 |
| $Al_2O_3$ | 10.4 % | Modulus of Rapture | [N/mm$^2$] | 6.0 |
| $SiO_2$ | 1.9 % | Cold Crushing Strength | [N/mm$^2$] | 35.0 |
| $Fe_2O_3$ | 7.3 % | | | |
| CaO | 0.8 % | | | |

# CHAPTER III

## ON CORROSION TESTING

In order to make a prediction of the behavior of refractories in real working conditions it is necessary to understand the possible interactions between the different phases involved. Corrosion tests, followed by an analysis of the results under simulative conditions, help to predict some expectable performances.

Numerous methods have been tried and some reasonable correlations have been obtained for very specific conditions, but very few methods have reached the status of standard operating practices and non have yet been accepted for universal use.

In this work, a rotary slag test method has been chosen to test the olivine-MgO castables, compare them between each other as well as to reference magnesia-chrome brick.

# 1. EXPERIMENTAL SET-UP

## 1.1. EQUIPMENT

The rotary slag test furnace, in accordance with ASTM C874-85 practice, is shown in ***Figure 5***.

The furnace consists of a cylindrical shell 16 inches long with 11 inches in diameter, two covers with holes in the middle for flame and slag charging on the other side respectively and a motor to rotate the cylinder during test.

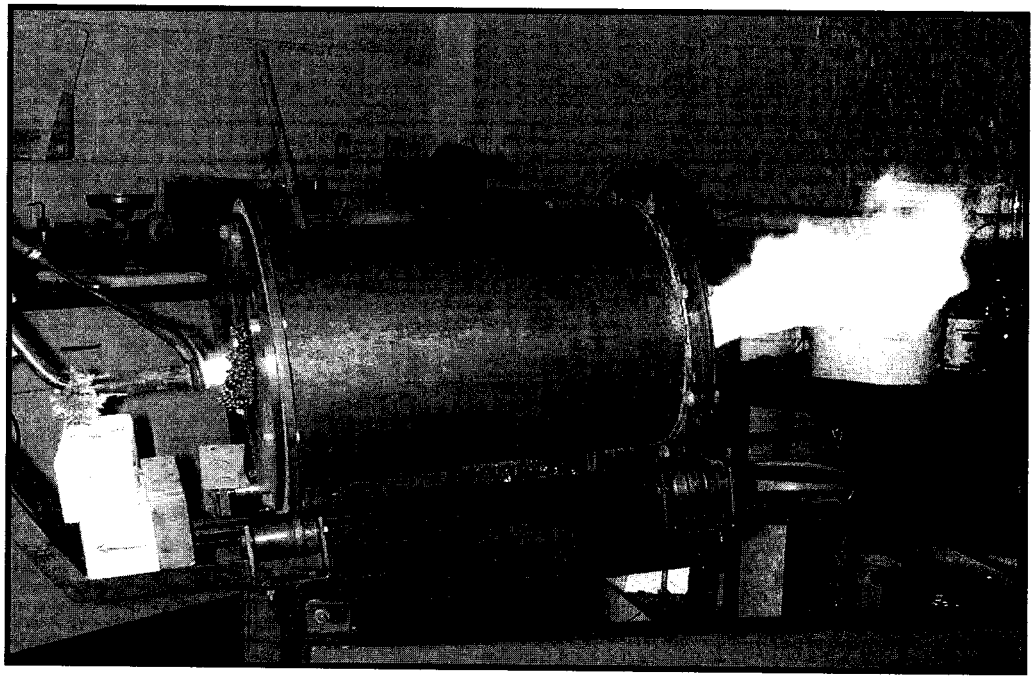

***Figure 5:*** *The rotary slag testing equipment – a general view*

## *1.2. SPECIMEN PREPARATION*

Castables samples for rotary slag test have been cast and vibrated in molds designed for that purpose. The molds were vibrated for 8-12 minutes on a vibration table with amplitude of 0.4mm and frequency of 50 Hz. The samples were demolded after 12-15 hours and than dried at room temperature for 5 - 8 hours. Samples were then dried further at 110°C for 12 hours. After drying, samples were fired in a furnace at 1450°C for 6 hours according to the heating program described in ***Figure 6***.

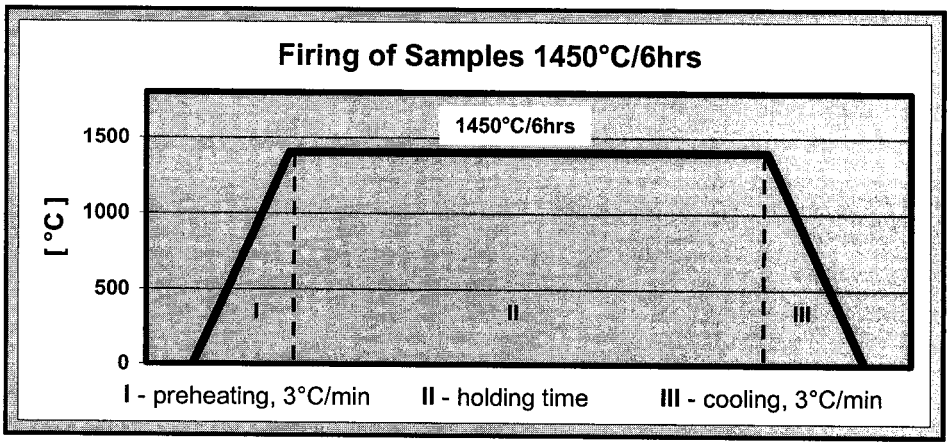


***Figure 6:*** *Heating program for the castable specimens prior to rotary slag test, and determination of physical properties*

Reference – REXAL 60 DB samples, present in each test, have been prepared by wet cutting with diamond blade then dried at 110°C for 12 hours. Final dimensions and shape of testing specimens is shown in ***Figure 7.***

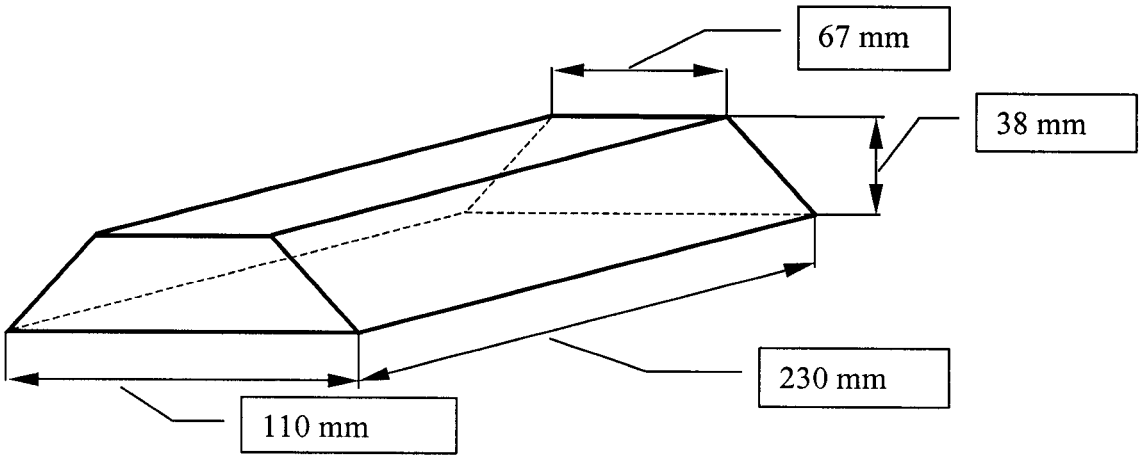


***Figure 7**: Shape and dimensions of a test specimen for rotary slag test*

## *1.3 CONFIGURATION OF THE TESTED SPECIMENS*

The six samples were put together as shown in ***Figure 8***. The samples had to be adjusted to make a tight side-to-side configuration. The gap between the inner wall of the steel cylinder and the cold face of specimens was filled up with granular (olivine - 0.3 mm.) refractory to hold specimens in a stable position. As "input" and "output" pieces mag – chrome bricks cut (6 x 6 x 1.5 and 6 x 6 x 5.5 inches respectively) then drilled (2.5 inches in diameter) were used

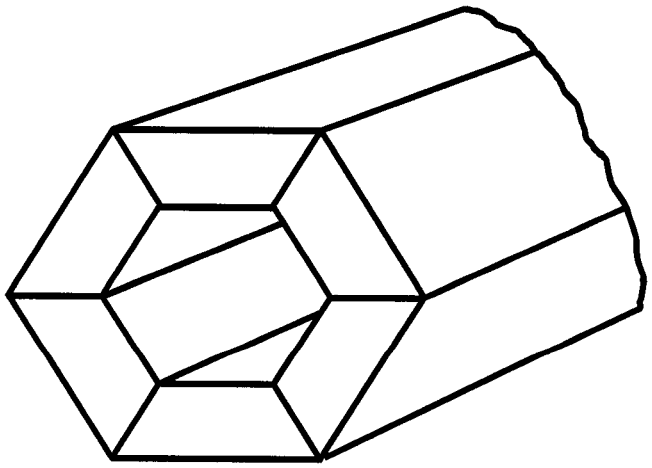

***Figure 8:** Configuration of 6 test samples*

## *1.4. SLAGS*

Fayalite and calcium ferrite slags of chemical compositions depicted in ***Table 13*** have been used as a corrosion medium. Slags have been crushed to the appropriate fraction (up to 10mm) to achieve fast melting and easy charging.

***Table 13:*** *Chemical composition of the testing fayalite and calcium ferrite slags.*

| | $(Fe_2O_3)t$ | $SiO_2$ | $Al_2O_3$ | MgO | CaO | $Na_2O$ | $K_2O$ |
|---|---|---|---|---|---|---|---|
| [%] | 77.6 | 18.3 | 0.87 | 0.29 | 0.3 | < 0.1 | 0.29 |
| | $(Fe_2O_3)t$ | $SiO_2$ | $Al_2O_3$ | MgO | CaO | $Na_2O$ | $K_2O$ |
| [%] | 57.3 | 1.2 | 0.23 | 1.6 | 18.7 | 0.05 | 0.03 |

## *2. PROCEDURE*

The furnace was tilted 12° axially toward the lower end as shown in ***Figure 9***. Heat is being provided using a gas-oxygen ($MAP/O_2$) flame equipped with a cooling system of the torch at the input end. Slag was charged into the upper (output) end of the tilted rotary furnace. The molten slag washed over the lining and escaped at the lower end of the furnace in front of the burner. The furnace was kept rotating at constant speed, at approximately 2.5 rpm.

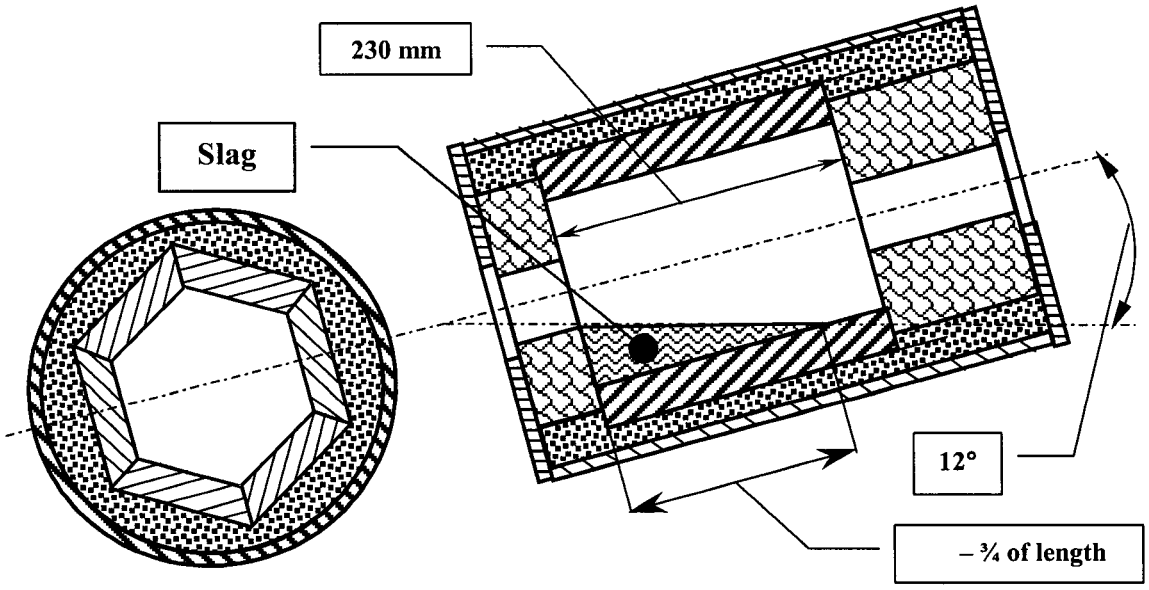


***Figure 9:*** *The rotary slag testing furnace – a longitudinal section view.*

During testing, temperature was measured by an optical pyrometer, which was directed to the roof between 3rd and 6th inches inside the furnace. After preheating (approximately 2 hrs), 1.4-1.6 kg of slag was charged in doses of 200g at 10 minutes intervals. When the furnace was filled up (first dropping of slag), charging of 200g of slag continued every 30 min for 8 hrs until the end of the test as shown in ***Figure 10***. Testing temperature was measured every 15 min, and kept at level of 1400°C ±15°C by controlling the gas/oxygen ratio.

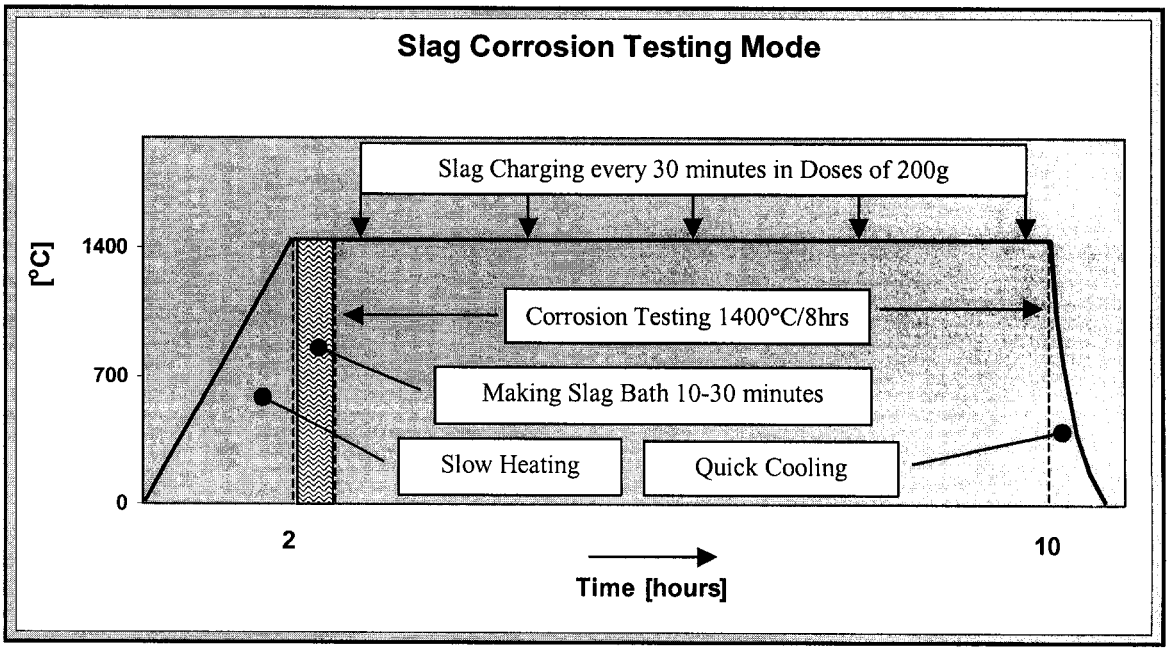


***Figure 10**: Rotary slag test – time/temperature evolution.*

At the end of each test, immediately after shutting off the oxygen, gas and motor, furnace was tilted to a vertical position to allow the remaining slag to drain. Fifteen hours after finishing of the test, testing cylinder was taken apart and tested samples were carefully separated from each other, cut longwise, dried and prepared for macro - evaluation of the corrosion resistance as well as for optical microscopy examination.

## 3 DETERMINATION OF DISSOLUTION – EROSION AND PENETRATION RATE

A measurement of samples before and after testing with subsequent calculation of areas in longwise section has been used as a method for the evaluation of ***dissolution-erosion rate***. Each sample was measured inch by inch, as shown in ***Figure 11***. Difference between initial height and height after test corresponds to dissolution-erosion

wear. Because of the temperature profile in within the furnace only the area between 2nd and 7th inch was considered to be representative of the dissolution - erosion rate.

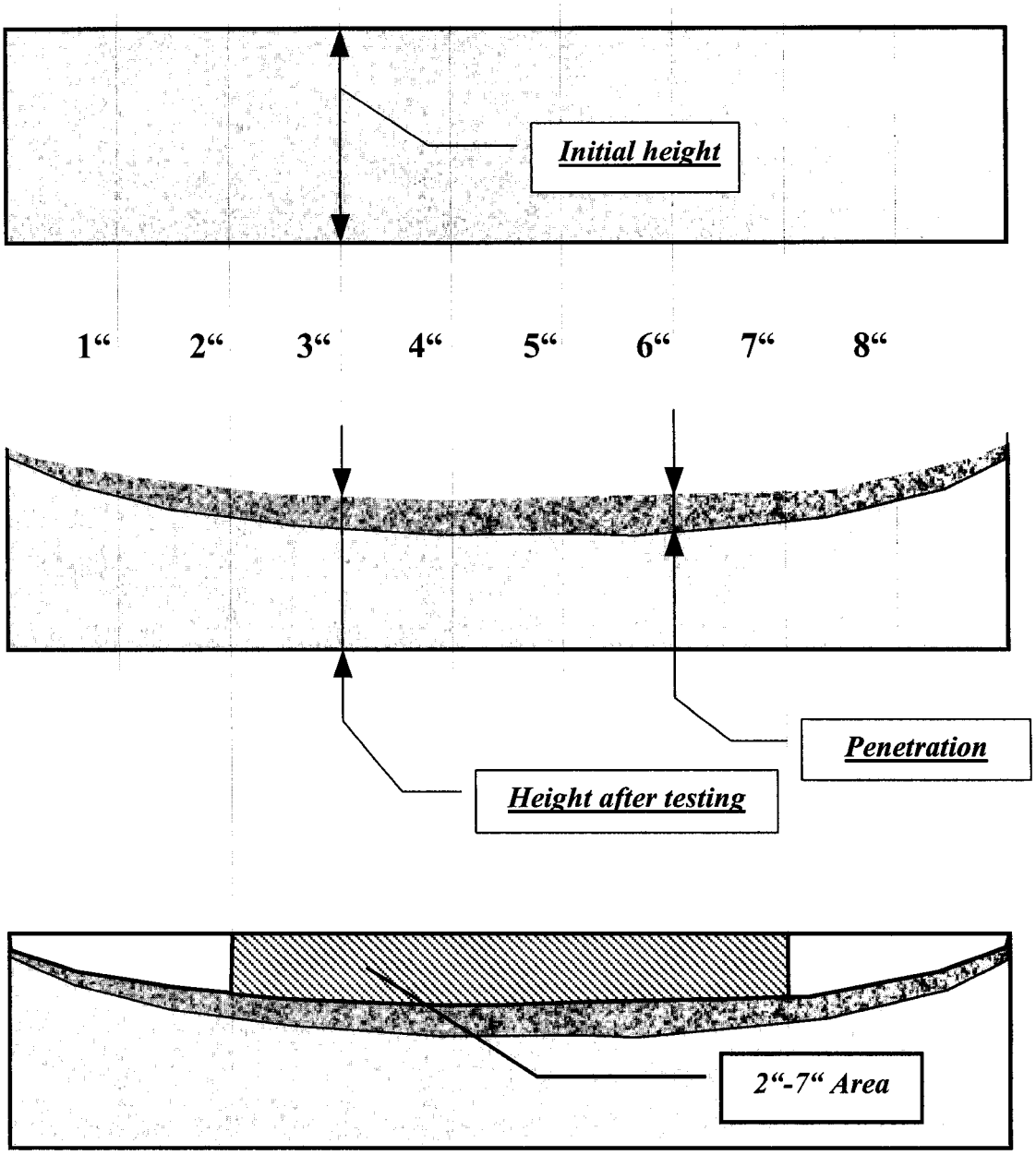


***Figure 11:*** *Way to determine of corrosion resistance of samples (penetration and dissolution-erosion).*

***Maximum penetration depth*** was localized visually and measured with calliper followed by optical microscopy examinations, as it will be discussed further later.

# CHAPTER IV

## EXPERIMENTAL RESULTS

### 1. DISSOLUTION – EROSION

The values depicted in ***Figures 12*** and ***13*** are averages of three identical repeated tests at 1400°C for 8 hours in fayalite and calcium ferrite slags respectively. The numbers represent dissolved – eroded area between 2nd and 7th inch in longwise section, as described in the previous chapter. Though a few eroded grains have been observed in slag, dissolution was the major factor in dissolution-erosion degradation.

In both slags, as expected, the reference magnesia – chrome bricks has shown the best performance for dissolution – erosion. The castable C-5 was dissolved – eroded the least from all tested castables in both slags. The determined values in fayalite slag (210 $mm^2$) and calcium ferrite slag (83 $mm^2$) are close to the reference where the dissolution – erosion rate was determined as 160 $mm^2$ in fayalite and 55 $mm^2$ in calcium ferrite slag respectively. Castable C-2 has been dissolved – eroded the most, followed by C-1 – the commercial olivine – MgO castable. The differences between C-1 and C-2 are small in both fayalite as well as calcium ferrite slags.

As far as dissolution-erosion rate is concerned, whether maximum depth or dissolution-erosion area in longwise section is taken into consideration (as shown in ***Tables 19*** and ***20*** in APPENDIX III) in both slags the same ranking is determined:
RFF < C-5 < C-4 < C-3 < C-1 < C-2. In both cases the rank is identical in all 6 tests – 3 in fayalite and 3 in calcium ferrite slag. Eventually the areas were preferentially taken over depth of dissolution-erosion in evaluation since it was considered more representative and made the results more distinguishable in between each other.

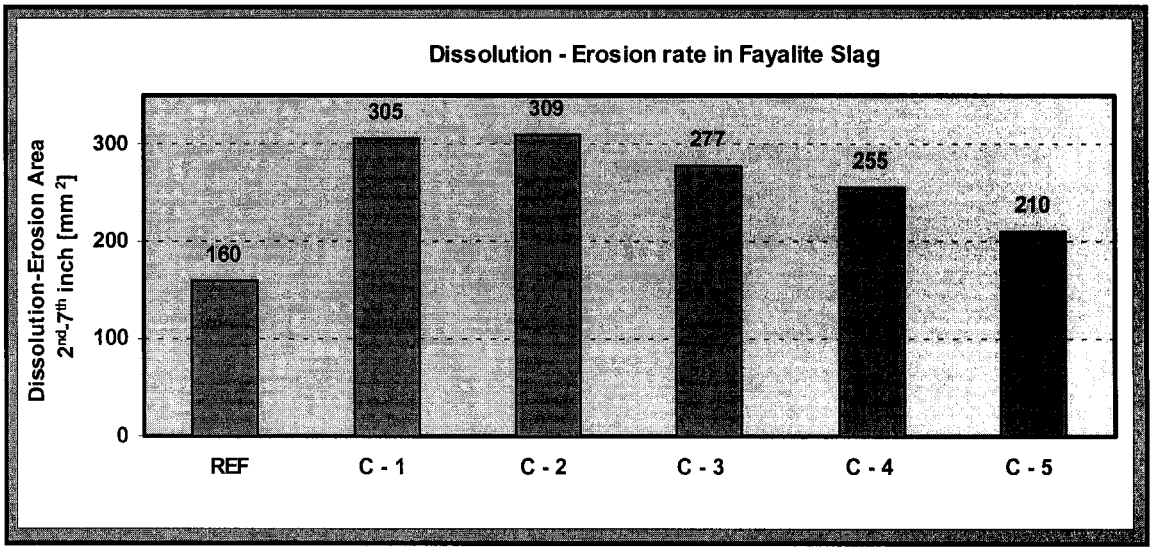


***Figure 12***: *Averages of dissolution – erosion rates of samples tested at 1400 °C for 8 hours in fayalite slag over three tests.*

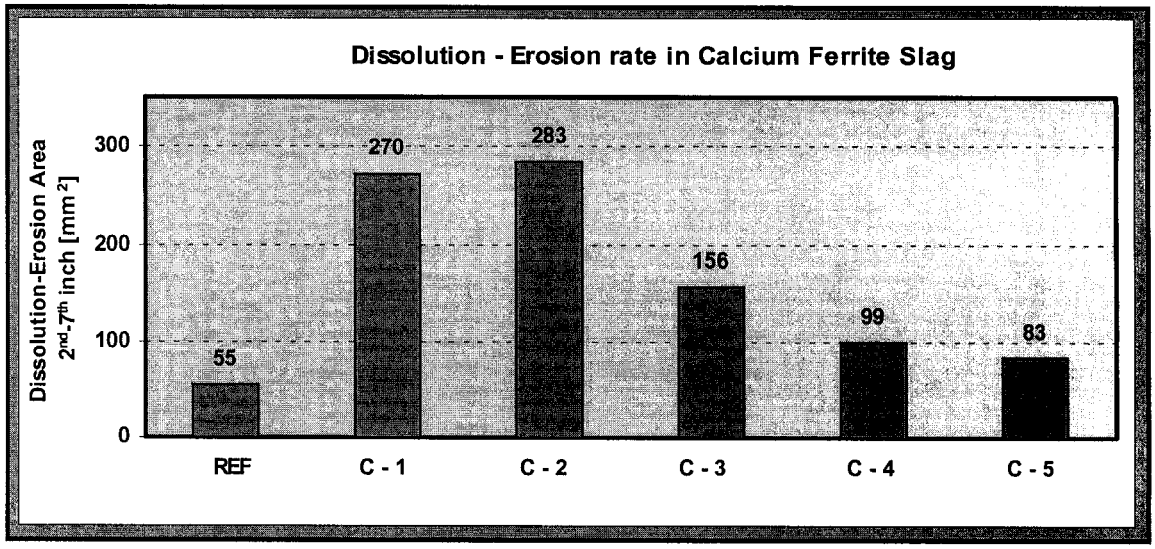


***Figure 13***: *Averages of dissolution – erosion rates of samples tested at 1400 °C for 8 hours in calcium ferrite slag over three tests.*

From those results it is evident that with increasing amount of MgO in the castables dissolution-erosion rate decreases. The trend of increasing resistance of castable with increasing MgO was identical in both slags. As shown in ***Figure 14***, in fayalite slag, contribution of MgO to resistance of the castable against dissolution-erosion is moderate and continuous. 15% of MgO addition to castable C-2 increases the resistance of the castable by approximately about 11% (from 309 to 277 $mm^2$). Another 15% of MgO addition (C-3 to C-4) increased the resistance by another 8% and finally dissolution-erosion resistance of castable C-5 containing 60% of MgO was determined as 18% better then C-4 containing 45% of MgO.

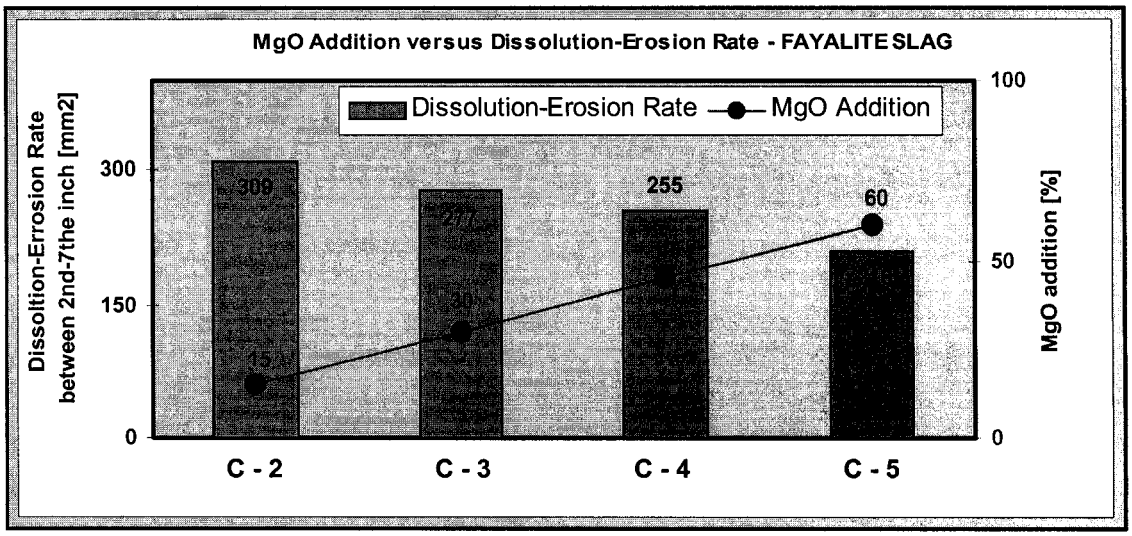


***Figure 14***: *Contribution of MgO additions to the total dissolution-erosion rate in fayalite slag.*

In ***calcium ferrite slag*** unlike the fayalite slag, as shown in **Figure 15**, MgO contribution to the total resistance of the castable against dissolution-erosion has been much more significant. 15% of MgO addition (from 15 to 30 % of MgO in the castable) to the castable C-2 on composition of C-3 decreased dissolution-erosion rate by 45% (from 283 to 156 $mm^2$) and similarly with another 15% of MgO addition to castable C-4 (45% of MgO) by 38% (from 156 to 99 $mm^2$). Castable C-5 containing 60% of MgO has increased resistance by only 16% comparing to castable C-4.

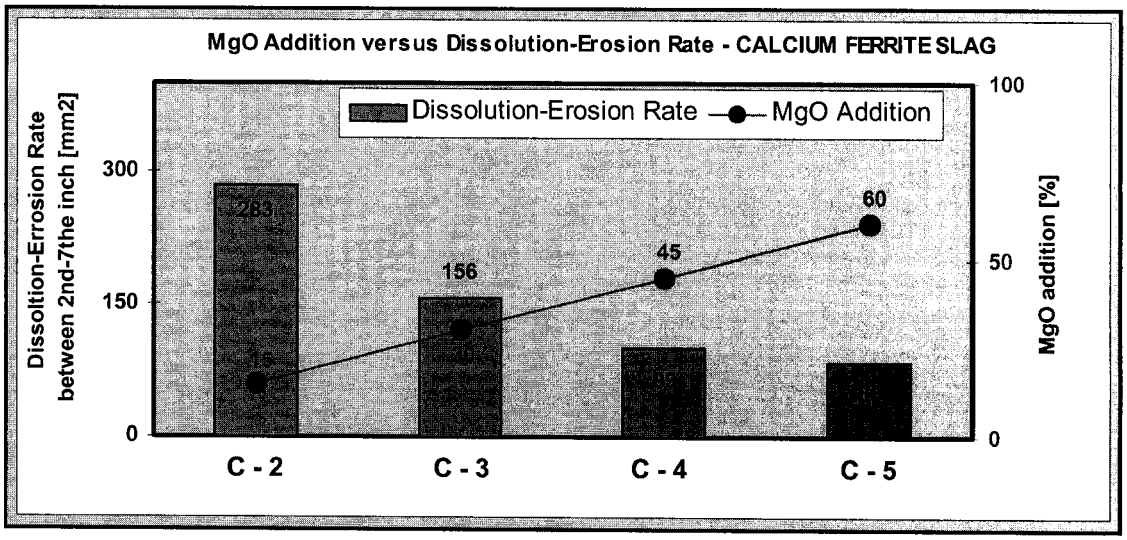


***Figure 15****: Contribution of MgO addition to total dissolution-erosion rate in calcium ferrite slag.*

Since the matrix in all 4 castables were made of the same constituents, with the same proportions (11% of crushed fine olivine –0.02mm and 15% of BMF MgO – 0.075mm) and the roughest fractions of MgO (1.7-3.35mm and 3.35-5mm) were only used in castable C-5, it appears that gradual replacing of intermediate olivine fractions of 0.2-0.5mm and 0.06-0.2mm by MgO of –0.3mm and olivine of 0.5-2mm by MgO of 0.3-1.18mm significantly improved the castable resistance in calcium ferrite slag.

Porosity of the castables influences dissolution process as well. The higher porosity the larger slag-refractory contact and the faster dissolution process is expected to be. As shown in ***Figure 16,*** apparent porosity of the castable C-3 (15.5%) was much lower that castables C-2 (20%) and it is believed that the difference naturally influenced the dissolution erosion rate as well. On the other side castable C-4 has even had higher porosity (17.1%) than C-3 (15.5%) and the dissolution-erosion rate was lower by 37%. Thus it appears that the composition of the castables mostly rules the behavior in both slags.

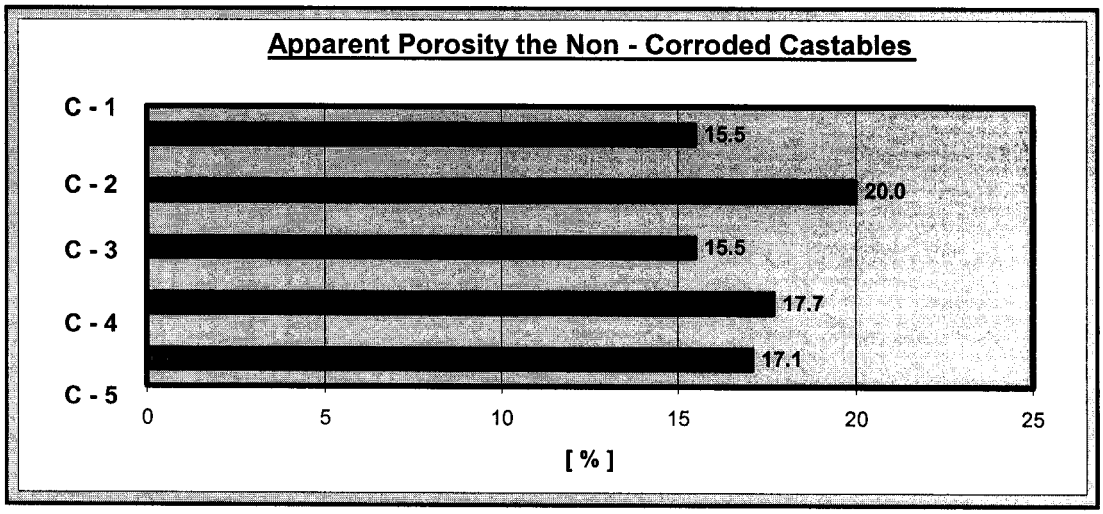


***Figure 16****: Apparent porosity of the castables after firing at 1450 °C/8 hrs.*

In the ***Figures 17*** and ***18*** are depicted the real values of the three repeated tests as measured (inch by inch) and calculated (area between $2^{nd}$ and $7^{th}$ inch in longwise section).

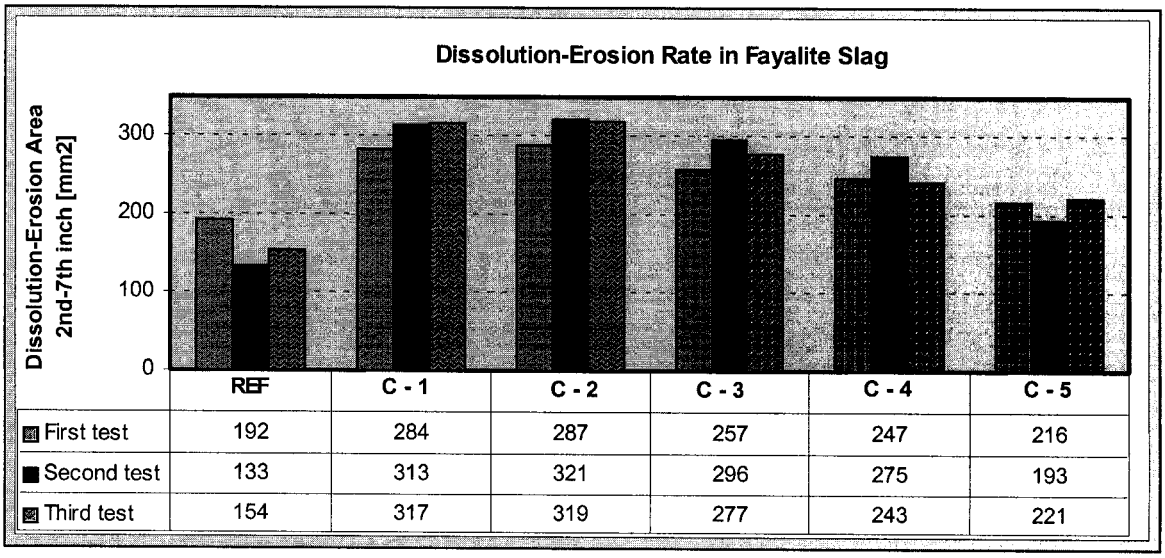


| | REF | C - 1 | C - 2 | C - 3 | C - 4 | C - 5 |
|---|---|---|---|---|---|---|
| First test | 192 | 284 | 287 | 257 | 247 | 216 |
| Second test | 133 | 313 | 321 | 296 | 275 | 193 |
| Third test | 154 | 317 | 319 | 277 | 243 | 221 |

***Figure 17***: *Dissolution-erosion rates of three tests in fayalite slag.*

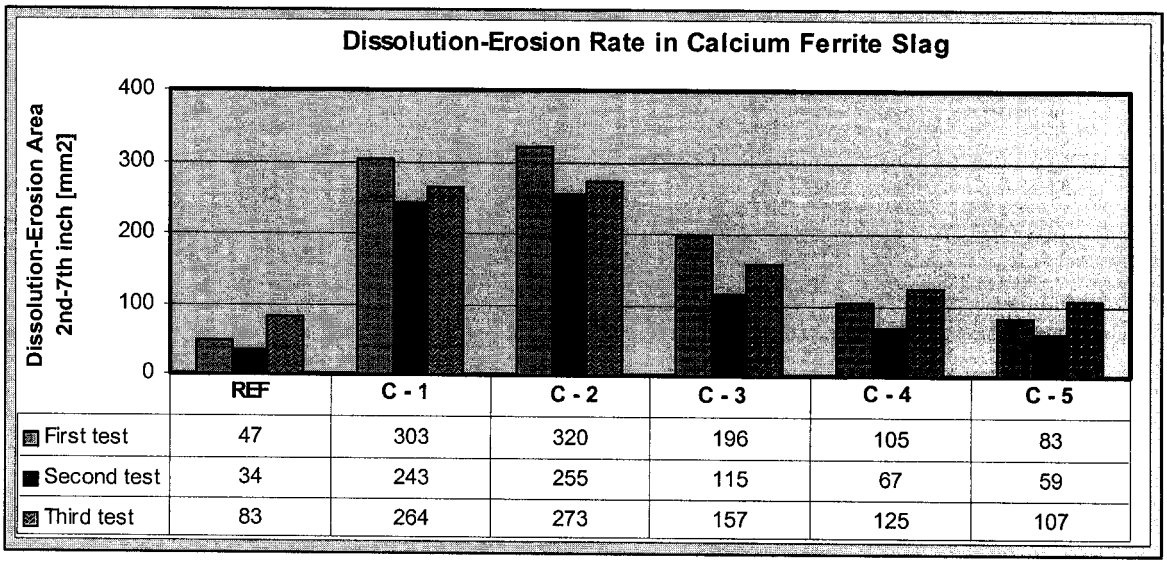


| | REF | C - 1 | C - 2 | C - 3 | C - 4 | C - 5 |
|---|---|---|---|---|---|---|
| First test | 47 | 303 | 320 | 196 | 105 | 83 |
| Second test | 34 | 243 | 255 | 115 | 67 | 59 |
| Third test | 83 | 264 | 273 | 157 | 125 | 107 |

***Figure 18***: *Dissolution-erosion rates of three tests in calcium ferrite slag*

The standard deviation values obtained from the three-repeated same test are shown in ***Tables 14*** and ***15.*** In fayalite slag, the reference magnesia-chrome brick was the one with the highest standard deviation (24). Magnesia chrome brick in first test was dissolved - eroded significantly more then two others in second and third test, which are quite close to each other. This was caused most probably by a heterogenity or alternatively a linear defect of some kind just in the section where dissolution-erosion rate was measured.

***Table 14****: Values of dissolution-erosion as measured and calculated averages and standard deviations for fayalite slag.*

| TESTS | | | | |
|---|---|---|---|---|
| First | Second | Third | **AVAERAGE** | **STANDARD DEVIATION** |
| 192 | 133 | 154 | 160 | **24** |
| 284 | 313 | 317 | 305 | **15** |
| 287 | 321 | 319 | 309 | **16** |
| 257 | 296 | 277 | 277 | **16** |
| 247 | 275 | 243 | 255 | **14** |
| 216 | 193 | 221 | 210 | **12** |

***Table 15****: Values of dissolution-erosion as measured and calculated averages and standard deviations for calcium ferrite slag.*

| TESTS | | | | |
|---|---|---|---|---|
| First | Second | Third | **AVAERAGE** | **STANDARD DEVIATION** |
| 47 | 34 | 83 | 55 | **21** |
| 303 | 243 | 264 | 270 | **25** |
| 320 | 255 | 273 | 283 | **27** |
| 196 | 115 | 157 | 156 | **33** |
| 105 | 67 | 125 | 99 | **24** |
| 83 | 59 | 107 | 83 | **20** |

Since the numbers obtained from tests in calcium ferrite slag are smaller and taking into account the same possible error of measurement, naturally the standard

deviations are bigger then in case of fayalite slag. However, results obtained from the rotary slag test doubtless provide a significant ranking of the 6 samples tested.

## 2. *PENETRATION*

The penetration of the slag into the refractories is a complex process and is generally non-uniform in nature. The penetration front does not usually show as a clear-cut boundary, but rather as a blurred region. In the areas, which have been penetrated, not all pores are filled with slag and the slag penetration through interconnected pores followed selective channels and pathways. This is then difficult to quantify the true depth of penetration. Macroscopical evaluation is not sufficient; it should be supported by microscopy examination. Occasionally macroscopical measurement can be, with previous experience in particular case, considered as sufficient. Samples have been evaluated visually (caliper measuring) first in whole length of section and observed under optical microscopy in areas where maximum penetration was expected (between $4^{th}$ and $6^{th}$ inch of the tested samples).

### 2.1. *VISUAL OBSERVATION*

Maximum penetrated depth in longwise section after testing has been determined and used as a way of evaluating of penetration rate - macroscopically. Similarly as in case of erosion-dissolution, both end sections between 0"-2" and 7"-9" were not taken into consideration. Unlike dissolution-erosion, measurement of penetration depth was very subjective matter.

Discoloration of refractory after testing, which is not penetration, often appears like penetration and by mistake can be considered as penetration, which is by the way valid vice-versa as well for "apparently non-penetrated mass". Very often, penetrated and non-penetrated zones differ from each other slightly and non-clear boundary can be established.

Results of maximum depth of penetration (in millimeters) in the reference magnesia-chrome brick and 5 tested olivine-MgO castables, as observed visually and measured with caliper, are depicted in ***Figures 19*** and ***20*** in fayalite and calcium ferrite slag respectively.

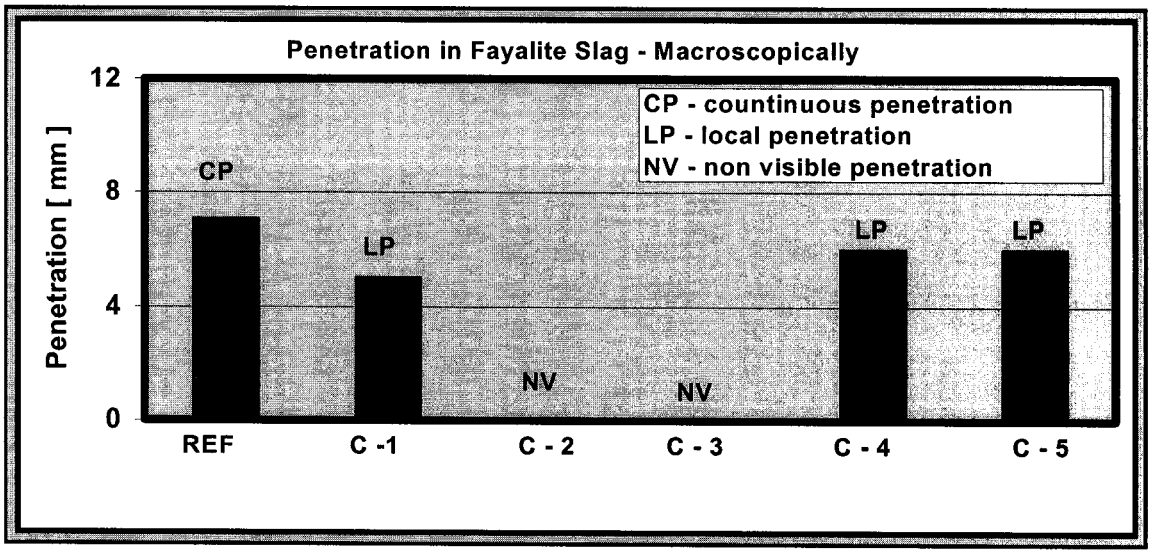


***Figure 19:*** *Depth of penetration as determined macroscopically for samples tested in fayalite slag at 1400°C for 8 hours.*

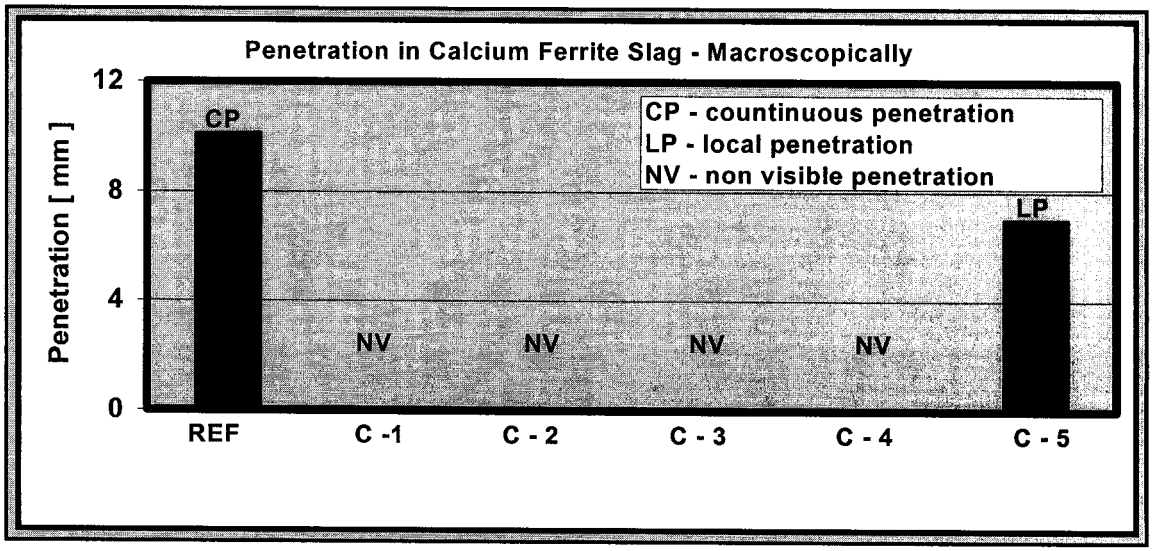


***Figure 20****: Depth of penetration as determined macroscopically for samples tested in calcium ferrite slag at 1400°C for 8 hours.*

In some cases, penetration has been observed in local zones. A mark of "LP" (local penetration) will symbolize that kind of penetration in subsequent evaluation. A mark of "CP" (continuous penetration) will represent a penetration with more or less clear boundary in whole length of section. If penetration has not occurred, or has not been seen visually by naked eye, a mark "NV"(non visible) has been used. Just for the record it has to be mentioned that it does not mean that there was no penetration but none was observed visually.

## 2.2. *OPTICAL MICROSCOPY*

Penetration has been evaluated microscopically. However, it should be always remembered that samples have been evaluated in whole length visually and just at limited part microscopically. Samples for microscopy examination were taken approximately from the middle of tested samples. ***Figure 21*** and ***Figure 22*** show values of depth of penetration determined by optical microscopy compared to conjectured depth determined by caliper measuring.

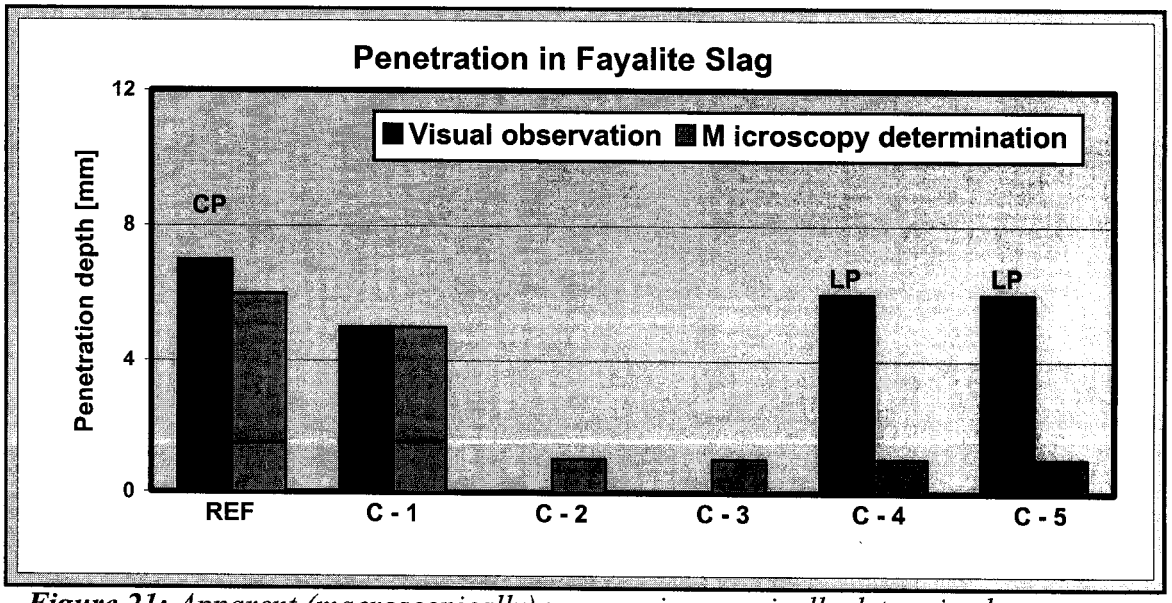


***Figure 21:*** *Apparent (macroscopically) versus microscopically determined penetration in fayalite slag, at 1400 °C for 8 hours.*

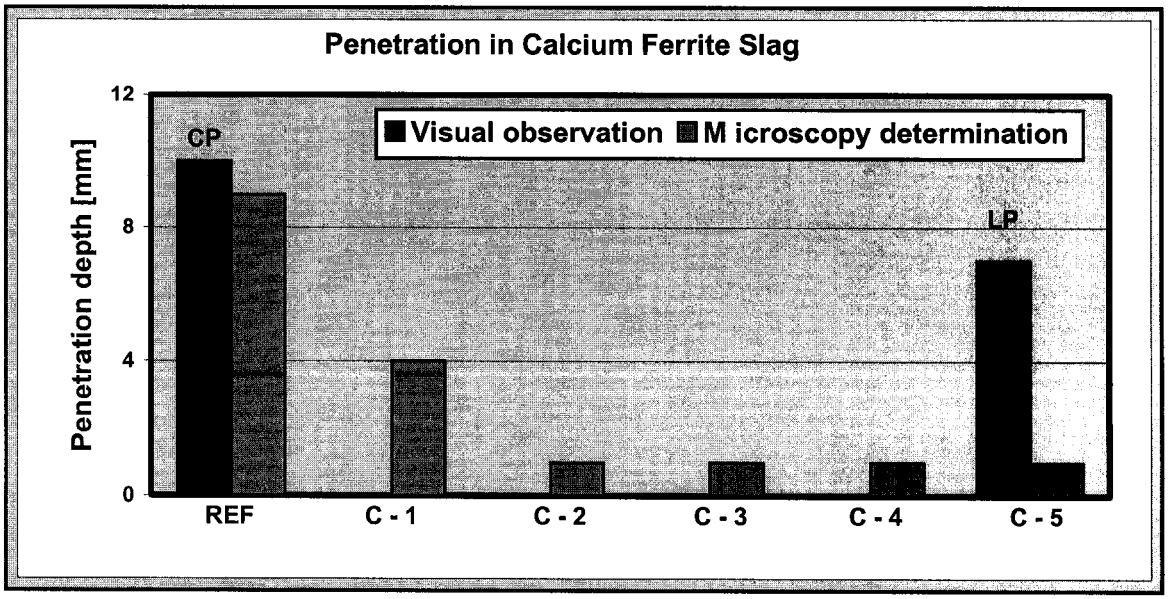


***Figure 22**: Apparent (macroscopically) versus microscopically determined penetration in calcium ferrite slag, at 1400°C for 8 hours.*

Microscopical examination has proven the fact that visual assessment of the depth of penetration can be misleading in some cases. Occasionally color of some olivine grains especially in contact with slag residuum, which is the same or a very similar color, at hot face, leads to incorrect estimation that matrix is penetrated as shown in ***Figure 23***.

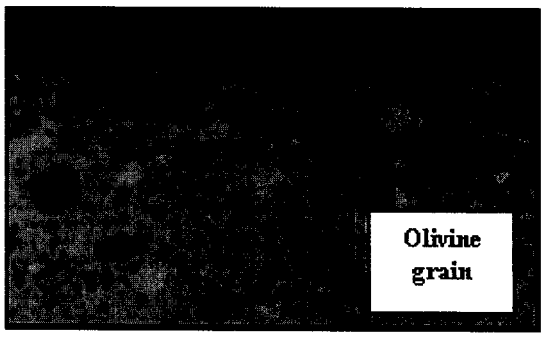


***Figure 23**: Olivine grain in contact with fayalite slag.*

Those samples for optical microscopy where a local penetration has been observed visually were taken from spots where particular irregularity occurred. Microscopical examination did not confirm occurrence of that so-called local penetration (LP), which was used to describe a sort of penetration in case of castable C-1, C-4 and C-5 in fayalite and C-5 in calcium ferrite slag. Depth of the "local penetration" has reached value up to 6 mm, in accord with the diameter of the biggest olivine grains in the castables and was

clearly identified as pure un-penetrated olivine grains. The color of the olivine grains when in contact with slag created that illusion of penetrated mass. However no local penetration has been observed by optical microscope.

On the other side with an exception of C-1 in fayalite slag, caliper-measurement has provided the results, which are very closed to microscopical observations. Optical microscopy examination has shown that castables C-2, C-3, C-4, C-5 with "non visible penetration" as determined by visual observation, are in fact penetrated up to 1 mm.

The macroscopical depth of penetration marked as "CP" (continuous penetration) was confirmed by microscopy as well. The values in both measurements are quite close to each other. Castables C-1 and C-4 in fayalite slag and C-2 and C-3 in both slags have been market as "NV" (visually non visible penetration) but optical microscopy revealed small depth of penetration up to 1 mm in all castables apart from C-2 where determined up to 4 mm.

Reference mag-chrome brick (REF) has been penetrated much deeper than the tested olivine-MgO castables. In addition to penetration by slag, the reference samples tested in calcium ferrite slag have been the only ones penetrated by metallic copper, which was find in considerable depth from the hot face (up to 12-15mm). The castables have had no evidence of penetrated copper in volume whatsoever. All olivine-MgO castables (C-2, C-3, C-4, C-5) have shown very good resistance against penetration, no matter what sort of slag has been used to test them. In all cases, depth of penetration has reached value up to 1 mm.

Macroscopic views of samples, which have been tested in fayalite slag, are shown in ***Figure 24*** and in calcium ferrite slag in ***Figure 25***.

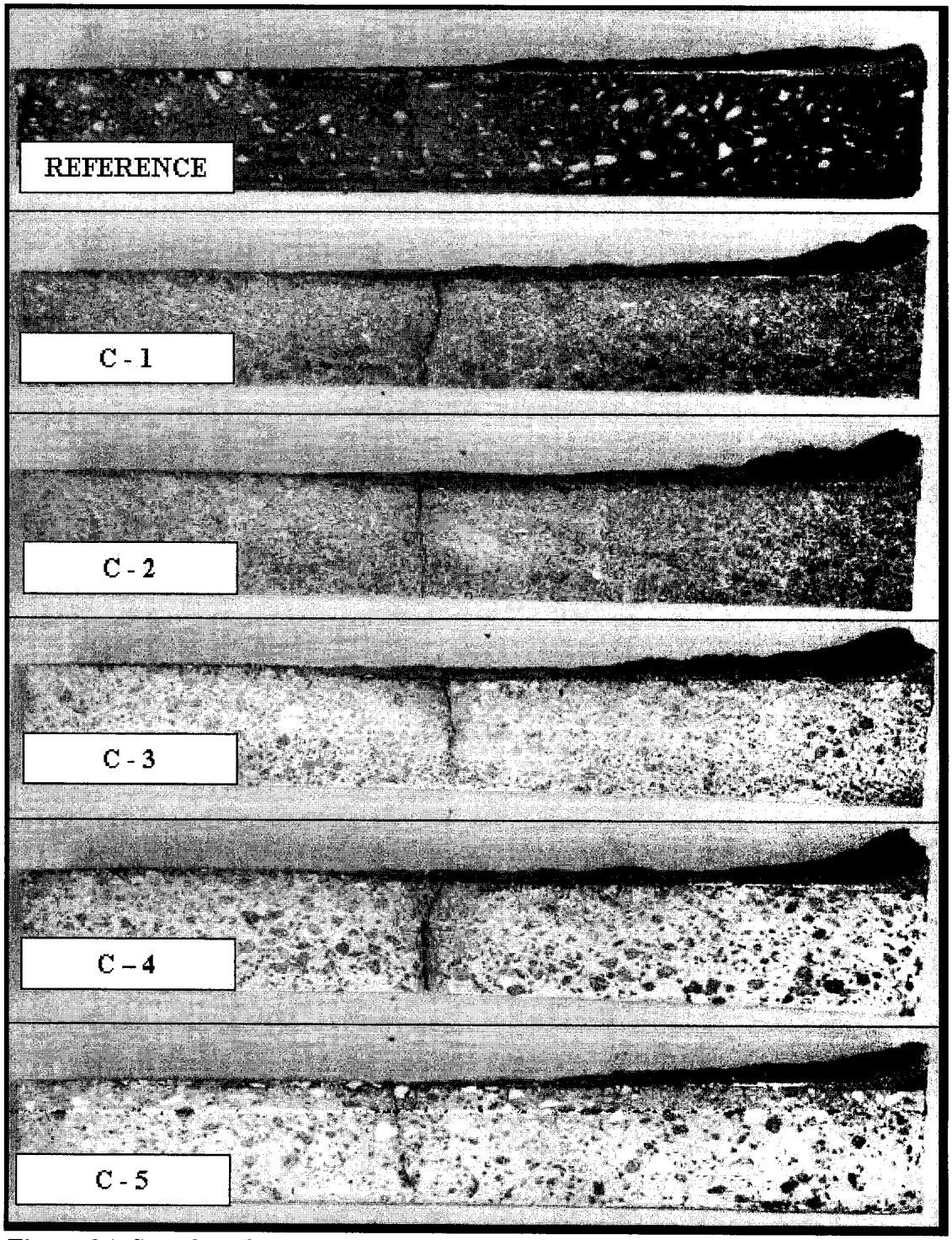


***Figure 24***: *Samples after 8 hrs in fayalite slag at 1400 °C*

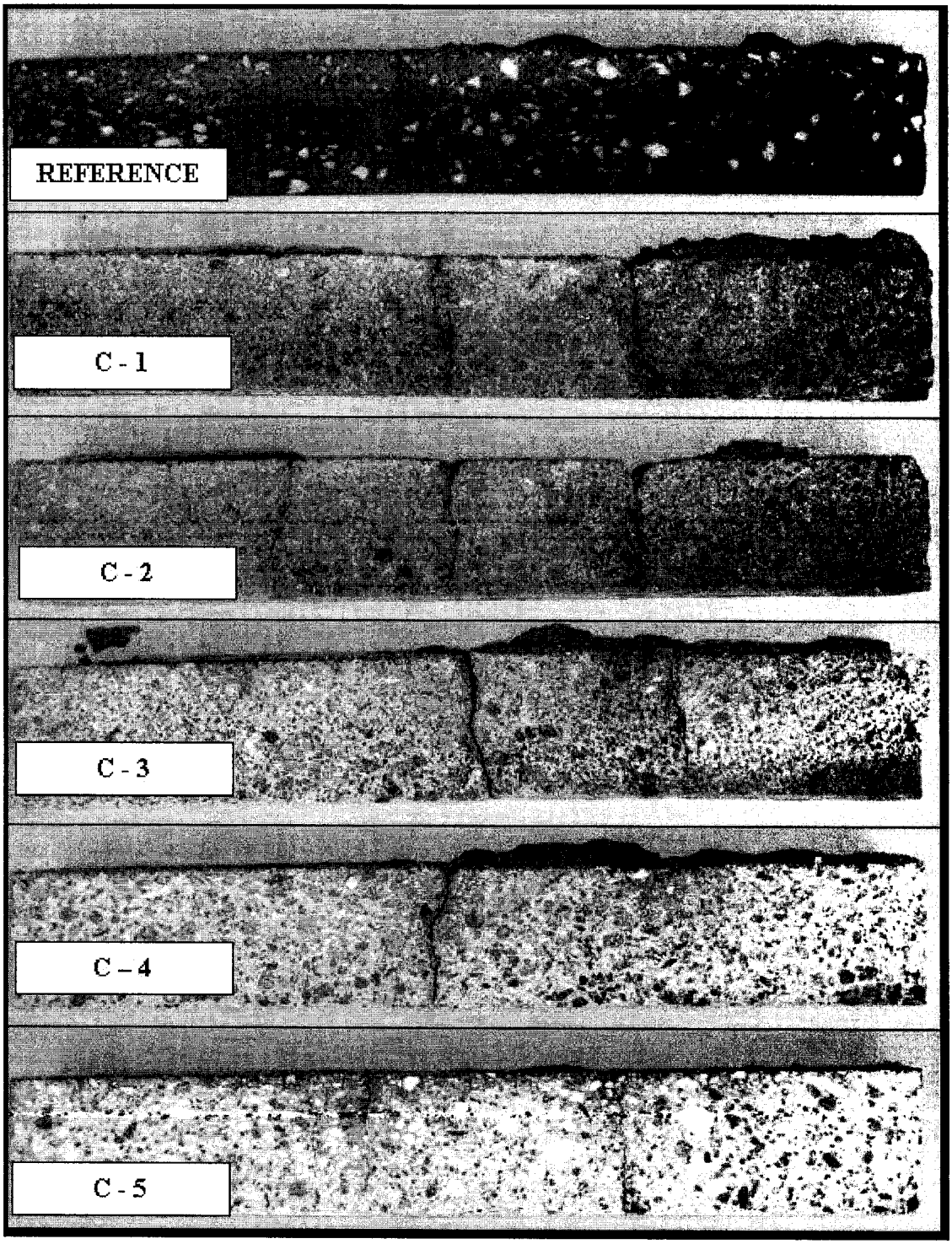


***Figure 25***: *Samples after 8 hrs in calcium ferrite slag at 1400 ℃*

The commercial olivine-MgO castable (C-1) lies between castables C-2 and C-3 as shown on **Figure 26** and has perfectly filled a spot in olivine-MgO ratio "puzzle" in terms of mineralogical composition and so a place in dissolution-erosion rank as well.

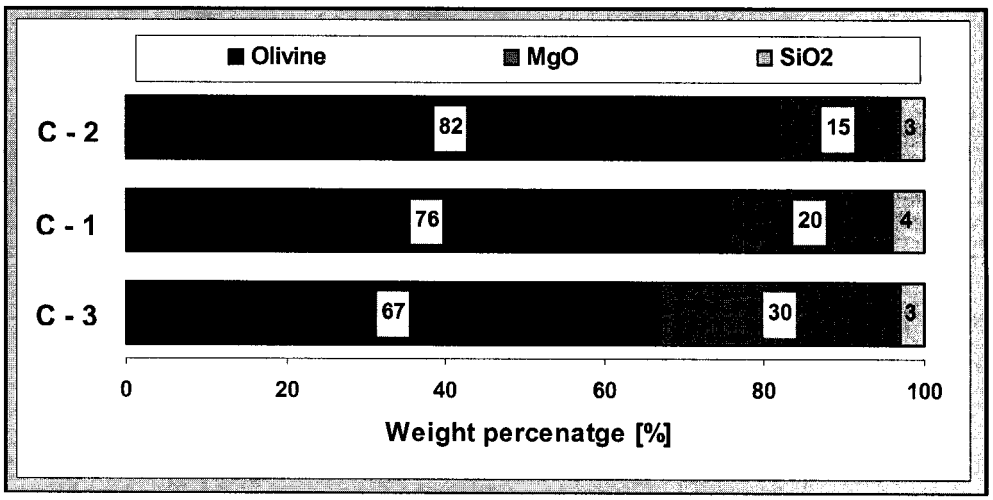


***Figure 26:*** *Olivine-MgO-$SiO_2$ proportion of the commercial (C-1) and CIREP's castable (C-2 and C-3)*

It is evident that olivine-MgO castables in spite of higher porosity in some cases then reference magnesia-chrome brick have much better resistance against penetration in both fayalite and calcium ferrite slags. It appears that some kind of self-protecting mechanism has something to do with interactions between olivine-MgO castable and both slags. Slag penetration into that kind of refractory as determined up to 1 mm is more than promising.

# CHAPTER V

## INTERPRETATION AND DISCUSSION

As stated at the beginning of this work, the objective was to evaluate an olivine-based castable refractory, as a possible new refractory to use in copper making units. To initiate the research, the rheological, mechanical and physical properties of various castables have been measured and then compared in terms of corrosion resistance to magnesia-chrome brick widely used in the copper industry.

This work was undertaken to understand in olivine - MgO castable - slag interactions, with either fayalite or calcium ferrite slag.

### 1. Olivine Castable in Fayalite and Calcium Ferrite Slag

Advantages and disadvantages of such slags from a metallurgical point of view have been summarized at the beginning of the thesis. However, refractory – slags interaction approach has nothing to do with metallurgical advantages and is a different issue.

Mole ratios of $FeO/SiO_2$ (3.2) in fayalite slag and $CaO/Fe_2O_3$ (0.95) in calcium ferrite slag calculated from the chemical composition depicted in ***Table 13*** reveal that fayalite is indeed the major component of the fayalite slag as well as calcium ferrite in calcium ferrite slag.

Refractory materials are usually composed of two or more major constituents, which gives the material certain level of heterogenity. The refractory – slag interactions are different in particular volumes. Besides, at certain temperature constituents of the refractory may react between each other.

The tested castables have been composed of two major components: MgO and olivine. Olivine for refractory application as already mentioned is a solid solution of forsterite ($Mg_2SiO_4$) and fayalite ($Fe_2SiO_4$) with unlimited solubility in each other in mutual ratio at least of 85/15 in favor of forsterite. For simplification, only forsterite's interactions have been taken into account instead of olivine.

The four interactions, considering olivine and MgO with both fayalite and calcium ferrite slag will be considered independently.

## *1.1. MgO - FAYALITE SLAG*

As shown in ***Figure 27***, MgO and FeO form a solid solution with unlimited mutual solubility. MgO dissolves into fayalite slag and simultaneously is able absorb unlimited amount of FeO from the fayalite ($Fe_2SiO_4$) slag as following formula (10) indicates.

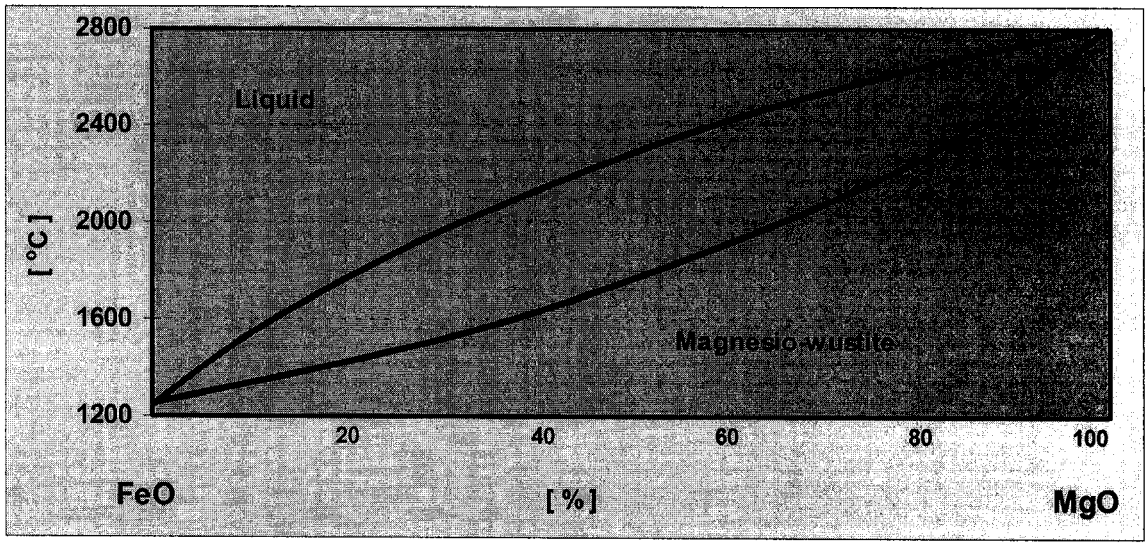


***Figure 27:*** *The FeO-MgO phase diagram.*

$$MgO_{(s)} + 2FeO.SiO_{2(l)} \Rightarrow (xMgO.yFeO)_{(ss)} + 2\left[\frac{(1-x)}{2}MgO.\left(1-\frac{y}{2}\right)FeO\right].SiO_{2(l,s)} \quad \textbf{(10)}$$

Since the reaction takes place in oxidizing atmosphere, partly oxidation of FeO to $Fe_2O_3$ takes place during test but mostly after the flame is shut down and oxygen gets into testing equipment. $Fe_2O_3$ unlike FeO has limited mutual solubility with MgO and the excess $Fe_2O_3$ forms magnesio - ferrite in shape of small crystals in a surface layer of MgO up to 200μm as it is shown at ***Figure 28***.

Dissolution of MgO to Fayalite slag causes change of composition of the slag. Melting point of the fayalite (1205°C) with increasing MgO amount in it is shifted toward higher temperatures as ***Figure 29*** shows. As more MgO is dissolved in the slag viscosity increases, ratio of liquid phase decreases and eventually a total solidification occurs (at testing temperature 1400°C) at MgO grain surface where the effect has the strongest influence.

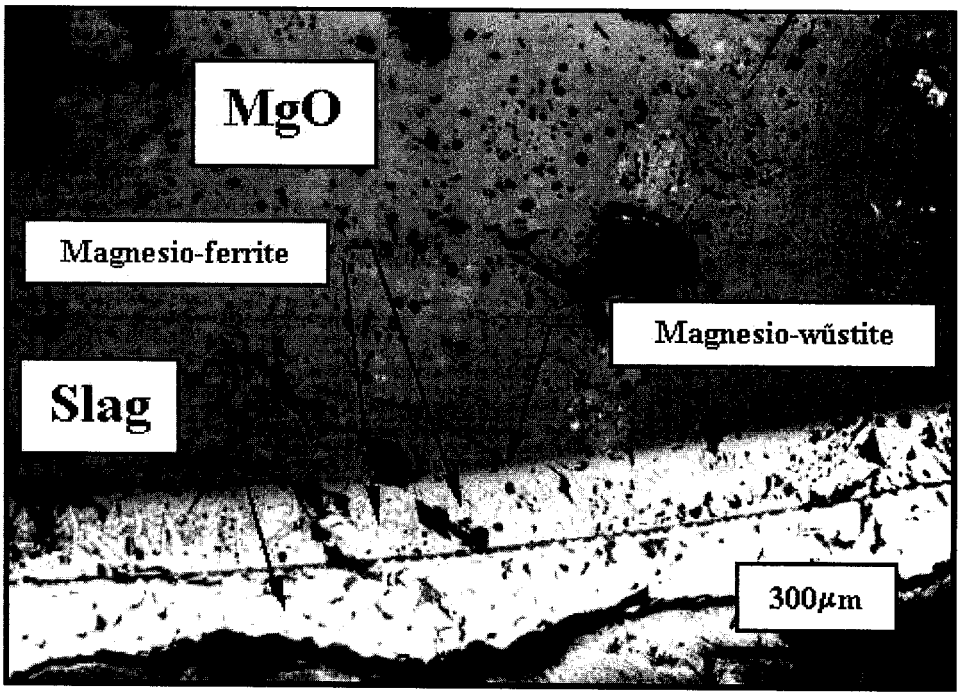


***Figure 28****: MgO - fayalite slag interface after rotary slag test at 1400°C/8hrs, 20x.*

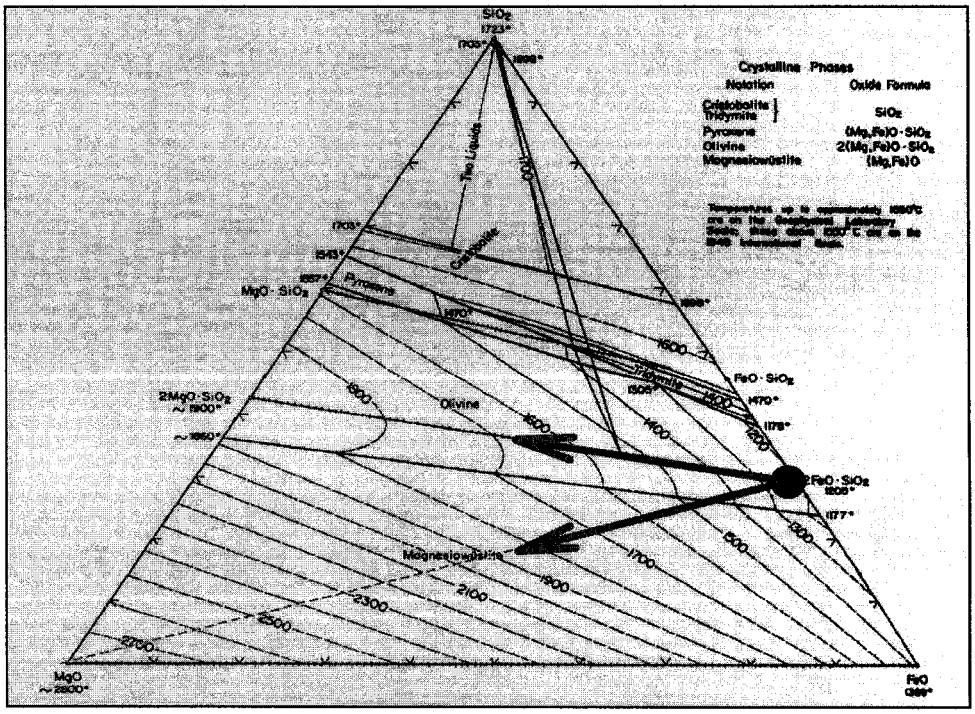


***Figure 29**: The FeO-$SiO_2$-MgO system.*

## 1.2. FORSTERITE - FAYALITE SLAG

Fayalite ($Fe_2SiO_4$) and forsterite ($Mg_2SiO_4$) form a solid solution with unlimited mutual solubility, as shown in ***Figure 30*** with melting points of 1205°C and 1890°C respectively. Fayalite and forsterite coexist (do not react with each other), but mutual solubility, as ***(11)*** describes, is being hold at all time. ***Figure 31*** proves this fact, by showing forsterite grain in contact with fayalite slag where the interface is scarcely visible and more or less continuously fayalite – forsterite transition can only be seen. The surface layer of olivine (forsterite) grain is enriched in FeO, while slag becomes, at the vicinity of the grain, richer in MgO.

$$\left[xMg_2SiO_4\right]_{(s)} + \left[yFe_2SiO_4\right]_{(l)} \Rightarrow \left(Mg_x; Fe_y\right)_2 SiO_{4(l,s)} \quad (11)$$

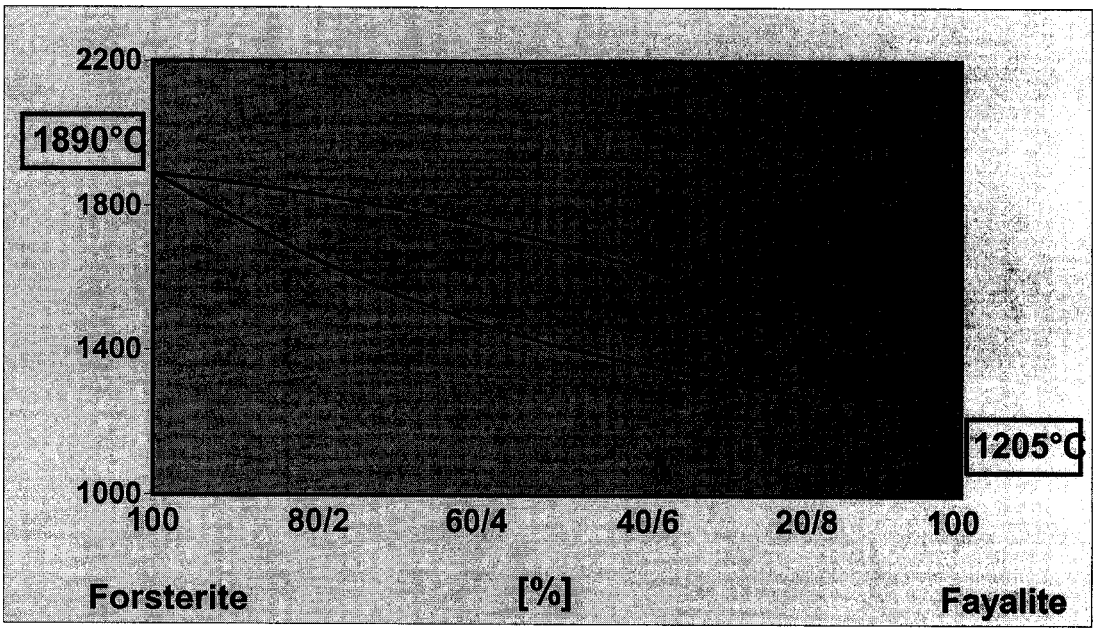


***Figure 30:*** *Forsterite - fayalite phase diagram.*

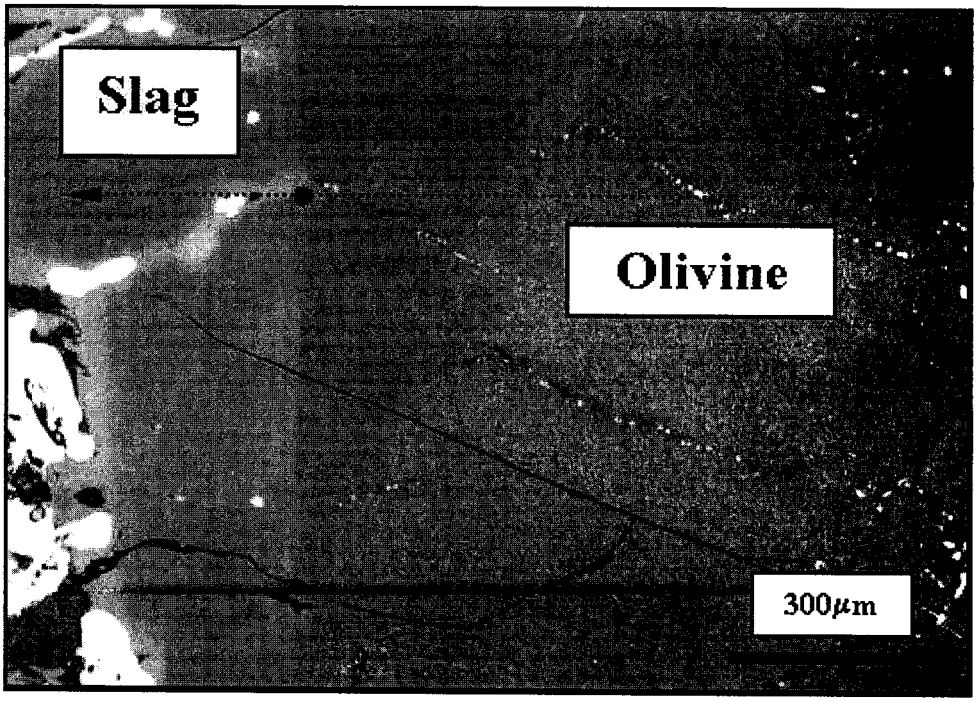


***Figure 31:*** *Olivine – fayalite slag interaction after rotary slag test at 1400℃/8hrs, 20x*

## *1.3. MgO - Calcium Ferrite Slag*

MgO coexists with dicalcium ferrite ($Ca_2Fe_2O_5$) but does not coexist with calcium ferrite ($CaFe_2O_4$) as shown in ***Figures 32*** and ***33***. The following chemical reaction may reflect the phenomena:

$$MgO_{(s)} + 2CaFe_2O_{4(l)} \Rightarrow MgFe_2O_{4(s)} + Ca_2Fe_2O_{5(s,l)} \qquad (12)$$

MgO (**M**) and $CaFe_2O_4$ (calcium ferrite – **CF**) can only reach mutual equilibrium by forming $MgFe_2O_4$ (Magnesio ferrite – **MF**) and $Ca_2Fe_2O_5$ (Dicalcium ferrite - **$C_2F$**) as shown in ***Figure 34*** with invariant point (occurrence of first liquid phase) for the system M – MF - $C_2F$ at temperature of 1335°C.

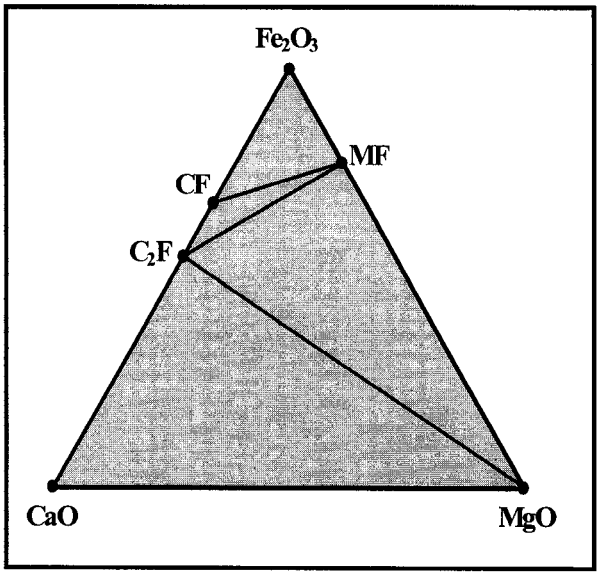


***Figure 32***: *The CaO-MgO-$Fe_2O_3$ phase diagram.*

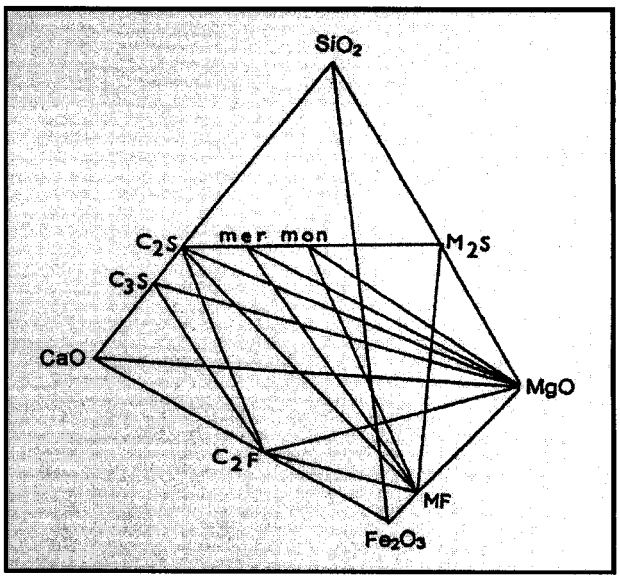


***Figure 33:*** *The $SiO_2$ – CaO – MgO – $Fe_2O_3$ system.*

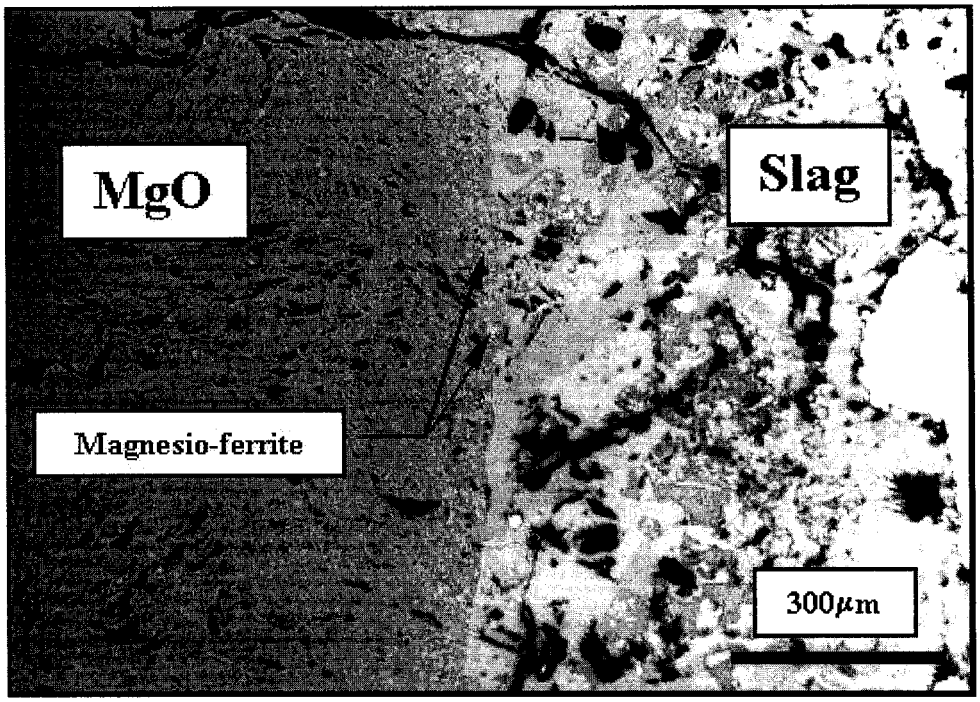


***Figure 34:*** *MgO – calcium ferrite slag interaction after 1400 °C/8hrs, 20x*

## *1.4. FORSTERITE - CALCIUM FERRITE SLAG*

Forsterite, as ***Figures 32*** and ***33*** indicate, does not coexist with calcium ferrite – the major constituent of the calcium ferrite slag and react following the reaction ***(13)***.

$$Mg_2SiO_{4(s)} + 2CaFe_2O_{4(l)} \Rightarrow 2MgFe_2O_{4(s)} + Ca_2SiO_{4(s)} \qquad (13)$$

The slag and olivine grain are decomposed at the mutual surface and lead to magnesio-ferrite and dicalcium silicate as reaction products.

Since forsterite ($Mg_2SiO_4$) and dicalcium ferrite ($Ca_2Fe_2O_5$) (from the reaction ***12***) do not coexist either, a further reaction goes on according to equation ***(14)***.

$$Mg_2SiO_4 + Ca_2Fe_2O_5 \Rightarrow MgFe_2O_4 + Ca_2SiO_4 + MgO \qquad (14)$$

Reaction layer (shown in ***Figure 35*** as well as in detail in ***Figure 36***) as a result of that reaction is composed of small crystals of magnesio ferrite ($MgFe_2O_4$) in MgO and dicalcium silicate ($Ca_2SiO_4$).

The reaction layer is strongly visible along each olivine grain in contact with calcium ferrite slag and the thickness is up to 100μm.

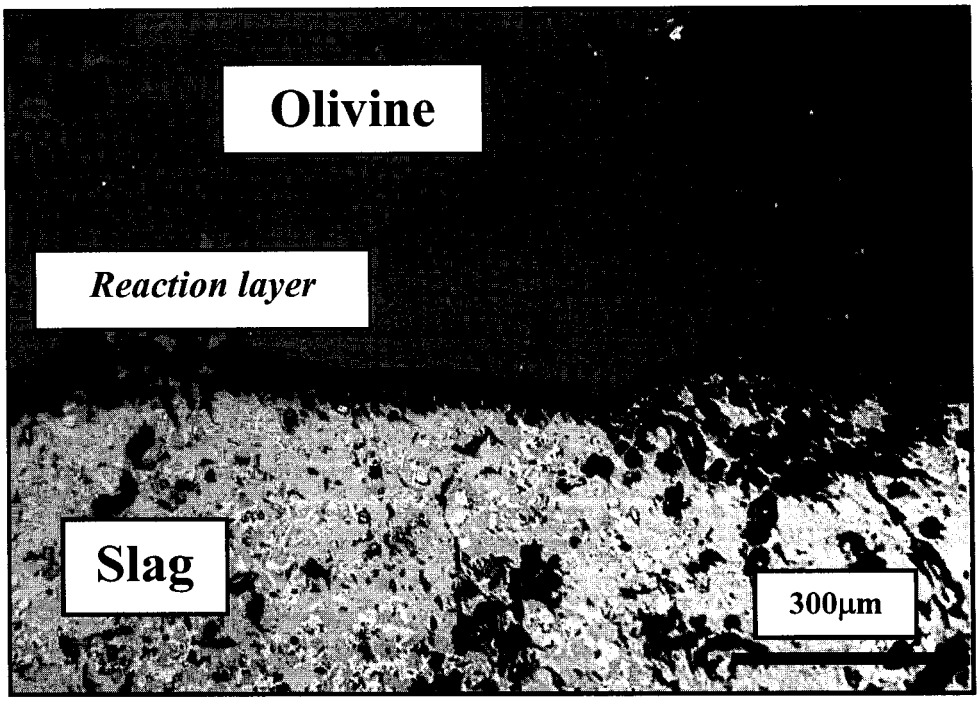


***Figure 35:*** *Olivine in contact with calcium ferrite slag, 20x.*

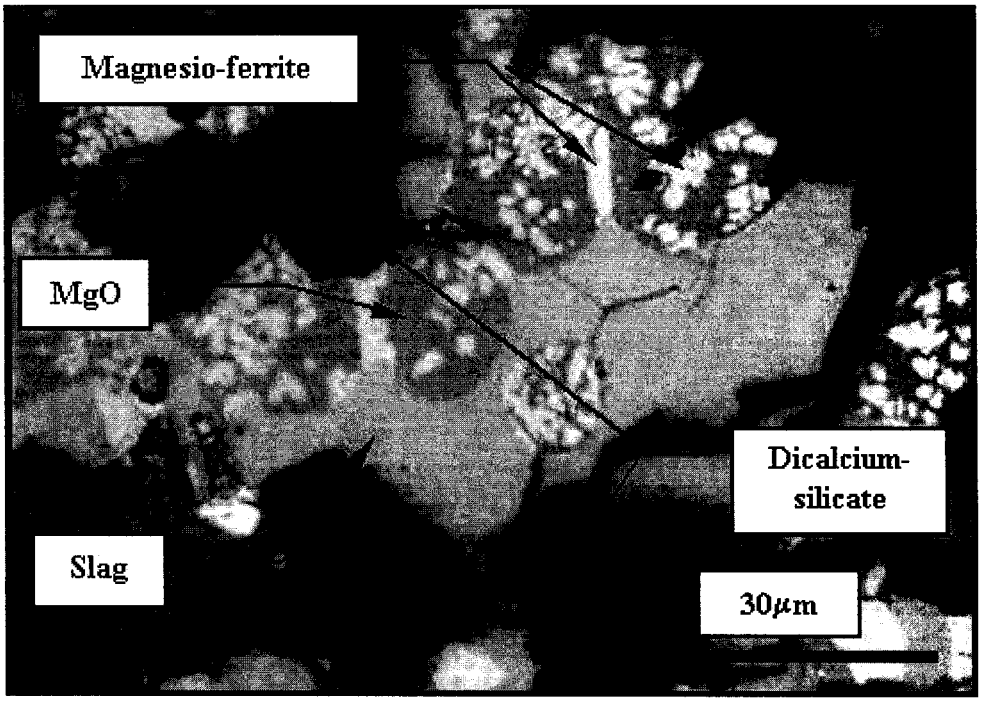


***Figure 36**: Reaction layer between olivine grain and calcium ferrite slag, 100x.*

## 2. GENERAL DISCUSSION

Corrosion mechanisms of olivine – MgO castables in fayalite and calcium ferrite slags are different. Characteristic feature in ***fayalite slag*** is unlimited mutual dissolution of both major constituents olivine and MgO into slag. Dissolution of both olivine and MgO, causes significant changes in composition of the fayalite slag. With increasing of amount of forsterite and MgO in slag, the melting point of the system is shifted to higher temperature, which causes increasing of viscosity. The slag enriched by forsterite or MgO at testing temperature, which is 1400°C can even reach composition where solidification occurs. The dissolution processes are being held primarily in thin layer of refractory – slag interface, which can be considered as a barrier for direct contact refractory and fayalite slag. Combination of high viscosity and good adhesion of the thin film on refractory "plays" self-protecting function against rinsing by slag of lower viscosity. Even regularly slag – renewing has no significant effect on the processes at interface.

According to the forsterite - fayalite phase diagram (***Figure 30***), composition needed for complete solidification at 1400°C is 50% of fayalite and 50% forsterite. Theoretically, 100g of fayalite (the layer) is needed to dissolve 100g of forsterite (olivine) to reach precipitation of a solid phase. Effect of MgO is even bigger and to get the same composition, only 23.4 g is needed to be dissolved. Differently said, MgO withstands attack of fayalite slag better and it is also noticeable in ***Figure 37***. Thus there is no surprise that with increasing amount of MgO, performance (dissolution – erosion rate depicted in ***Figure 16***) of the olivine-MgO castable is better.

Temperature in most copper making units rarely reaches values over 1200-1250°C. At this temperature the solidus composition in binary forsterite – fayalite system

is at 85% of fayalite, which means that the solubility of forsterite in fayalite slag would be substantially lower and the effect of corrosion-dissolution of olivine grains will be less critical than determined at testing temperature of 1400°C.

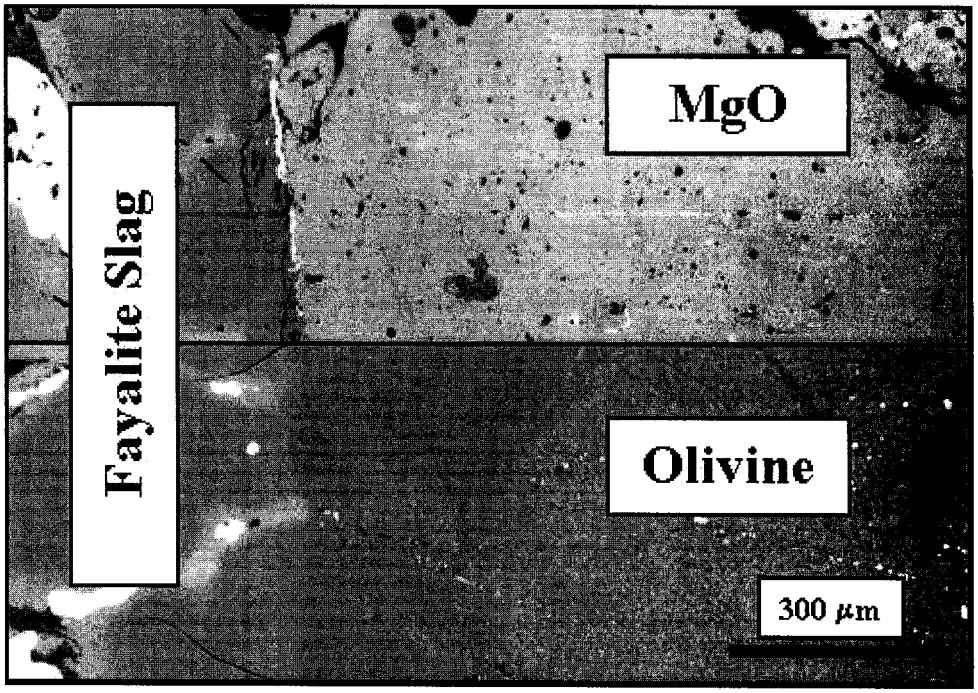


***Figure 37**: MgO and olivine grains in contact with fayalite slag, 20x.*

Characteristic features for interaction between olivine and ***calcium ferrite slag*** are chemical reactions leading to mutual equilibrium. Generally speaking the calcium ferrite slag is less aggressive then fayalite slag. Interaction between forsterite and calcium ferrite ($CaFe_2O_4$) as a major component of calcium ferrite slag lead to magnesio ferrite ($MgFe_2O_4$), dicalcium silicate ($Ca_2SiO_4$), MgO and dicalcium ferrite ($Ca_2Fe_2O_5$), which coexist and do not react further. MgO basically withstands the calcium ferrite better then olivine, as illustrated in ***Figure 38***; the case is similar to the fayalite slag interaction with increasing amount of MgO in olivine-MgO castable: the corrosion resistance increases.

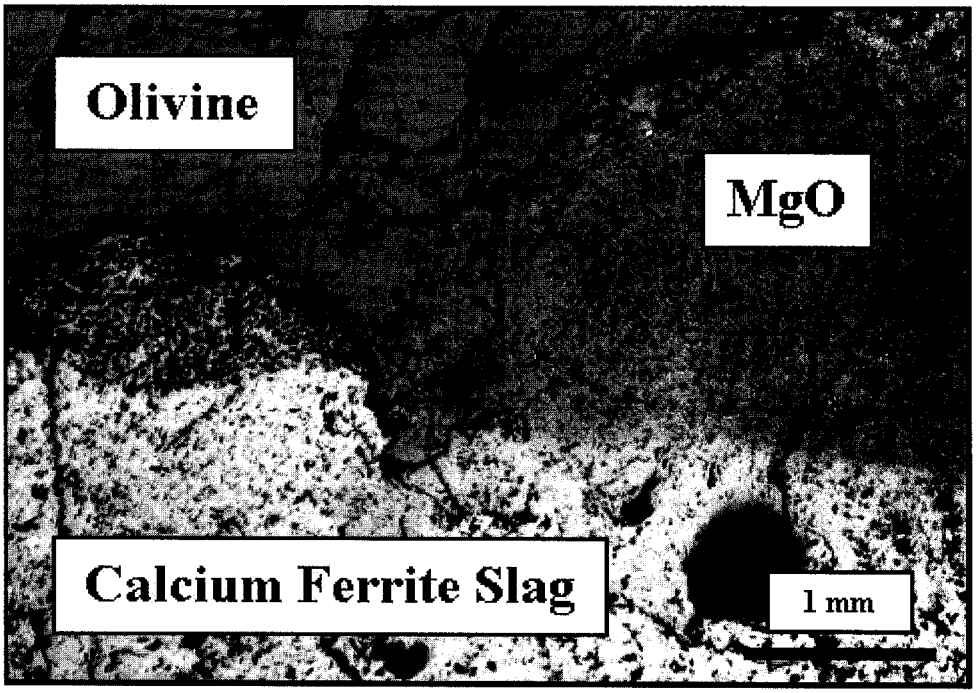


***Figure 38**: MgO and olivine in contacts with fayalite slag, 5x.*

Naturally there is a direct connection between composition of the slag and the rate of penetration into refractory. Physical – chemical processes are illustrated in ***Figures 39*** and ***40***. When olivine – MgO castable are in contact with either fayalite or calcium ferrite slag, there is net increase in the slag. Viscosity of the slag is one of the major factors, which rules the rate of penetration. It appears that, olivine containing refractory has a self-protecting mechanisms that reduces the penetration in both cases, which explains the fact that penetration depths in olivine-MgO castables determined by optical microscopy as depicted in ***Figures 22*** and ***23*** were much lower than in the mag-chrome brick, as a reference.

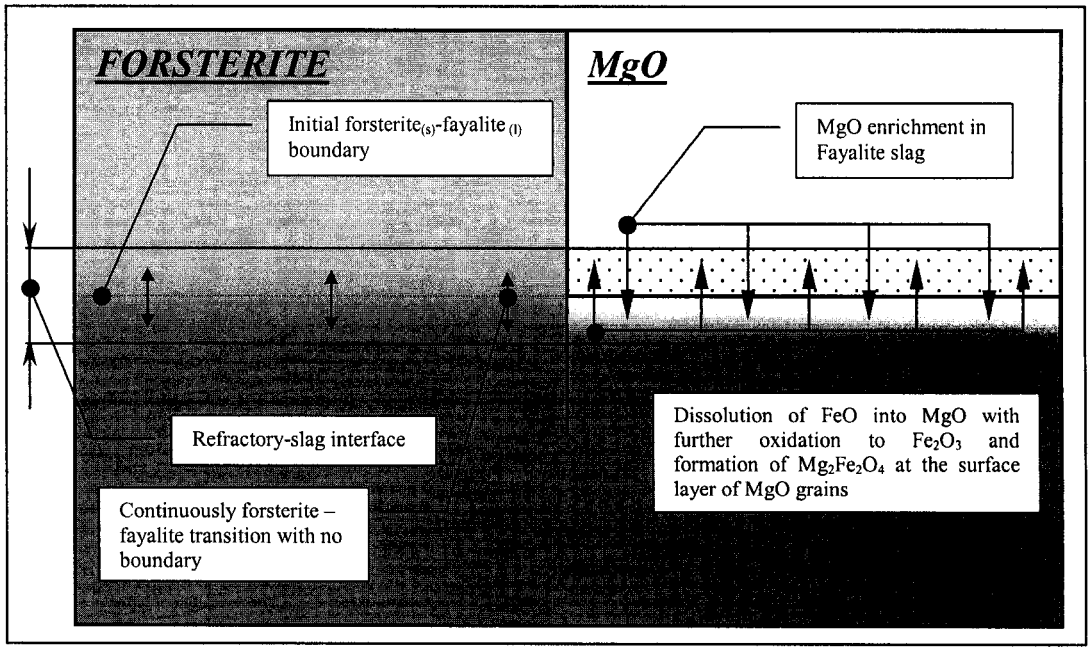


***Figure 39***: Features of olivine – MgO – fayalite slag interactions.

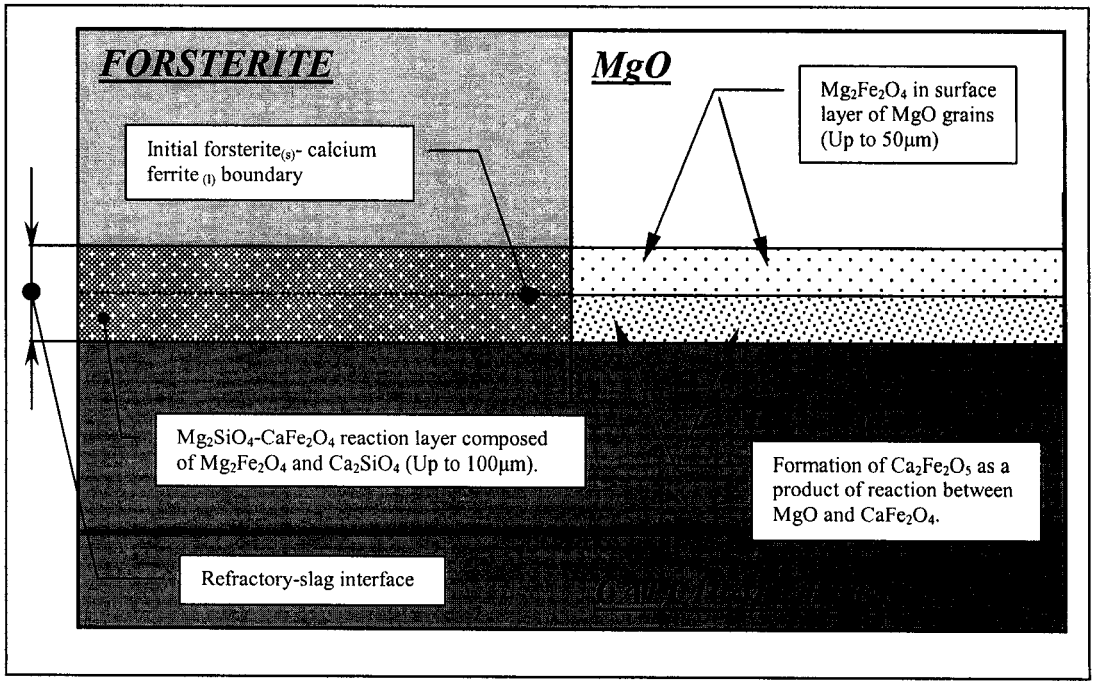


***Figure 40***: Features of olivine – MgO – calcium ferrite slag interactions.

# CHAPTER VI

## CONCLUSIONS AND RECOMMENDATIONS

Four olivine – MgO castables (C-2, C-3, C-4 and C-5) with graded MgO addition, which have been designed and prepared at CIREP, were selected for corrosion testing in fayalite and calcium ferrite slags. Magnesia – chrome bricks (REF) as a reference and a commercial olivine – MgO castable (C-1) as an additional reference were involved in testing and used as a comparison. The increasing dissolution – erosion resistance with increasing amount of MgO was determined in both slags. In fayalite slag the resistance increased steadily from C – 2 with 82% of olivine and 15% of MgO to C – 5 composed of 37% of olivine and 60% of MgO. In calcium ferrite slag already 30% of MgO (C – 3) significantly increased resistance of the castable against dissolution – erosion comparing to castable with 15% of MgO addition (C – 2). MgO amount above 45% (C – 4) appears not to have considerable contribution to total resistance of the olivine – MgO castable. The commercial castable (C – 1) used as second reference, has chemically fitted in between castable C – 2 and C – 3 and so dissolution – erosion rate was determined as well. In both slags, the values of dissolution-erosion of olivine-MgO castables were higher than of the reference magnesia-chrome brick.

However castable C – 5 composed of 60 % of MgO and 37% of olivine has got close to REF in both fayalite and calcium ferrite slag.

As far as penetration is concerned, all CIREP's castables (C-2, 3, 4, 5) were penetrated up to 1 mm in both slags. Olivine – MgO system has a self – protecting mechanism, which reduces penetration. In both slags, interactions between olivine, MgO and fayalite ($Fe_2SiO_4$) and calcium ferrite ($CaFe_2O_4$) as major constituents of the fayalite and calcium ferrite slag respectively, lead to increasing viscosity of the slags at the

vicinity of the interface. The thin layer (up to100μm) at the interface, as a result of mutual dissolution of phases, protects the refractory from penetration. On the other side the magnesia - chrome brick (REF) has been penetrated much deeper in both fayalite (up to 6mm) and calcium ferrite (up to 9mm) slags.

Matrix of the castables has been composed of BMF MgO, fine crushed olivine and 3% of microsilica. $SiO_2$ forms forsterite through reaction with MgO added in to castable as well as with MgO coming from the decomposition of olivine. As have been discussed, mutual dissolution of forsterite and fayalite is a significant proportion in the corrosion of olivine - MgO castable in fayalite slag. Microsilica addition on the one hand improves rheological behavior of the castables but on the other hand increases the amount of forsterite in matrix. If an alternative material could replace the microsilica in matrix, amount of forsterite would be decreased and total dissolution of the castables should be lower than have been determined for microsilica containing olivine-MgO castables.

An introduction of graphite into the castables seems to be another possible improvement of the olivine-MgO castables. The latest research on CIREP indicates, that dissolution – erosion wear of silica-free refractory with the addition of graphite pellets and metallic antioxidants (Al, Si) as a protection of the graphite against oxidation, can be even lower that magnesia-chrome brick. Penetration into that kind of refractory can be minimized to even less than 1 mm.

Corrosion testing has been carried out at higher temperature (1400°C) than in real working temperature. Corrosion testing completed at 1250°C did not allow determining any dissolution – erosion rate and increasing testing temperature was the only way to make the corrosion wear of several refractory materials recognizable. Refractory lining is commonly in use for months even years and it cannot be simulated in laboratory conditions. Even if olivine – MgO castable have not reached dissolution – erosion

resistance as good as magnesia – chrome brick, there is grounded supposition of much better performance of that kind of refractory at temperature of 1200-1250 °C.

With both fayalite and calcium ferrite slags, a test with the same configuration of the specimens was repeated three times. The results obtained from the tests showed that reproducibility of the test is satisfactory. As for the rotary slag test as a testing method itself can be stated that for comparing of several refractory samples tested in one run the method is sufficient. Relative corrosion wear of different samples can be compared and samples ranked from best to worst or vice versa.

Knowledge obtained from experimental work and collected in this work indicate that:

- Olivine-MgO castables could be considered as possible candidate for application in copper making units. The low penetration of fayalite and calcium ferrite slag indicates a potential for good structural spalling resistance of this type of refractory in copper applications.

- Relatively high solubility of olivine grain in fayalite, and high reactivity in calcium ferrite slag, excludes this refractory material from applications in zones in copper making units where temperature would much exceed 1250°C generally considered as a copper making temperature.

- Further study of the olivine – MgO castables with different granulometry and dispersants may lead to lower porosity and increase corrosion resistance. In this study porosity of castable fluctuated between 15.5 and 17%.

- Introducing anti-wetting additives like graphite and metals into olivine-MgO castables, which have begun lately [21], appears to be a way to increase corrosion resistance against, at least, fayalite slag.

- Theoretically, fine $Al_2O_3$ could be considered as a possible replacement of microsilica in matrix of olivine –MgO castable. Theoretically, MA spinel as a product of $Al_2O_3$ with MgO in matrix would decrease the amount of forsterite, which is easy dissolved in fayalite slag, and is formed through reaction of $SiO_2$ with MgO in matrix and that could increase corrosion resistance of the castables against fayalite slag.

- Hypothetically, introducing of limited amount of $Cr_2O_3$ into olivine castables could be considered. Well-known anti-wetting effects of $Cr_2O_3$ as well as its proven good resistance against dissolution into slags, would surely improved the performance at least in fayalite slag, where $Cr_2O_3$ would cause no health hazard whatsoever.

# ***REFERENCES***


1. J. Mosser, G. Karhut, "Refractories at the Turn of the Millennium", Proceeding UNITECR '99, Berlin, Germany, September 1999, pp. XXV-XXX.
2. R.I. Robertson, P.L. Smith, J. White, "Research of Metallurgical Slags at Glasgow and its Contribution to Refractory Research", Ironmaking and Steelmaking, Vol. 12, No. 3, 1985, pp. 124-135.
3. K. Goto, W.E. Lee, " The Direct Bound Magnesia Chromite and Magnesia Spinel Refractories", J. Am. Ceram. Soc. Vol. 78, No. 7, 1995, pp. 1753-1760.
4. K. Hiragishi, H. Fukuoka, K. Asano, K. Hayashi, " Corrosion of Various Basic Bricks By $CaO$-$SiO_2$-$Fe_2O_3$-$MgO$ Slag", Taikabutsu Overseas, Vol. 5, No. 1, 1985, pp. 12-20.
5. N. Usaki at al., "Development of Magnesite-Chrome Refractories with high Thermal Shock Resistance", Interceram, Vol. 40, No. 5, 1991, pp. 279-283.
6. K. Cherif, V. Pandolfelli, M. Rigaud, "Factors Affecting the Corosion By Fayalite Slags and the Thermal Shock Performance of Magnesia-Chrome Bricks", Jour. Can. Cer. Soc., Vol. 66, No. 3, 1997, pp. 210-216.
7. M. Dionne, M. Rigaud, " Comparative Study of Various Magnesia-Based Refractory for the Copper Industry, Internal Report, 1995.

8. M. Rigaud, CIREP Report on NSERC Collaborative R&D Project," Characterization and Evaluation of New Refractories for the Copper Industry", 9 reports between 1994 and 1996.

9. M.D. Crites et al., " Interaction of Chrome-Free Refractories with Copper Smelting and Converting Slags 2, Proceedings Advances in Refractories for the Metallurgical Industries III, Quebec City, Quebec, 1999, pp 203-214.

10. M.E. Schlesinger et al., "Chrome-Free Refractories for Copper Production Furnaces", Proceeding UNITECR '97, New Orleans, LA, 1997, pp. 1703-1708.

11. S. Palco, M. Rigaud, " Results of Laboratory Tests of Three Classes of Refractories for the Copper Industry", Report of Investigation, September 1999.

12. G.R. Rigby, B. Hamilton," A study of Basic Bricks from Copper Anode Furnaces", J. Am. Cer. Soc., Vol. 44, No. 5, 1961, pp. 201-205.

13. G.R. Rigby, "A study of Basic Brick from Various Copper Smelting Furnace", Transactions of the Metallurgical Society of AIME, Vol. 224, October 1962, pp. 887-892.

14. H.M. Mikami, A.G. Sidler, " Mechanisms of Refractory Wear in Copper Converters", Transactions of the Metallurgical Society Of AIME. Vol. 227, October 1963, pp. 1229-1245.

15. H. Pressley, J White, Phase Relationship and Microstructures in certain Copper Oxide-Containing Systems and their Bearing on the Attack of Copper Slags On Basic Refractories" Trans. J. Br. Ceram. Soc., Vol. 78, No. 1, 1979, pp. 4-10.

16. M. Mäkipää, P. Taskinen, " Rfractory Wear In Copper Converters: Part I, Blister Copper-Refractory Interactions", Scandinavian Journal of Metallurgy, 9, 1980, pp. 273-281.

17. A.H. Jagari. S.A. Davoodi, H.R. Hassani, K.Bagheri, "Hot Corrosion Mechanisms of Magnesite-Chromite Refractories used at Reverberatory Furnaces in Iran's Sarcheshmeh Copper Complex and Development of Iranian Refractory Productions" Proceedings Advances in Refractories for Metallurgical Industries III, Quebec City, Quebec, 1999, pp. 217-229.

18. R.A. Landy, " Postmortem of Rexal 60 DB from the Tuyere line of Pierce-Smith Converter, Horne Smelter, Noranda" Report, 1998

19. A. Yazawa, Thermodynamic Considerations of Copper Smelting", Canadian Metallurgical Quarterly, Vol. 13, No. 3, 1974, pp. 121-125.

20. L. Molnar, P. Vadasz, M. Kozlovsky, " Study of Interactions at the Slag-Basic Refractory Boundary", Ceramics-Silicaty, Vol. 37, No. 3, 1993, pp. 121-125

21. E. Kosc, E. Paransky, S. Palco, M. Rigaud, "Olivine-based refractory for copper industry", accepted for EMC 2003, September 16-19, Hannover, Germany

# APPENDIX I

## 1. OLIVINE

Olivine is greenish magnesium silicate mineral made up of a solid solution of forsterite ($Mg_2SiO_4$) and fayalite ($Fe_2SiO_4$) as shown in ***Figure 41***. The name "olivine" was first applied by Werner in 1790 because of its olive-green colour.

Forsterite is named after the German naturalist, Johan Forster. It is one of two minerals that are simply known as **olivine** Forsterite is the magnesium rich member with a pure formula of $\mathbf{Mg_2SiO_4}$, corresponding to 57,3 % magnesia (MgO) and 42.7 % silica ($SiO_2$) [22]

Fayalite is named after the Island of Fayal of the Azores. It is the iron rich member with a pure formula of $\mathbf{Fe_2SiO_4}$. Due to its iron content has a higher index of refraction, is heavier and has a darker colour than forsterite. Melting temperatures of forsterite and fayalite is 1890°C and 1250°C respectively as shows on in ***Figure 41.***

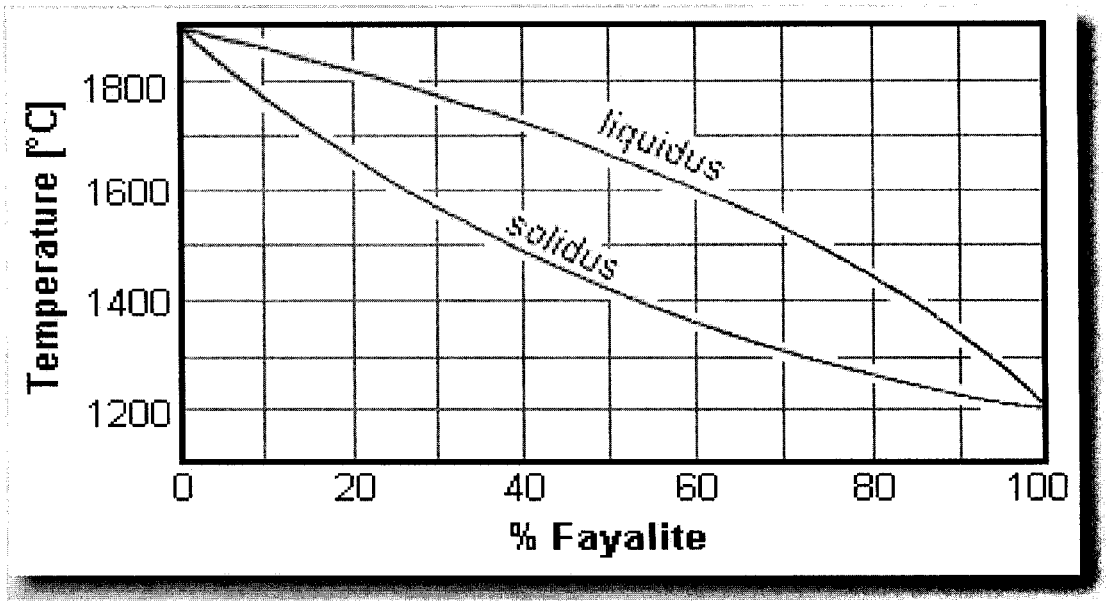


***Figure 41:*** Binary system forsterite ($Mg_2SiO_4$) – fayalite ($Fe_2SiO_4$) showing total miscisity in the molten and solid state.

## *1.1. MINERALOGY AND MODE OF OCCURRENCE*

Olivine is a group of orthosilicate minerals in isomorphous series, with magnesium-rich forsterite ($Mg_2SiO_4$) and iron-rich fayalite ($Fe_2SiO_4$) as end points. In commercial practice, olivine applies to deposits containing a mixture of forsterite and fayalite in solid solution with fayalite content usually limited to less than 15% and forsterite more than 85%.

The chemical composition of olivine is slightly different according to different region, which is expressed in ***Table 16***.

***Table 16:*** Chemical analyses of some commercial olivine (%).

(**1** – Ste.Anne des Monts, P.Q. Canada; **2** – Leoben. Austria; **3** – Aaheim, Norway; **4** – Norddal, Norway; **5** – Burnsville, NC, USA; **6** – Hamilton, WA, USA; **7** – Capaleda, Spain; **8** – Vidracco, Italy)

| | 1 | 2 | 3 | 4 | 5 | 6 | 7 | 8 |
|---|---|---|---|---|---|---|---|---|
| MgO | 47.5 | 43-44 | 49.0 | 47.7 | 46.4 | 46.9 | 37-38 | 41-43 |
| $SiO_2$ | 40.4 | 24-35 | 42.6 | 40.8 | 42.5 | 40.8 | 38-39 | 42-44 |
| $Fe_2O_3$ | 9.0 | 7.6-7.7 | 6.0 | 7.5 | 8.0 | 9.4 | 0.08 | 6.5-8.9 |
| other | 2.5 | 0.7-0.8 | 1.8 | 1.9 | 2.4 | 3.2 | | 3.5-7.1 |
| LOI | 0.8 | ? | 1.6 | 2.0 | 0.5 | 0.6 | 10 | |

Commercial olivine occurs as alpine-type and zoned dunite bodies. There is general agreement about the origin and mode of emplacement that most olivine have been emplaced in a partially crystallised condition (much) and that in part at least, foliation present in many unmetamorphosed dunites results from flowage during emplacement prior to complete crystallisation.

Unlike pure magnesite, magnesium silicate deposits are so abundant in nature that they can be considered to be virtually inexhaustible. For example, there are extensive

olivine deposits of varying quality in Albania, Austria, Norway, Russia, Sweden and The USA [23].

In Norway alone the high quality deposits in Aaheim have reserves that have been estimated to amount of more than two billion tons. In the USA, significant deposits of high quality dunites are found in Western North Carolina and Georgia and also in the Puget Sound region of the state of Washington. The dunites in North Carolina and Georgia from a belt 175 miles wide, extending from Watunga County, North Carolina south-westward to White County, Georgia [24].

At some localities, those dunites have been altered to serpentine and talc, however, in general, the deposits are fairly free from serpentine and other impurities. In the state of Washington the principal dunite deposit occurs 20 miles inland from Bellingham in the Twin Sisters Mountains [25]. That deposit forms a northwest range about10 miles long in Skaget and Whatcom Counties between Seattle, Washington in the U.S. and Vancouver, British Columbia in Canada. That entire range of peridotites consists of approximately 90% of unaltered dunite with serpentines and pyroxenites comprising the other 10%.

At the present, more than 3 million tons/year of olivine are produced in Norway alone (A/S Olivin Åaheim). The olivine deposits in Åaheim, containing 90% olivine with weight content at 50% magnesium oxide, has calculated reserves of 2 billion tons, and is thereby world's largest known deposit of high-quality olivine [26].

Worldwide consumption totals about 6 million tons, including 2 million tons in Japan. About 10% of the total quantity is used in traditional fields such as foundries, abrasives and refractories.

In special cases olivine forms as the igneous rock olivenites which can be directly applied as an industrial refractory material. Through the action of moisture, olivenites are often heavily weathered on the surface. This results in the transformation of same of the olivine into the hydrous magnesium silicate, serpentine ($(Mg, Fe)_6Si_4O_{10}(OH)_8$), and perhaps also some brucite ($Mg(OH)_2$) and magnesite ($MgCO_3$). Unless the brucite and magnesite remain within the rock, it may become severely depleted in magnesia (MgO).

As evident from the phase diagram for the MgO-$SiO_2$ system, ***Figure 42***, such MgO loss will create a substantial reduction in the refractoriness [27].

Certain natural magnesium silicates, known as dunites, which consist of olivine and serpentine do not undergo large volumetric changes when they are fired. They can actually be used as refractories in their natural state. However, it has not been possible to develop an economical method of shaping or sawing these natural olivinites and dunites, which, unlike talc (only 1 on the Mohs scale), are much harder (about 7 on Mohs scale) and are quite brittle [28]. Some physical properties of olivine are shown in ***Table 17*** [29].

***Table 17***: Physical properties of olivine.

| | |
|---|---|
| Specific Gravity | 3.1-3.3 g/cm$^2$ |
| Bulk Density (Dry sand; Unpacked) | 1.4-1.7 g/cm$^2$ |
| Bulk Density (Dry sand; Compacted) | 1.7-1.9 g/cm$^2$ |
| Bulk Density (Dry sand; Moulding sand) | 1.7-1.9 g/cm$^2$ |
| Hardness (Moh's scale) | 6.5-7 |
| Expansion (25-1200°C without crystal change) | 1.6% |
| Specific Heat (25-1500°C) | 0.20-0.33 cal/g/°C |
| Grain Shape | Angular |
| PH-Value | 9 |

## *1.2. FORSTERITE ($Mg_2SiO_4$)*

The stoichiometric compound forsterite ($Mg_2SiO_4$) consists of 57.2% MgO and 42.8%$SiO_2$ by weight. It crystallises on the orthorhombic structure. At one atmosphere pressure this material is known to exist in only the one crystal form. It has a density of 3.21 g/cm$^3$ and a melting point of 1890°C. Since it has a high melting point (1890°C), forsterite is considered to be a potentially useful commercial refractory material.

Unfortunately, no deposits of pure forsterite are known to exist [30]. Natural magnesium orthosilicate is only known to occur as solid solutions with the ferrous orthosilicate, fayalite ($Fe_2SiO_4$). These solid solutions are known as olivines, for which the chemical formula is usually written as $(Mg, Fe)_2SiO_4$, even though the Mg and Fe are not in 1:1 ratio as it may be implied. The melting temperature of pure fayalite (1250°C) is quite low relative to that of pure forsterite (1890°C). As the content of the ferrous component is increased, the melting point of olivine is severely reduced, as shown in fayalite-forsterite phase diagram, ***Figure 41***. Nevertheless, olivines containing 10-15% of FeO, a compositional level that occurs in many natural deposits, are quite suitable as raw material for producing industrial forsterite refractories [31].

Forsterite has an orthorhombic crystal structure with an "a" lattice parameter of 4.756 Å, a "b" of 10.207 Å and "c" of 5.980 Å at room temperature. The average principal linear thermal expansion coefficient between room temperature and 600°C have been reported by Skinner [32] to be: $\alpha_a = 9.2 \times 10^{-6}/°C$, $\alpha_b = 12.6 \times 10^{-6}/°C$ and $\alpha_c = 11.3 \times 10^{-6}/°C$. Smyth and Hazen [33] have reported $\alpha_a = 8.0 \times 10^{-6}/°C$, $\alpha_b = 14.1 \times 10^{-6}/°C$ and $\alpha_c = 10.8 \times 10^{-6}/°C$. Kahn [34] has estimated similar principles thermal expansion coefficient for forsterite ($Mg_2SiO_4$) based on theoretical calculations applying polyhedral thermal expansion concepts. From these values, it is evident that forsterite possesses considerable thermal expansion anisotropy for $\alpha_b > \alpha_c > \alpha_a$. The average thermal expansion of forsterite is about $10 \times 10^{-6}/°C$, slightly greater than that of alumina ($8.0 \times 10^{-6}/°C$), but considerably less than that of magnesia ($14.5 \times 10^{-6}/°C$).

Forsterite is reported to fracture conchoidally and is generally considered to be brittle. It has a Mohs hardness of about 7. Olivine is usually crystallised with thick, tabular, striated grains or crystals that often exhibit wedge shaped terminations. It usually occurs as massive, compact or granular embedded grains, irregular or rounded [35].

## *1.2.1. FORSTERITE REFRACTORIES*

The system magnesia-silica ($MgO$-$SiO_2$) for which the phase diagram is depicted in ***Figure 1*** has been of primary importance to the refractories industry for at least half a century [36]. From that perspective the magnesia-silica system is practically equivalent in significance to the alumina-silica ($Al_2O_3$-$SiO_2$) system, for between pure alumina and pure silica there are a series of compositions, which constitute the bulk of aluminosilicate mineral-based refractories [37]. The magnesia-silica ($MgO$-$SiO_2$) system in analogous, as forsterite refractories are those which contain from 40.8 to 57.3% $MgO$ about a $2MgO{:}SiO_2$ ratio. During the processing, or use of these refractories, the mineral forsterite ($Mg_2SiO_4$) develops. Although pure forsterite melts at 1890°C, $MgO$-rich compositions may be liquid-free up to 1850 °C.

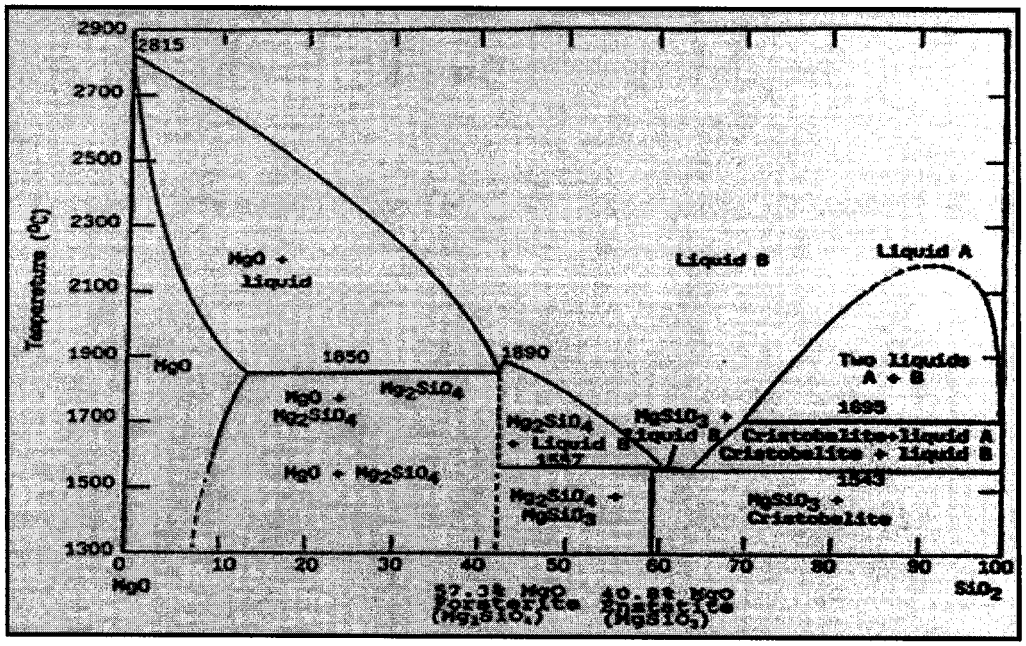


***Figure 42***: The binary system $MgO$ – $SiO_2$ after Bowen and Anderson [35].

To form forsterite the reactants are often pulverised dunite, serpentine, olivenite and other magnesium silicates with additions of caustic or sintered magnesite (dead-fired) to react with the excess silica ($SiO_2$) to form additional $Mg_2SiO_4$. These also react

with the $R_2O_3$ components to yield spinel phases. Different levels of magnesia may be added depending on the chemical and phase composition of the initial raw materials. For example about 7% magnesia must be added to olivenites, but only 4% to dunites, 16% for serpentines, and 36% to talcs. The formation of forsterite and the various spinel ($ROR_2O_3$) phases makes it possible to produce refractoriness for a given initial composition [38].

From economics perspective, the lower the amount of pure magnesia that must be added to achieve the forsterite composition, the more valuable is the mineral as refractory raw material. For example, if talc is used to synthesise forsterite refractories, there occurs the opportunity to choose complementary raw materials containing a considerable amount of magnesite (talc-magnesites), which means that less MgO as pure magnesia must be added.

## *1.3. MAGNESIUM METASILICATE ($MgSiO_3$)*

The magnesium metasilicate, enstatite ($MgSiO_3$), consists of 40.8 % MgO and 59.2 % $SiO_2$. It generally occurs in isomorphous mixtures with the metasilicate of iron, ferrosilicate ($FeSiO_3$). The density of enstatite is 3.18 g/cm$^3$. However, enstatite transforms at 1140°C to clinoenstatite, a compound those formula is also $MgSiO_3$, but which possesses a different crystal structure and properties. For example, enstatite crystallises in the orthorhombic system while clinoenstatite is monoclinic [39].

Magnesium metasilicate ($MgSiO_3$) melts incongruently with the precipitation of forsterite. The melting initiates at 1557°C and is completed by 1600°C on heating. Thus, the magnesium metasilicate, unlike forsterite, is not very satisfactory for steelmaking refractories. When technologically processed for refractory applications, the metasilicate must by combined with magnesia and converted into the orthosilicates (forsterite) according to the reaction:

$$MgSiO_3 + MgO \quad Mg_2SiO_4 \qquad (1)$$

This reaction proceeds rapidly in the solid state at temperature greater than about 1450°C.

Similar to forsterite, pure magnesium metasilicate is only rarely found in nature. The magnesium oxide is usually partially replaced by iron oxide to form a solid solution of the hypersthenes type $(Mg, Fe)_2Si_2O_6$.

The MgO may also be replaced by CaO or MnO in some deposits. The metasilicates in the form of these solid solutions are mineralogically known as pyroxenes. Minerals containing predominantly pyroxenes are known as pyroxenites. They are even more abundant in nature than olivinites, but unfortunately have widely variable compositions and contain considerable levels of impurities. It is the impurities, which prevent those minerals from being extensively used as raw materials in refractory industry [40].

## *1.4. SERPENTINE ($(Mg, Fe)_3Si_2O_5(OH)_4$)*

Serpentine is a rock-forming mineral commonly found in nature. It sometimes forms almost entirely without other impurities. It occurs frequently and usually in quite large deposits [41]. In the pure magnesia form, serpentine consists of 43 % MgO, 44.1 % $SiO_2$, and 12.9 % $H_2O$. It exists in two crystal forms: antigorite and fibrous chrysotile (chrysotile-asbestos). Both of these minerals crystallise in the monoclinic system and have densities from 2.5 – 2.8 g/cm$^3$. Serpentines may be magmatic or metamorphic. They are often the products of the hydration of anhydrous magnesium silicates, for example by the reaction:

$$2Mg_2SiO_4 + 2H_2O + CO_2 \quad Mg_3Si_2O_5(OH)_4 + MgCO_3 \qquad (2)$$

The fibrous forms of serpentine (chrysotile-asbestos) are industrially important as soundproofing, heat insulating, and electrically insulating materials. They are also extensively utilised as fillers for rubber and asbestos-cement products.

Forsterite and magnesium metasilicate are formed when serpentines are heated and the chemically bound water is liberated. The refractoriness of most serpentines is only about 1500°C because of the impurities, which are present. Hence, to obtain improved refractory products, additional magnesia must be added. During firing the

MgO reacts with the thermal decomposition products of the serpentine to yield pure forsterite. It also liberates water according to the reaction:

$$Mg_2Si_2O_5(OH)_4 + MgO \quad 2Mg_2SiO_4 + 2H_2O \qquad (3)$$

Also of significant importance are the dunites, which lie somewhere between olivenite and serpentine in composition. These can be processed to develop a superior refractory (refractoriness about 1700°C). However, dunites may contain water to level as high as 13 % in contrast to olivenites, so that considerable dimensional changes may be expected to occur upon firing. Similar to olivenites, some dunites can also be utilised as nonfired refractories in their natural state. Their hardness is also high (about 6.5) and they are quite brittle as well.

## 2. *THERMAL DECOMPOSITION OF OLIVINE ($(Mg, Fe)_2SiO_4$)*

Forsterite ($Mg_2SiO_4$) is a very stable material with a melting point of 1890°C, but fayalite ($Fe_2SiO_4$) has a melting point of only 1205°C. During the heating of olivine, two major changes occur [42-45]. First is the decomposition of the fayalite producing FeO and free $SiO_2$. The second one is the decomposition of serpentine and talc impurities, which may cause a molten material to be formed at relatively low temperature, about 1460°C to 1500°C.

Stone [46] has reported the decomposition of fayalite. As fayalite it liberates one $SiO_2$ and yields two FeO for each $Fe_2SiO_4$ of fayalite. The FeO oxidised to $Fe_2O_3$. Fayalite begins to decompose at about 500°C on heating and is completely oxidised at about 700°C. The absence of free $SiO_2$ in thin sections indicates that the $SiO_2$ remains in the forsterite matrix in very fine state. Simultaneously, the Fe migrates to the grain boundaries and there undergoes a series of changes. Between the temperatures of 20°C and 680°C the Fe, which has migrated to the grain boundaries, is oxidised to form $Fe_2O_3$.Then as the temperature is raised to 1480°C the conversion of $Fe_2O_3$ to $Fe_3O_4$ begins. The $Fe_3O_4$ migrates short distances to form tiny crystals on the cleavage planes and on the grain boundaries of the forsterite. At 1480°C most of the Fe has migrated to

the grain boundaries and has formed flakes or nodules of appreciable size. These flakes may react with the forsterite grains and the impurities which are present to form a very fluid magnesia-ferrous iron-silicate liquid. Also, by 1480°C considerable recrystallization of the forsteritic material has occurred, especially in the regions to which the iron oxide has migrated.

Birch and Harvey [45] have reported that when pure olivine is fired to 1450°C a considerable amount of molten material develops. They have observed that even thought the top of a specimen appeared normal; the pores at the bottom were often completely saturated with a glass. Since the firing temperature was 1450°C, a full 100°C below the eutectic of the $MgO$-$SiO_2$ system, it was obvious that components other than the MgO and $SiO_2$ from the forsterite had entered into that glass composition.

Birch and Harvey have concluded that the liquid was caused by the decomposition of serpentine and talc, which occurs as impurities in the olivine [40]. Serpentine ($(Mg, Fe)_3Si_2O_5(OH)_4$) contains equal amount of $SiO_2$ and MgO by weight. Talc ($(Mg, Fe)_3Si_2O_5(OH)_2$) corresponds to half as much MgO as $SiO_2$ by weight. At 1559°C, serpentine will form 60.5 % forsterite and 39.5 % of a siliceous liquid, while at 1554°C pure talc will become 4.4 % cristobalite and 95.6 % liquid phase of metasilicate. The presence of this amount of liquid phase can cause a considerable decrease in the load bearing ability of the refractory. The liquid formation and drainage can be prevented by the addition of sufficient MgO to convert the magnesium silicates, the talc and the serpentine, to forsterite during firing, and combine with the FeO, which is present to form the magnesioferrite spinel ($MgO.Fe_2O_3$).

## 2.1. MgO Additions to Olivine

From the $MgO$-$SiO_2$ phase diagram (***Figure 42***) is evident that composition between about 43 % and 61 % of $SiO_2$, will develop a liquid phase at the incongruent melting point of clinoenstatite. Thus, any olivine composition which contains $SiO_2$ levels above the forsterite composition will develop a liquid phase above 1557°C and might even form liquid phases as low as 1543°C under nonequilibrium condition. Liquid formation will occur at even lower temperatures if there are large amount of impurities present. The impurities can yield silica rich phases such as the phase diagram indicates. As MgO is added to olivine the percentage of free silica is reduced and the resulting compounds are shifted to the MgO side of the phase diagram, increasing the temperature of liquid formation to 1850°C.

A study of MgO additions to electrically fused olivine [46] demonstrated that the addition of 16% MgO by weight raised the "load-failure" temperature of an olivine refractory by 250°C, from 1500°C to 1750°C. The reason for the increase in the load failure temperature was that the MgO reacted with the low melting magnesium metasilicate (enstatite; $MgSiO_3$) to form the orthosilicate (forsterite; $Mg_2SiO_4$). MgO additions in excess of the amount needed to react with the free silica were also prepared and it was observed that the excess MgO concentrated as regions of periclase between the olivine grains. This further increased the hot load strength of the refractory as it prevented the olivine grains from sliding over one another during deformation preceding failure.

Stone [47] has studied the effects of MgO additions in varying amounts on the phase composition of fired olivine bodies. The reason that excess MgO is added to the olivine is to form secondary forsterite with the silica resulting from the decomposition of the fayalite and other products such as talc and serpentine. It can also be from magnesioferrite ($MgFe_2O_4$) with the iron oxide from the fayalite. Through microstructural observations of the fired olivine and MgO bodies, it was observed that the silica from the fayalite did not react. This was because it is not present at the grain

boundaries. On the other hand the FeO from the fayalite and the silica from the impurities does react with the MgO. In practice, additions of about 4% by weight of MgO prevented any shrinkage from occurring during firing. The theoretical amount of MgO for the reaction with all the SiO2 present from all of impurities was 12%.

Stone [48] has summarised four reasons why the olivine-MgO mixtures should be fired to at least 1590°C.

- First, at lower temperature, complete formation of secondary forsterite from the $SiO_2$ and $MgSiO_3$ does not occur.
- Second, the iron oxides do not readily react with the MgO to form magnesioferrite below 1590°C. It was observed that the spinel-forming reaction becomes more rapid at 1650°C.
- Third, forsterite will form from the $MgO{\bullet}SiO_2$ liquid arising within the grains of forsterite material at that temperature.
- Fourth, the temperature must be sufficiently high to permit the crystal growth of magnesioferrite and secondary forsterite. The higher the firing temperature, the more complete the above reactions, and that will lead to an improved olivine-MgO refractory.

# APPENDIX II

## PENETRATION

The penetration of the slag into the refractories is a complex process and is generally non-uniform in nature. The penetration front does not usually show as a clear-cut boundary, and very often rather as a blurred region. In the areas, which have been penetrated, not all pores are filled with slag and the slag penetration though interconnected pores followed selective channels and pathways. It is difficult to quantify the true depth of penetration. Obviously any such depth should be treated as an average whether it is determined by the amount (weight) of the slag penetrated, or by visual microscopic examination [49].

It is useful to distinguish between physical penetration and chemical invasion. Physical penetration, without dissolution at all, occurs when strictly nonweting liquid is forced into the pores of a solid by gravity or external forces. Chemical invasion occurs when dissolution and penetration are tied together. Both physical and chemical penetrations are favored by effective liquid-solid wetting and by low-viscosity liquid. Silicates, particularly silicate glasses, are usually viscous; simple oxidic compounds and basic slags are less viscous; and halides and elemental molten metals are, in general, the most fluid liquids.

Penetration is the result of interplay between capillary forces (surface tension), hydrostatic pressure, viscosity, and gravidity. Mercury penetration in a capillary glass tube is the best example of physical penetration. The rate of penetration in horizontal pore *dl/dt*, with a pore radius *r*, is given by following expression:

$$\frac{dl}{dt} = \frac{r\gamma_{lg}\cos\theta}{4\eta l}$$

Where $l_g$ is the surface tension of mercury in air, $\theta$ the wetting angle of mercury on the glass wall, $\eta$ the viscosity of the penetration liquid, Hg, over a length, *l*, at time, *t*.

This expression is valid only at constant temperature, where $\gamma_{lg}$ and $\gamma$ are liquid properties greatly influenced by temperature. Such an equation has often been used to describe the penetration of liquids in refractories without distinction between physical and chemical invasion. However, in the case of the chemical invasion, the penetration – dissolution causes changes in composition (which, in turn, affect the values of $\gamma_{lg}$ and $\gamma$), and changes in porosity geometry.

When the pore size distribution is narrow (i.e., pores of the same size), penetration and filling of the porosity by capillarity produce a relatively uniform front moving gradually from the hot face and remaining parallel to it. When pores size distribution is wide (i.e. very large and very small pores) or when open joints, cracks or gaps between bricks in a refractory wall are accessible at the hot face, rapid, and irregular liquid intrusion does occur. There are many penetration paths in a refractory, and the texture of material is of primary importance; it is important to distinguish between interconnected versus isolated porosity, between open and total porosity, pore size and unbounded boundaries between grains (aggregates and/or matrix) due to thermal mismatches during heating.

For a given temperature gradient, the pertinent eutectic temperature of the penetrating liquid determines its maximum liquid penetration depth [50].

# *APPENDIX III*

***Table 18**: Calculation packing density using Andreasen formula for coefficient n=0.26, 0.27 and 0.28*

| n = 0.26 | | | n = 0.27 | | | n = 0.28 | | |
|---|---|---|---|---|---|---|---|---|
| I. | II. | III. | I. | II. | III. | I. | II. | III. |
| 5.000 | 100.00 | | 5.000 | 100.00 | | 5.000 | 100.00 | |
| | | 21.20 | | | 21.92 | | | 22.63 |
| 2.000 | 78.80 | | 2.000 | 78.08 | | 2.000 | 77.37 | |
| | | 21.18 | | | 21.67 | | | 22.14 |
| 0.600 | 57.62 | | 0.600 | 56.41 | | 0.600 | 55.23 | |
| | | 14.32 | | | 14.48 | | | 14.62 |
| 0.200 | 43.30 | | 0.200 | 41.93 | | 0.200 | 40.60 | |
| | | 9.75 | | | 9.76 | | | 9.75 |
| 0.075 | 33.56 | | 0.075 | 32.18 | | 0.075 | 30.85 | |
| | | 33.56 | | | 32.18 | | | 30.85 |
| | Sum | 100 | | Sum | 100 | | Sum | 100 |

Where:

**I.** **- Diameter of the biggest grain in particular fraction**

**II.** **- Cumulative percentage of particles finer than "I".**

**III.** **- Volume percentage of fraction between two "I"s**

**Table 19**: Inch – by – inch dissolution – penetration depth [mm] determination – fayalite slag

| First test | 1' | 2' | 3' | 4' | 5' | 6' | 7' | 8' | Area 2' - 7' [mm²] |
|---|---|---|---|---|---|---|---|---|---|
| REF | 0.44 | 0.51 | 1.26 | 2.44 | 2.53 | 2.70 | 1.71 | 1.75 | 226 |
| C - 1 | 0.00 | 0.46 | 1.17 | 2.91 | 3.97 | 3.82 | 0.83 | 1.12 | 284 |
| C - 2 | 0.22 | 0.86 | 1.83 | 2.58 | 3.21 | 3.54 | 1.46 | 0.96 | 283 |
| C - 3 | 0.89 | 0.76 | 1.35 | 2.42 | 2.98 | 3.19 | 1.81 | 0.98 | 257 |
| C - 4 | 0.77 | 0.82 | 1.44 | 2.22 | 2.53 | 3.52 | 1.69 | 1.80 | 253 |
| C - 5 | 0.85 | 0.42 | 1.29 | 2.06 | 2.49 | 3.12 | 1.43 | 1.42 | 227 |

| Second test | 1' | 2' | 3' | 4' | 5' | 6' | 7' | 8' | Area 2' - 7' [mm²] |
|---|---|---|---|---|---|---|---|---|---|
| REF | 0.33 | 0.29 | 1.17 | 1.57 | 1.32 | 1.43 | 0.61 | 0.17 | 133 |
| C - 1 | 0.70 | 1.16 | 2.52 | 3.57 | 3.62 | 2.03 | 1.83 | 1.15 | 294 |
| C - 2 | 0.00 | 1.86 | 2.67 | 3.71 | 3.92 | 2.73 | 1.49 | 0.98 | 330 |
| C - 3 | 0.59 | 1.28 | 1.98 | 3.68 | 3.98 | 2.55 | 1.03 | 0.52 | 296 |
| C - 4 | 0.71 | 0.67 | 2.41 | 3.31 | 4.15 | 1.52 | 1.25 | 0.86 | 275 |
| C - 5 | 0.75 | 1.09 | 1.32 | 1.66 | 2.70 | 1.67 | 0.95 | 0.38 | 193 |

| Third test | 1' | 2' | 3' | 4' | 5' | 6' | 7' | 8' | Area 2' - 7' [mm²] |
|---|---|---|---|---|---|---|---|---|---|
| REF | 0.21 | 0.76 | 1.03 | 1.62 | 2.46 | 1.02 | 0.60 | 0.28 | 154 |
| C - 1 | 0.46 | 1.99 | 2.17 | 4.12 | 4.49 | 1.88 | 1.75 | 0.93 | 321 |
| C - 2 | 0.11 | 0.86 | 2.53 | 3.85 | 4.32 | 2.23 | 1.10 | 0.69 | 308 |
| C - 3 | 0.01 | 0.18 | 1.78 | 2.65 | 3.29 | 1.78 | 1.20 | 0.91 | 228 |
| C - 4 | 0.12 | 0.95 | 2.07 | 2.53 | 2.78 | 2.07 | 1.20 | 0.71 | 238 |
| C - 5 | 1.46 | 1.52 | 1.90 | 2.23 | 2.44 | 1.65 | 1.59 | 1.01 | 222 |

**Table 21**: Inch – by – inch dissolution – penetration depth [mm] determination – calcium ferrite slag.

| First test | 1' | 2' | 3' | 4' | 5' | 6' | 7' | 8' | area 2' - 7' [mm$^2$] |
|---|---|---|---|---|---|---|---|---|---|
| REF | 0.00 | 0.63 | 0.36 | 0.02 | 0.98 | 0.01 | 0.35 | 0.08 | 47 |
| C - 1 | 0.00 | 2.95 | 2.83 | 2.56 | 3.03 | 2.23 | 1.95 | 2.19 | 303 |
| C - 2 | 3.96 | 3.66 | 2.95 | 2.64 | 2.71 | 2.64 | 2.05 | 2.13 | 320 |
| C - 3 | 1.13 | 1.97 | 1.51 | 0.97 | 2.27 | 1.67 | 1.53 | 1.31 | 196 |
| C - 4 | 0.58 | 0.82 | 0.01 | 0.71 | 1.45 | 1.36 | 1.04 | 0.74 | 105 |
| C - 5 | 0.66 | 0.42 | 0.22 | 0.88 | 1.02 | 0.87 | 0.93 | 1.28 | 83 |

| Second test | 1' | 2' | 3' | 4' | 5' | 6' | 7' | 8' | area 2' - 7' [mm$^2$] |
|---|---|---|---|---|---|---|---|---|---|
| REF | 0.00 | 0.14 | 0.08 | 0.41 | 0.55 | 0.19 | 0.05 | 0.09 | 34 |
| C - 1 | 2.83 | 3.20 | 2.09 | 2.62 | 2.11 | 1.78 | 1.14 | 1.46 | 243 |
| C - 2 | 3.81 | 3.03 | 2.23 | 2.55 | 2.52 | 1.71 | 1.38 | 1.14 | 255 |
| C - 3 | 1.17 | 1.14 | 1.47 | 1.45 | 0.68 | 0.67 | 0.68 | 1.19 | 115 |
| C - 4 | 0.82 | 0.77 | 0.46 | 0.42 | 0.80 | 0.55 | 0.47 | 0.50 | 67 |
| C - 5 | 0.11 | 0.33 | 0.71 | 0.24 | 0.67 | 0.32 | 0.63 | 0.13 | 59 |

| Third test | 1' | 2' | 3' | 4' | 5' | 6' | 7' | 8' | area 2' - 7' [mm$^2$] |
|---|---|---|---|---|---|---|---|---|---|
| REF | 0.00 | 0.26 | 0.95 | 1.13 | 1.07 | 0.49 | 0.07 | 0.09 | 83 |
| C - 1 | 0.00 | 2.79 | 2.71 | 2.49 | 2.72 | 1.73 | 0.99 | 0.56 | 264 |
| C - 2 | 3.65 | 3.60 | 3.05 | 2.53 | 2.69 | 1.25 | 1.20 | 0.76 | 273 |
| C - 3 | 0.93 | 1.47 | 1.68 | 1.96 | 1.23 | 1.03 | 0.89 | 0.84 | 157 |
| C - 4 | 0.87 | 1.09 | 1.12 | 1.32 | 1.29 | 0.90 | 0.72 | 0.57 | 125 |
| C - 5 | 0.78 | 0.98 | 1.03 | 1.05 | 1.08 | 0.78 | 0.54 | 0.61 | 107 |

# ***REFERENCES FOR APPENDIX***

22. Harbison-Walker Refractories Company,: Modern Refractory Practice, Fourth Addition,: Forsterite Refractories, 288, Pittsburgh, Pennsylvania

23. V. A. Orlov, Y. M. Kuznestsov, A. A. Kortel and M. Y. Konov,: Refractories Made of Olivenites from Kola Reinseela, UNITECR, Global Advances in Refractories, 382-386, Aachen, Germany, 1991

24. A. F. Greaves-Walker and R. L. Stone,: Opportunities for Increasing Olivine Output, Industrial Minerals, 12, Feb. 1970

25. H. W. Wilson and K. G. Skinner,: Review of Four Years of Research on Refractory Properties of Pacific North-west Olivines, J. Am. Ceram. Soc., 23, 136-137, 1940

26. A/S Olivin, Sand Products, Propagation Material, 2000

27. R. E. Raymond, E. Birch and F. A. Harvey,: Forsterite and Other Magnesium Silicates as Refractories

28. C. A. Sorrell,: Rocks and Minerals, Golden Press, 164, New York, 1973

29. N. Wang.,: Olivine and Its Application, December 1992

30. P. P. Budnikov a kol,: Technologie Keramiky a Zaruvzdorneho Zbozi, 270, 1960( In Czech language)

31. N. L. Bowen and J. F. Schairer,: The System MgO-FeO-$SiO_2$, Am. Jour. Sci., 29, 151-217, 1935

32. B. J. Skinner,: Thermal Expansion of Ten Minerals, U. S. Geol. Surv. Prof. Paper, 450D, 109-112, 1962

33. J. R. Smyth and R. M. Hazen,: The Crystal Structures of Forsterite and Hortonolite at Several Temperatures up to 900°C, Am. Min., 58, 588-593, 1973

34. A. A. Kahn,: Computer Simulation of Thermal Expansion of Non-Cubic Crystal: Forsterite, Anhydrite and Scheelite, Acta Cryst., A32 11-16, 1976

35. W. L. Roberts, T. J. Campbel and G. R. Rapp, Jr.,: Encyclopedia Of Minerals, Van Nostrand Reinhold Company, 291-292, New York, 1989

36. N. L. Bowen and O. Anderson,: The Binary System $MgSiO_2$, Am Jour. Sci., 4th Sep., 37, 487-500, June 1914

37. F. W. Clarke, Data of Geochemistry, U. S. Geol. Serv. Bull., No. 770, 1924

38. P. P. Budnikov and B. N. Bogomolov,: Forsterite Refractories and Their Use in Different Branches of Industry, Vol. 5, No. 2, 140-148, 1960

39. N. L. Bowen and O. F. Tuttle,: The System of $MgO$-$SiO_2$-$H_2O$, Bull. Geol. Soc. Am., 60, 439-460 March 1949

40. E. A. Gee, C. E. McCarthey, F. S. Riordan and M. T. Pawel,: Magnesia form Olivine, U. S. Bureau Mines, Rep. Invest. 3938

41. F. A. Norton, Fine Ceramics, McGraw-Hill Book Company, New York, 249-250, 1970

42. A S. Berezhnoy,: Physical-Chemical Fundamentals of the Technology for Forsterite Refractories, Coll. Scientific Proc. Refractory Institute, No. 2, Metallurgizdat, Moscow, 1958

43. F. Singer and S. S. Singer, Industrial Ceramics, Champan and Hall Ltd., London 422, 1963

44. R. L. Stone,: Thermochemistry of North Carolina Olivine in the Manufacture of Forsterite Refractories, J. Am. Ceram. Soc., 22, 342, 1939

45. R. E. Birch and F. A. Harvey,: Forsterite and Other Magnesium Silicate as Refractories, J. Am. Ceram. Soc., 22, 342, 1939

46. R. L. Stone,: Electrically Fused Forsterite-Olivine, J. Am. Ceram. Soc., 26, 405, 1942

47. R. L. Stone,: Thermochemistry of North Carolina Olivine In the Manufacture of Forsterite Refractories, J. Am. Ceram. Soc., 22, 344, 1939

48. R. L. Stone,: Thermochemistry of North Carolina Olivine In the Manufacture of Forsterite Refractories, J. Am. Ceram. Soc., 22, 348, 1939

49. D. Xie, T. Tran, S. Jahanshahi,: In-Situ Gravimetric Of Wetting, Penetration and Wear of refractories by Molten Slags, Australia

50. M. Rigaud,: Corrosion of Refractories and Ceramics, Uhlig's Corrosion Handbook, 395-410, 2000